Structural transitions and fibril formation of the prion protein *in vitro*

Inaugural - Dissertation

zur

Erlangung des Doktorgrades der

Mathematisch-Naturwissenschaftlichen Fakultät

der Heinrich-Heine-Universität Düsseldorf

vorgelegt von

Karl-Werner Leffers

aus Oldenburg

Düsseldorf 2003

Gedruckt mit der Genehmigung der Mathematisch-Naturwissenschaftlichen Fakultät der Heinrich-Heine-Universität Düsseldorf

Referent: Prof. Dr. D. Riesner

Koreferent: Prof. Dr. J. H. Hegemann

Tag der mündlichen Prüfung: 23.01.2004

„If you want to waste your life doing stuff like this, just go on!"

Stanley B. Prusiner, 2000

Danksagung

Mein besonderer Dank gilt Prof. Dr. Detlev Riesner, der mir die Durchführung dieser Doktorarbeit ermöglichte. Dabei ist nicht nur die stete kritische Diskussion hervorzuheben, sondern auch die Möglichkeit selbständigen, flexiblen Arbeitens sowohl im eigenen Institut als auch im Austausch mit anderen Forschungsgruppen.

In this context I would like to thank Prof. Dr. Stanley Prusiner from the University of California at San Francisco who gave me the possibility to carry out important experiments of my project in his lab. Also I would like to thank Ana Serban and Guiseppe Legname for the constant supply with protein material and antibodies. A special thanks goes to everybody in the “lunch-crew” who created a great atmosphere in the lab, especially Svetlana, Camille, Marcela, Holger, Sam, Gerold and Patrick.

Ich danke Holger Wille für die geduldige Einführung in die Geheimnisse der Elektronenmikroskopie, für die gehaltvollen Diskussionen über meine Arbeit, für das noch geduldigere Ertragen der einen oder anderen Wissenslücke meinerseits und natürlich für die Einführung in die „lunch-crew“, die erholsamen Campingtrips und nicht zuletzt den Fernseher!

Frau Gruber danke ich für die Unterstützung in allen organisatorischen Fragen, vor allem in Bezug auf meine Auslandsaufenthalte.

Der gesamten Prion-Gruppe danke ich für die nette Arbeitsatmosphäre, insbesondere meinen beiden „Ex-Lehrlingen“ Andreas Schmidt und Jan Stöhr, die mir mit ihrer täglichen Begrüßung („Tach Chef!“) das Gefühl gaben, dass die akademische Ausbildung einen respektabel in der Gesellschaft positioniert… also Jungs, ihr wisst, wofür ihr arbeitet!
Des Weiteren danke ich allen Mitgliedern des Instituts für viele nette Stunden bei der Arbeit, auf Retreats, bei Betriebsausflügen und bei sonstigen Feiern.

Ich danke meiner Familie für den starken Rückhalt, der unabhängig macht und komplette Freiheit im Denken und Handeln erlaubt; diese Dinge sind wertvoller als alles andere.

Sandra, danke für alles vom ersten Tag bis heute!

Ich danke außerdem den Mitgliedern der Hero-Quest Runde für effektive Freizeitgestaltung sowie Eva & Tom für perfekte Nachbarschaft.

Zuletzt möchte ich mich noch bei allen bedanken, die die Zeit im Institut, in Düsseldorf und in San Francisco zu dem schönen Erlebnis gemacht haben, dass es geworden ist.

Eine spezieller Dank natürlich auch an Hobbel und Beavis für, like, you know…

Table of Contents

Abbreviations

µg	microgram
µl	microliter
BSE	bovine spongiform encephalopathy
°C	degrees Celsius
cf.	see further
CJD	Creutzfeld-Jakob disease
cm	centimetre
CWD	chronic wasting disease
d	days
Da	Dalton
e.g.	for example
et al.	and others
fCJD	familiar CJD
FFI	fatal familial insomnia
Fig.	figure
FSE	feline spongiform encephalopathy
FSI	fatal sporadic insomnia
g	gram
g	average acceleration due to the gravity on the surface of the earth
GSS	Gerstmann-Sträußler-Scheinker Syndrome
h	hour
HEPES	N-[2-Hydroxyethyl]piperazine-N'-[2-ethansulfonic acid]
iCJD	iatrogenic CJD
i.e.	in detail
kDa	kilodalton
l	litre
log	logarithm
M	molar (mol/l)
mA	milliampere
MeOH	methanol
min	minute

ml	millilitre
mM	millimolar
µM	micromolar
NaP_i	sodium phosphate buffer
ng	nanogram
µg	microgram
NMR	nuclear-magnetic resonance
nt	nucleotide
PAGE	polyacrylamide-gelelectrophoresis
PBS	Phosphate Buffered Saline
PK	proteinase K
PMSF	Phenylmethylsulfonylfluorid
PrP	prion protein
PrP 27-30	prion protein from prion rods
PrP^C	cellular prion protein
PrP^{Sc}	PrP Scrapie (abnormal, infectious form of PrP)
PVDF	polyvinylidenfluorid
rpm	revolutions per minute
rec PrP (90-231)	recombinant PrP with the amino acid sequence of PrP 27-30
RT	room temperature
S	Svedberg units
sec	seconds
sCJD	sporadic CJD
SDS	sodium dodecyl sulphate
sol PrP 27-30	solubilized PrP 27-30
sol PrP 27-30 elu	solubilized and gel-eluted PrP 27-30
Tab.	table
TBS-T	Tris buffered saline, tween
TEMED	N,N,N‘,N‘-Tetramethylethylendiamine
TME	transmissible mink encephalopathy
Tris	Tris-[hydroxymethyl-]aminomethane
TSE	transmissible spongiform encephalopathy
V	Volt

1. Introduction

1.1 Neurodegenerative diseases and amyloid deposits – cause or effect?

Neurodegenerative diseases like Alzheimer's disease (AD), Parkinson's disease (PD) or Transmissible Spongiform Encephalopathies (TSEs) are a group of late-onset progressive diseases. Surveys e.g. in Germany revealed that a great number of people are affected by these diseases: AD is the most prevalent neurodegenerative disease in Germany with one million cases followed by PD with 250.000 cases. All neurodegenerative diseases are characterized by clinical symptoms that are caused by loss of certain brain functions: While AD-patients typically lose cognitive functions, PD is characterized clinically by difficulty in initiating movements and often by a resting tremor. The majority of neurodegenerative diseases have sporadic etiologies, but the cause can also be genetic. In the special case of TSE's the disease can even be transmissible which will be in the focus of this study.
At autopsy, neurodegenerative diseases can be characterized by the presence of abnormal proteinaceous deposits, often showing fibrillar morphology (*for review*: Caughey & Lansbury, Jr., 2003; Taylor *et al*., 2002). These deposits are distributed in areas of the brain where neurodegeneration is most extreme. Histopathologic studies looking at the morphology of the deposits classified them as amyloid plaques. The amyloid character of protein deposits can be used for their detection in various ways: The term "amyloid" was introduced by Virchow (Virchow *et al*., 1851) originally defining "carbohydrate-like" properties of deposits found by histopathologic studies of brains using iodine and sulfuric acid as dyes. Later it was shown that these deposits actually contain proteins leading to a new definition for the term "amyloid"(*for review*: Sunde & Blake, 1997; Rochet & Lansbury, Jr., 2000):

1.) Amyloid structures can be specifically labeled using the dye congo-red. This label results in specific gold-green birefringence under polarized light.

2.) Amyloid structures contain relatively straight, rigid and unbranched fibrils with a diameter of 8-15 nm as revealed by electron microscopy.

3.) Amyloid structures reveal cross-β structure with β-strands perpendicular to and backbone hydrogen bonds parallel to the fibril axis.

Hence, currently the term "amyloid" is mostly used to describe fibrillar protein deposits associated with neurodegenerative diseases (cf. Table 1.1).

Table 1.1 Most common neurodegenerative diseases. All of these diseases are characterized by protein aggregation and deposits.

Disease	Cause	Deposits	Protein
Alzheimer's disease	95 % sporadic 5 % genetic	Extracellular amyloid plaques, fibrillar Aβ	Amyloid Precursor Protein (APP), Tau
Parkinson's disease	Mostly sporadic, increasing evidence of genetic causes	Lewy bodies, fibrillar α-synuclein	α-Synuclein
Huntington's disease	Genetic (dominant autosomal)	Intranuclear neuronal inclusions, fibrillar Huntingtin	Huntingtin
Transmissible spongiform encephalopathies	90 % sporadic 8 % genetic 2 % transmissible	Extracellular plaques of a patho-logical isoform of the prion protein	Prion Protein (PrP)
Amyotrophic lateral sclerosis (ALS)	90 % sporadic 10 % genetic	Intraneuronal inclusions, insoluble SOD 1	Superoxide-dismutase 1

One of the first questions that were addressed after detecting amyloid plaques in connection to neurodegenerative diseases was how these deposits form. It is known that the process of protein folding from a totally unfolded, newly generated amino acid sequence to a correctly folded, functional protein involves intermediates of partial folding. If a polypeptide chain fails to reach its functional, three-dimensional structure from these intermediates or fails to maintain its native structure, aggregates or pre-fibrillar assemblies can appear. Normally chaperones indirectly suppress the appearance of unwanted aggregates through minimizing

the population of partially folded molecules by assisting the correct folding of the nascent chain. Furthermore the "unfolded protein response" usually targets incorrectly folded proteins for degradation by the proteasome (cf. Figure 1.1). Another cause for the appearance of higher concentrations of only partly folded intermediates which can then lead to uncontrollable aggregation including formation of highly ordered, amyloid fibrils are mutations in the amino acid sequence of a protein that sometimes lead to destabilization of the native fold (Dobson *et al*., 1999).

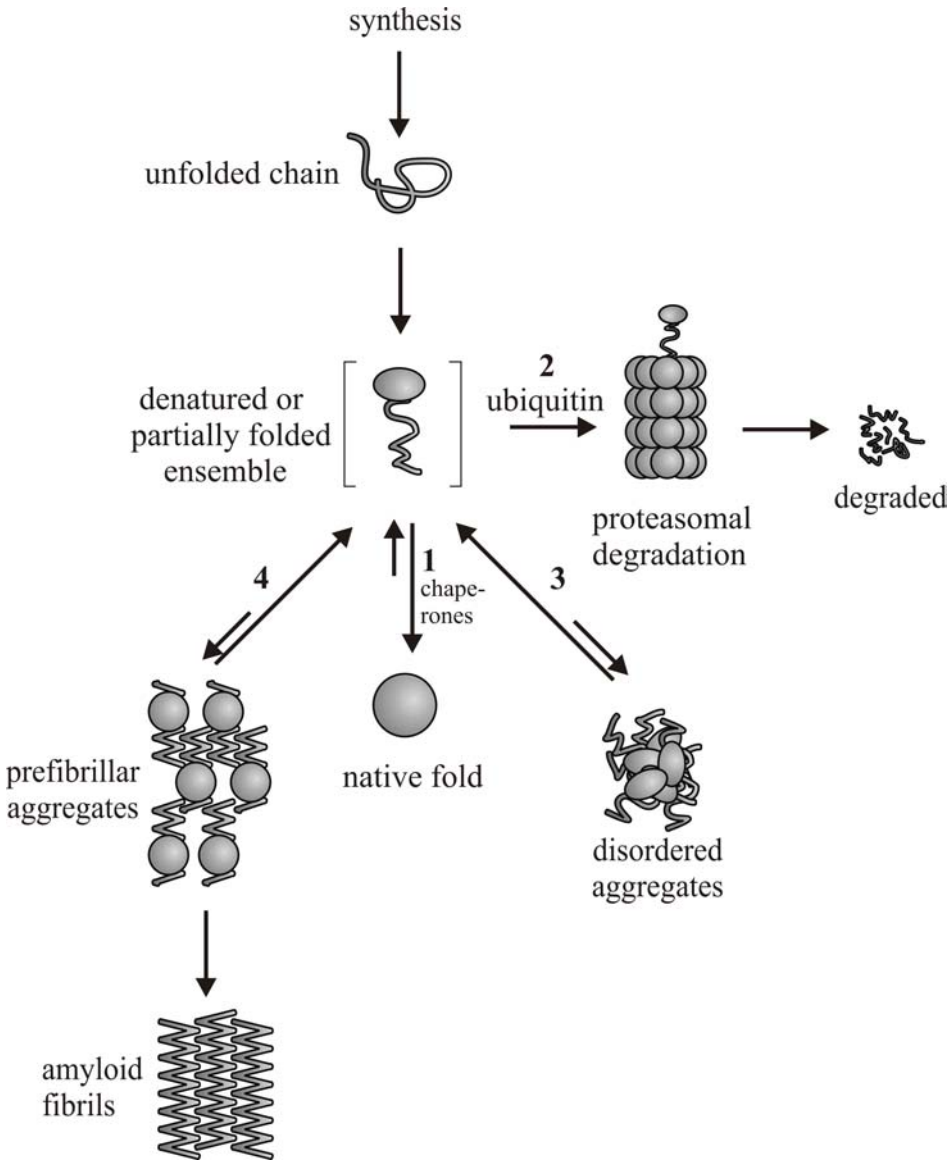

Figure 1.1: Possible fates of a newly synthesized polypeptide chain. Usually the equilibrium (**1**) is strongly favoring the native fold. Mutations or destabilizing solution conditions can lead to increased concentrations of partially folded or misfolded intermediates which are then usually degraded by the proteasome ("unfolded protein response") (**2**). If this mechanism is impaired, these species can form disordered aggregates (**3**) or prefibrillar aggregates that end up as amyloid fibrils (**4**). Modified from Dobson, 2002.

Studies of amyloid deposits in connection with neurodegenerative diseases led to the question if protein aggregation is a cause or one of the consequences of neurodegeneration. Evidence from multiple sources suggests that protein aggregation is rather a cause than the effect of neurodegeneration (*for review*: Caughey & Lansbury, Jr., 2003):

a.) Genes linked to familial forms of the diseases encode the aggregated protein, e.g. for the case of PD the gene α-synuclein encodes for the major fibrillar component of Lewy bodies found associated to PD, the protein α-Synuclein.

b.) Colocalization of cell death and aggregates: Amyloid deposits are often found in proximity to vacuolated regions of the brain.

c.) Disease-associated mutations promote *in vitro* aggregation in many cases: Point-mutations can lead to unstable intermediates in the folding process of proteins. These intermediates may then preferably lead to aggregation prone forms of the disease-associated protein.

d.) Overexpression of the aggregated protein in animal models produces the disease-associated phenotypes (Wang *et al*., 2002).

e.) Rates of cell death, disease onset and progression are consistent with a nucleation-dependent process for the majority of neurodegenerative diseases (Clarke *et al*., 2000).

More detailed studies on protein fibrils and their precursors detected in association with neurodegenerative diseases led to models that suggest that not the fibrillar endproduct, but instead an oligomeric intermediate or protofibrils may actually be the neurotoxic agent (*for review:* Caughey & Lansbury, Jr., 2003). This hypothesis is supported by increasing experimental evidence, e.g. in the case of Alzheimer's disease (Walsh *et al*., 2002) and Parkinson's disease (Conway *et al*., 2001).
However, the consequence from the collected data about aggregating proteins involved in neurodegenerative diseases must be to avoid conditions of oligomerization and aggregation and thereby to prevent the disease (Lansbury *et al*., 1999).

1.2 Transmissible spongiform encephalopathies (TSEs)

Transmissible spongiform encephalopathies (TSEs) are a particularly challenging kind of neurodegenerative disorders since unlike the other neurodegenerative diseases they cannot only be of genetic or sporadic, but also of transmissible etiology. TSEs are always lethal; they appear in animals as well as in humans. The most commonly known TSEs are scrapie in sheep, bovine spongiform encephalopathy (BSE) and Creutzfeldt-Jakob Disease (CJD). The latter is divided into sporadic CJD (sCJD), familial CJD (fCJD), iatrogenic CJD (iCJD), and the (new) variant CJD (vCJD) in regard to their sporadic, genetic or in the last two cases transmissible nature (cf. Table 1.2).

Typical symptoms of TSEs are dementia (often observed in CJD-cases) or ataxia (often observed in BSE-cases). These clinical symptoms often appear after a long, symptomless time (Wells *et al*., 1987).

Table 1.2: TSEs. Modified after Prusiner 1998 (Prusiner, 1998).

Disease	Host	Reference
Sporadic Creutzfeldt-Jakob disease (sCJD)	Human	Creutzfeldt *et al*., 1920; Jakob *et al*., 1921
Familial Creutzfeldt-Jakob disease (fCJD)	Human	
Iatrogenic Creutzfeldt-Jakob disease (iCJD)	Human	
Variant Creutzfeldt-Jakob disease (vCJD)	Human	Will *et al*., 1996
Gerstmann-Sträussler-Scheinker-syndrome (GSS)	Human	Gerstmann *et al*., 1936
Fatal Familial Insomnia (FFI)	Human	Lugaresi *et al*., 1986
Kuru	Human	Gajdusek & Zigas, 1957
Bovine spongiform encephalopathy (BSE)	Cattle	Wells *et al*., 1987
Scrapie	Sheep	McGowan *et al*., 1922
Chronic wasting disease (CWD)	Mule deer, elk	Williams *et al*., 1980

It took a long time before scientists found out that the diseases listed in Table 1.2 all belong to the same group of diseases; mainly the common histopathology of these diseases led to the link between the different diseases. Generally a spongiform degeneration of the brain occurs, i.e. a vacuolization of the neuropil going along with cell-death of neurons. At the same time an astrocytic gliosis and microgliosis can be observed, i.e. astrocytes and microglia grow and proliferate more than usual (Masters & Richardson, Jr., 1978). Additionally, as a characteris-

tic for all neurodegenerative diseases, protein deposits that sometimes have fibrillar character (called amyloid plaques) can be detected by electron microscopy (Jeffrey *et al*., 1992; Jeffrey *et al*., 1994). In the case of TSEs these protein deposits are mainly composed of a protein called the "prion protein" or PrP (*for review*: Prusiner 1998), which will be characterized in more detail below (cf. 1.3).

The transmissible nature of TSEs differentiates them from all other neurodegenerative diseases. In the early 80's the suspicion was raised that on of these diseases, i.e. BSE, might have crossed the species barrier to humans. Basis for this suspicion were the observations that were made in context to the BSE-epidemic in Great Britain: The procedure for making meat and bone meal from carcasses of cattle was changed to lower temperatures during the sterilization step. This allowed the agent causing BSE to resist degradation during this step (Wilesmith & Wells *et al*., 1991). As a consequence the BSE-agent was spread when the meat and bone meal resulting from this procedure was fed to animals, i.e. mostly cattle again. This opened the door for a big epizootic in the UK during the late 80's and early 90's with up to 36.500 cases of BSE per year in 1992 (Hörnlimann *et al*., 2001). Also other animals that had been fed with this meat and bone meal developed clinical signs of diseases similar to BSE (Wells & McGill, 1992; Bons *et al*., 1996). Furthermore the first cases of vCJD were reported in Great Britain 1996 (Will *et al*., 1996; Collinge *et al*., 1999) raising the suspicion that a transmission from BSE-infected cattle to humans had occurred through consumption of products from these animals.

To evaluate whether the agent causing TSEs had crossed the barrier to humans in the form of vCJD, further experiments were carried out: Studies with BSE- or CJD-infected macaques support the hypothesis that vCJD is caused by the transmission of BSE to humans (Lasmezas *et al*., 1996). These results were questioned for a long time, since another TSE that has been known for a long time, i.e. scrapie in sheep, had never noticeably crossed the species-barrier to humans. One of the hypotheses for the origin of BSE is that it may have been transferred from sheep to cattle (Prusiner *et al*., 2001). Another model suggests that BSE arose from a sporadic form in cattle which then had been transmitted to other animals (Fraser *et al*., 2000).

Clinical surveys revealed that the average age at onset of vCJD is 28 (Belay *et al*., 1999), whereas in the case of to sCJD and fCJD the average age of the patients at onset of the disease is around 60 years.

1.3 Identification of the agent causing TSEs

The fact that clinical symptoms of prion diseases often occur after a long, symptomless time, led to the hypothesis that these diseases are "slow-virus-diseases" (Sigurdsson *et al*., 1954). The agent causing the TSEs was thought to be more-or-less a normal virus, i.e. composed of nucleic acids and proteins. The experiments of Alper (Alper *et al*., 1967) revealed that this hypothesis was difficult to support : The agent causing scrapie resisted high doses of UV- (254 nm) and ionizing-radiation for a long time. In contrast, viruses or other agents composed of nucleic acids get irreversibly damaged when exposed to low doses of radiation. These results led to many discussions about the nature of the agent including models that suggested replicating membrane proteins as the causative agent of scrapie (Gibbons & Hunter, 1967). In the same issue Griffith postulated that a protein isoform could amplify in an autocatalytic manner and in this way be responsible for the transmission of scrapie (Griffith *et al*., 1967). However, the hypotheses of Griffith gained no acceptance, particularly because to few experiments could support them. Prusiner followed and extended systematically the approach of Alper et al.: He developed a protocol to purify the scrapie-agent from experimentally infected hamsters and found that the extract containing the agent mainly was composed of protein (Prusiner *et al*., 1980). The infectivity of this extract could be reduced with methods that denature proteins but not with methods that degrade or denature nucleic acids (Prusiner *et al*., 1981; Prusiner *et al*., 1982). In conclusion he called the agent causing scrapie "prion" as a short form for "*pro*teinaceous *in*fectious particle" indicating that the main and most important component of prions is a protein (Prusiner, 1982). A single protein was subsequently purified and called PrP for "*pr*ion *p*rotein". Moreover, these discoveries led to using the term "prion diseases" for transmissible spongiform encephalopathies.

Surprisingly it was found that PrP is a protein that is present in all animals and humans: PrP was found to be a membrane protein which is mainly expressed in the central nervous system (CNS), but also in most organs of the body except liver and pancreas (Kretzschmar *et al*., 1986a; Weissmann *et al*., 1993). The human PrP gene called "Prnp" is located on chromosome 20 and was first sequenced in 1986 (Kretzschmar *et al.*, 1986b). The observation that the gene encoding PrP is expressed throughout life and that PrP is present in infected as well as non-infected humans and animals supported the conclusion that PrP can adapt different conformations: One normal, harmless conformation designated PrP^{C} (for *c*ellular PrP) and one abnormal, harmful conformation designated PrP^{Sc} (for *sc*rapie).

Even today there are still discussions whether nucleic acids play a role in the pathway of scrapie-infection and -pathogenesis: The strongest argument for scrapie-associated nucleic acids is the phenomenon of scrapie-strains. These strains are characterized by different incubation times, lesions, etc. The characteristics of strains are conserved in serial passages in mice even if they have the same genetic background (Bruce *et al*., 1992). This may be a sign of a nucleic acid that carries the information of strain-specifications from one generation to the next. Despite many attempts no such nucleic acids could be found in experiments. To the contrary these experiments revealed that nucleic acids of more than 50 nucleotides length per infectious unit are absent (Meyer *et al*., 1991; Kellings *et al*., 1992). To the current knowledge nucleic acids that are smaller than 50 nucleotides may have regulatory functions but not the ability to encode a number of strain-specifications as required by the described hypothesis.

Another approach to explain properties of prion diseases and species specificity in particular was taken in studies including a cellular “factor X”, which interacts with the C-terminus of PrP (Telling *et al*., 1994; Telling *et al*., 1995). In a study using mice as a model system the interaction site was characterized in more detail: The amino acids 168, 172, 215 and 219 are very close to each other in the 3D-structure of the protein and form a discontinuous epitope interacting with “factor X” (Scott *et al*., 1997).

Other experiments suggest that the information for the strains is encoded in the conformation of the prion protein (Safar *et al*., 1998): Using a conformation-dependent immunoassay (CDI) it could be shown that PrP of different prion strains has distinct stabilities against denaturation by denaturing agents and degradation by proteinase K.

1.4 The prion protein

The primary translation product of the prion protein gene is composed of about 250 amino acids and carries two signal sequences: The first 22 amino acids at the N-terminus encode a signal that directs the protein into the endoplasmatic reticulum (ER) and is cleaved off when the protein enters the ER-lumen. The second signal sequence of 23 amino acids length is located at the C-terminus and encodes for the attachment of a glycosyl-phosphatidyl-inositol-anchor (GPI-anchor) that is attached to the protein in the ER-lumen (Stahl *et al.*, 1990). Additionally a disulfide-bridge forms between C179 and C214. Two N-linked oligosaccharides can be attached to N181 and N197 resulting in a heterogeneous glyco-sylation-pattern. Further posttranslational modifications occur in the Golgi-apparatus including modifications of the N-linked oligosaccharides and the GPI-anchor. In the end a membrane protein designated PrP^C with M_r = 33-35 kDa results that is transported to the cell surface (cf. Figure 1.2). Here it is located in caveolae- or raft-like domains which are rich in cholesterol and sphingolipids (Kaneko *et al*., 1997a; Taraboulos *et al*., 1995; Vey *et al*., 1996). It is unclear which role PrP^C plays in the cell metabolism once it has reached the cell surface. Considering the high grade of conservation of the Prnp-gene it can be assumed that the role is of some functional relevance. Therefore it was surprising that $PrnP^{0/0}$-mice developed normally besides some relatively minor disturbances in the circadian rhythm (Bueler *et al.*, 1992; Prusiner *et al.*, 1993; Weissmann *et al.*, 1993; Manson *et al*., 1994). Experimental evidence suggested a role in the copper metabolism of neurons (Brown *et al*., 1997) and a role similar to superoxidedismutase-1 (SOD-1), i.e. degradation of radicals (Brown *et al*., 1999). However, these results could not be confirmed by others (Hutter *et al.*, 2003). Studies aiming at finding interaction-partners of PrP identified the neural cell-adhesion molecule (N-CAM) (Schmitt-Ulms *et al*., 2001) and various interactions in signal transduction pathways (Mouillet-Richard *et al.*, 2000; Gauczynski *et al*., 2001).

To further characterize PrP^C, biophysical and biochemical studies were carried out: PrP^C can be purified and solubilized in mild detergents. It reveals a high α-helical content when analyzed by CD-spectroscopy (Pan *et al*., 1993). The structure was later resolved with atomic resolution using NMR-spectroscopy revealing the presence of 3 α-helices in PrP^C (Zahn *et al*., 2000). Upon digestion with proteinase K the protein is degraded within a few minutes (McKinley *et al*., 1983). In its cellular form the prion protein is not infectious.

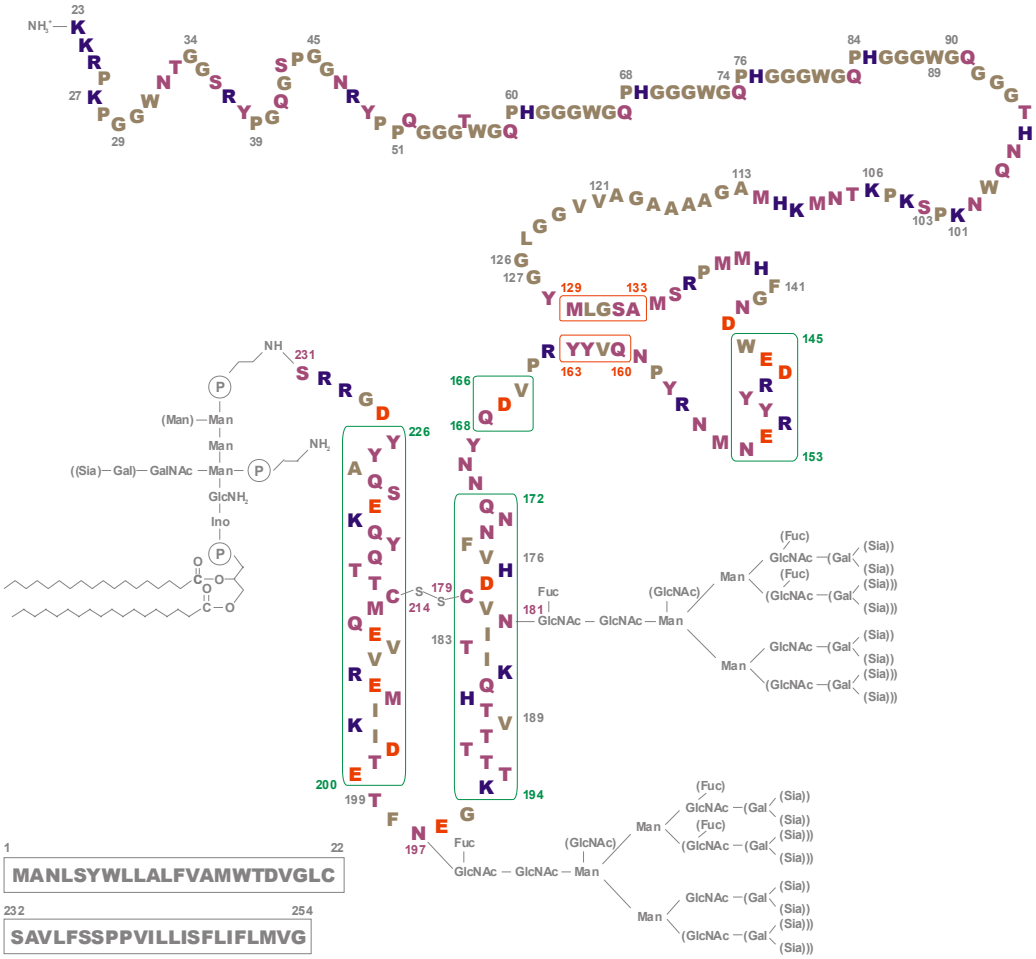

Figure 1.2 Schematic picture of the cellular prion protein from Syrian hamster.

Amino acids (aa) 1-22 and 232-254 are the signal sequences for transport to the ER-lumen and GPI-anchor (lower left). The α-helices are located at aa 145-153, aa 166-168, aa 172-194 and aa 200-226. Short β-sheet strands are located at aa 129-133 and aa 160-163. Two N-linked oligosaccharides can be attached to N181 and N197, the GPI-anchor is attached to S231. A disulfide bond forms between C179 and C214.

Red = negatively charged aa; blue = positively charged aa; violet = neutral hydrophilic aa; brown = hydrophobic aa (all at pH 7.0). Figure taken from Dumpitak, 2003.

1.5 PrP^{C} vs. PrP^{Sc}

What is the relation between PrP^{C} and PrP^{Sc} and how does PrP^{Sc} cause a prion disease? Both forms are chemically identical: It could be shown that the amino acid sequence is identical and there are no covalent modifications in PrP^{Sc} that cannot be found in PrP^{C} (Stahl *et al.*,

1993). It should be noted though that one infectious unit is composed of 10^5 PrP-molecules, therefore it cannot be excluded that a small portion of the infectious molecules may actually be modified but are not detectable (Prusiner *et al*., 1991). However, if PrP is isolated either from non-infected hosts or as highly infectious material, its biophysical properties are drastically different:

Comparative biophysical studies of PrP^C and PrP^{Sc} revealed major differences regarding some central properties of the protein (*for review*: Cohen & Prusiner, 1998; Ironside *et al*., 1998): Whereas PrP^C is soluble, has a mainly α-helical secondary structure and is sensitive to degradation by proteases, PrP^{Sc} forms insoluble, β-sheet-rich, protease resistant aggregates (cf. Table 1.3).

Table 1.3: Comparison of biophysical properties of PrP^C and PrP^{Sc}.

Property	PrP^C	PrP^{Sc}
Solubility	+	-
Secondary structure	mainly α-helical	β-sheet-rich
PK-resistance	-	+
Infectivity	-	+

When PrP^{Sc} is subjected to digestion with proteinase K, an N-terminally truncated form designated PrP 27-30 consisting of residues 90-231 with an approximate molecular weight of 27-30 kDa results. This protease resistant core has the ability to form amyloid fibrils (Prusiner *et al*., 1983) and 2D crystals (Wille *et al*., 2002). Further studies on these 2D-crystals led to an advanced model of glycosylated PrP 27-30 oligomers featuring a β-helical structure (cf. Figure 1.3):

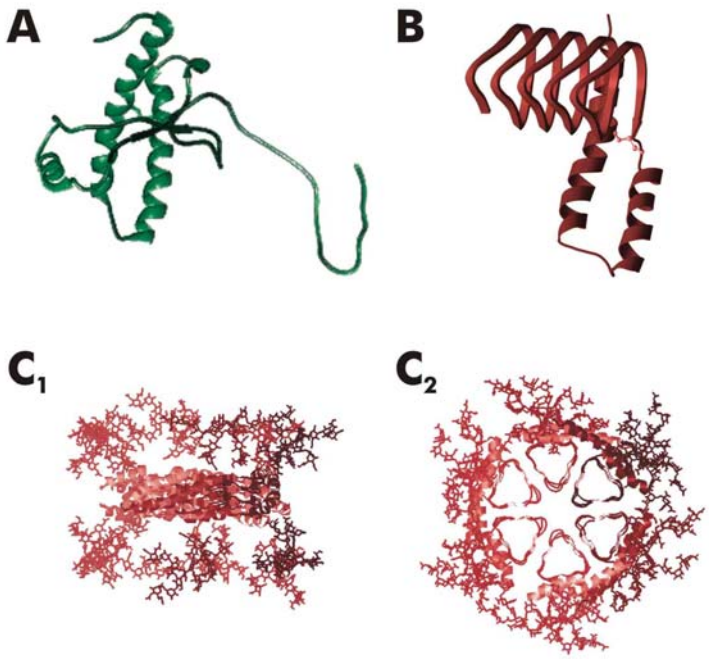

Figure 1.3: PrP^{C} vs. PrP^{Sc}.

A: NMR-structure of recombinant SHa PrP (90-231) (modified after Liu *et al*., 1999) which is accepted as a PrP^{C}-like structure. **B:** Model of SHa PrP^{Sc} as derived from electron microscopic data of 2D-crystals. The depicted monomer is part of a trimer of dimers or dimer of trimers. $\mathbf{C_1}$ and $\mathbf{C_2}$ show the side view and the top view of the suggested hexamer (modified after Wille *et al*., 2002).

Since it cannot be differentiated between a β-sheet structure and a β-helix structure by the methods used in this study, i.e. CD-spectroscopy, the term β-structure will be used.

Under certain circumstances this β-structure allows formation of amyloid fibrils: It could be shown that formation of large quantities of amyloid fibrils during the purification process of PrP 27-30 is dependent upon both detergent extraction and limited proteolysis (McKinley *et al*., 1991). However, it could also be shown that amyloid fibrils sometimes occur in infected brains: Electron microscopic studies of infected tissue and membrane fractions containing PrP^{Sc} sometimes display small amounts of amyloid fibrils besides large quantities of amorphous plaques (Jeffrey *et al*., 1992; Jeffrey *et al*., 1994). These amyloid fibrils are also known as scrapie associated fibrils or SAF's (Merz *et al*., 1981).

Amyloid fibrils are of central interest in prion research; on the one hand because they are highly infectious and on the other hand because they exhibit a highly ordered structure similar to those found in many neurodegenerative disorders like in Alzheimer's Disease (AD), Parkinson's disease, etc. (cf. above).

1.6 Prion-replication

According to the prion-concept and its simplest formulation, i.e. the "*protein-only*"-hypothesis, the agent causing prion diseases is the prion protein that replicates. The general difficulty in creating a model that explains this replication process is that this model needs to explain transmissible cases as well as genetic and sporadic cases. Three major models are currently discussed in context of the "*protein-only*"-hypothesis: The "*template assistance*"-model by Cohen & Prusiner (Cohen & Prusiner, 1998), the "*cooperative Prusiner*"-model suggested by Eigen (Eigen, 1996) and the "*seeded nucleation*"-model by Rochet & Lansbury (Rochet & Lansbury, Jr., 2000). The $PrP^{C} \rightarrow PrP^{Sc}$ transition is an autocatalytic process that occurs as long as new PrP^{C} is synthesized. A similar process, i.e. induction of a certain protein structure by another protein, is already known from chaperones.

1.6.1 Template assistance model

Early theoretical considerations led Prusiner to the formulation of a "*heterodimer*"-model (Cohen *et al*., 1994). This model suggests that PrP^{C} exists in an equilibrium with a second state designated PrP*. PrP* is viewed as a transient intermediate and participates in PrP^{Sc} formation through an interaction with PrP^{Sc}. This formation of a heterodimer is the critical step in the transition process. Once formed, PrP^{Sc} induces the structural transition from PrP* to PrP^{Sc} resulting in a PrP^{Sc} homodimer. This homodimer can then dissociate and initiate a replication cycle. This reaction corresponds to a linear autocatalysis that leads to exponential formation of PrP^{Sc}. The equilibrium must be on the side of PrP^{Sc} because otherwise there wouldn't be a driving force for the catalytic turnover. Thermodynamic calculations by Eigen (Eigen, 1996) led to the conclusion that the spontaneous conversion must occur extremely slow because otherwise PrP^{Sc} would accumulate even without an infection. To induce such a slow spontaneous transition within the lifespan of a human or animal, a catalytic acceleration of 10^{15} would be required. A catalytic acceleration in this order of magnitude is rather unlikely considering the known enzymatic processes in nature. Since genetic evidence points to the existence of an auxiliary factor ("factor X"; cf. above) in the transition process, the "*heterodimer*"-model was extended by this factor to a model designated the "*template assistance*"-model (Cohen & Prusiner, 1998): According to this new model, the mentioned

factor X preferentially binds PrP^C which exists in equilibrium with a partially folded intermediate designated PrP*. When e.g. exogenous PrP^{Sc} invades the organism, it interacts with the PrP*/protein X-complex and induces transition to a PrP^{Sc} homodimer while factor X is liberated. When this homodimer dissociates a replication cycle is initiated. Similar scenarios also involving factor X and following replication cycles are described to explain spontaneously or genetically caused prion diseases.

1.6.2 Cooperative Prusiner model

After carrying out the thermodynamic calculations mentioned above Eigen extended the "*heterodimer*"-model and created a model designated "*cooperative Pruinser*"-model (Eigen 1996). According to this model several molecules of PrP^{Sc} have to bind cooperatively to PrP^C to induce a transition to PrP^{Sc} (cf. Figure 1.5). Therefore the catalytic effect of one PrP^{Sc}-molecule is lower than in the "*heterodimer*"-model. This model is similar to the mechanism of allosteric binding of ligands. Again the equilibrium between PrP^C and PrP^{Sc} is on the side of PrP^{Sc}, but the non-catalytic formation of PrP^{Sc} is so slow, that degradation of PrP^{Sc} is faster than spontaneous formation of PrP^{Sc}. Every molecule of PrP^{Sc} that binds to the PrP^C/PrP^{Sc}-complex leads to changes in the conformation of PrP^C which raises the affinity for binding more monomeric PrP^{Sc} resulting in a n-mer that is capable of inducing the transition process. This model was designed from calculations assuming kinetic constants in realistic orders of magnitude but it lacks experimental data.

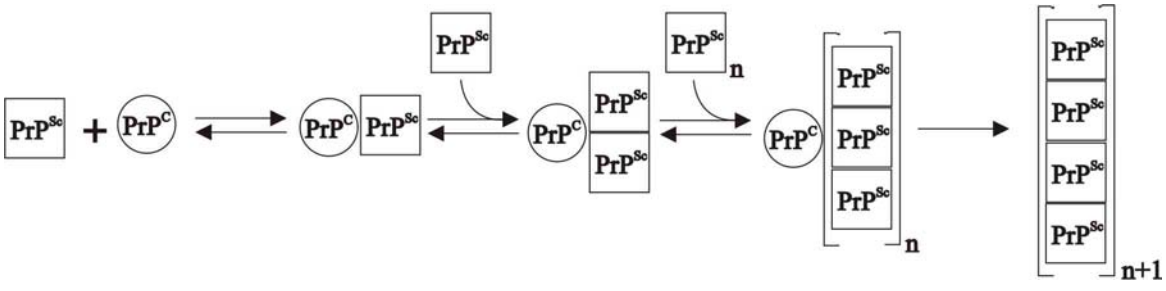

Figure 1.5 Cooperative Prusiner Model. Several molecules of PrP^{Sc} have to bind to PrP^C to result in a complex that is capable of inducing the transition of the PrP^C to PrP^{Sc}. Modified from Eigen (Eigen 1996).

1.6.3 Seeded nucleation model

Lansbury derived a model for prion replication from a model for seeded nucleation that has been described for many other aggregation processes in neurodegenerative diseases (Rochet & Lansbury 2000). This model follows the principle of linear crystallization: In contrast to the previous models this model suggests that the equilibrium between PrP^C and partially structured conformers is on the side of PrP^C. The partially structured conformers have an increased β-sheet content and therefore amyloidogenic character. This conformer may then be stabilized by ordered self-assembly to form a nucleus enriched with β-sheet. Alternatively, large amorphous aggregates can be formed. The presence of these aggregates provides a high local concentration of amyloidogenic intermediates and might therefore facilitate formation of nuclei. Once a nucleus is formed, it can grow by β-sheet extension to form prefibrillar aggregates and later amyloid fibrils (cf. Figure 1.6). The nucleus is the first stable intermediate. From here growth is faster than degradation.

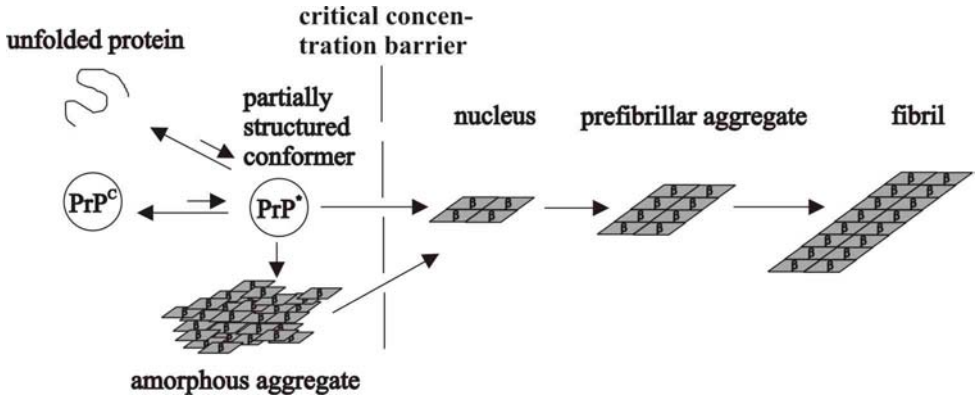

Figure 1.6: Seeded Nucleation Model. PrP^C or the unfolded protein are in an equilibrium with a partially structured conformer with increased β-sheet content designated PrP*. This conformer can form amorphous aggregates or, when a critical concentration barrier is crossed an ordered nucleus enriched with β-sheet. Growth of the nucleus by β-sheet extension leads to prefibrillar aggregates and later amyloid fibrils. Modified from Rochet & Lansbury (Rochet & Lansbury, 2000).

1.7 *in vitro* conversion

The insolubility of amyloid fibrils composed of PrP^{Sc} or PrP 27-30 has hampered biophysical studies on prion diseases. Evaluation of the "*protein-only*"-hypothesis is the subject of many studies on prion diseases (cf. above). Therefore the creation of an *in vitro*-system, that allows solubilization of the protein and at the same time enables investigation of the transition from PrP^{C} to PrP^{Sc} under controllable and well-defined conditions, is of major importance.

One of the central problems of working with the prion protein *in vitro* is the difficult analysis of the resulting protein in regard to its functionality: Since no activity test exists that can confirm that the protein in the sample is actually the biologically functional PrP^{C} as found *in vivo*, it can only be regarded to as "PrP^{C}-like isoform". This PrP^{C}-like character is confirmed by analysis of commonly accepted markers, i.e. solubility, PK-resistance, secondary structure and infectivity (cf. Table 1.3). PrP^{C} or PrP^{C}-like isoforms can be manipulated *in vitro* in a way that PrP adopts a conformation with structural features of PrP^{Sc}, but all attempts to generate *de novo* infectivity *in vitro* have failed so far (Caughey *et al*., 1995; Caughey *et al*., 1997; Post *et al*., 1998; Hill *et al*., 1999). Therefore the term "PrP^{Sc}-like isoform" will be used in this context throughout the present study.

In the attempts to generate *de novo* infectivity *in vitro* several approaches were made: Using partly denaturing conditions e.g. by adding guanidinium hydrochloride, low pH and sodium chloride, oligomers of recombinant PrP with β-structure were found that can form insoluble fibrils after long incubation times (Jackson *et al*., 1999). These results were confirmed by other groups using similar setups during this study (Swietnicki *et al*., 2000; Baskakov *et al*., 2001). Furthermore, it could be shown recently that treating recombinant PrP with detergents like sarkosyl can also lead to formation of fibrils (Xiong *et al*., 2001). Taking a closer look at the respective incubation conditions in all of these studies it can be summarized that not only longer incubation times lead to the formation of more or longer fibrils: The presence of an appropriate salt, i.e. sodium chloride, also seems to be essential for the formation of such fibrils. These observations were taken into account during this study resulting in modulated protocols for aggregation studies (cf. below). Moreover it can be observed that fibril formation is inducible in a pH-range from 3-6.5.

Failure to generate *de novo* infectivity *in vitro* in all of these studies might have different reasons: The conversion conditions used in the respective experiments might be inappropriate: *In vitro* conversion studies are generally carried out in solution whereas *in vivo* PrP^{C} is presented attached to a membrane. Furthermore, missing secondary components could

be responsible: The $PrP^{C} \rightarrow PrP^{Sc}$ conversion might only occur in the presence of a cellular factor X (Telling *et al*., 1994; Telling *et al*., 1995; Kaneko *et al*., 1997b) (cf. above). Also, small amounts of specific lipids (Klein *et al*., 1998) and substantial amounts, i.e. about 10 % of a polyglucose scaffold (Dumpitak, 1998; Appel *et al*., 1999) have been found in association with prion rods composed of PrP 27-30. So far it remains unclear which specific role these or other components might play e.g. in the conversion process, for structure stabilization or for the attachment of prions onto the cell.

Since there is experimental evidence that the $PrP^{C} \rightarrow PrP^{Sc}$ transition occurs in membrane domains enriched in sphingomyelin and cholesterol, i.e. rafts or caveolae-like domains (Vey *et al*., 1996; Kaneko *et al*., 1997a), studies have been carried out to determine the interaction between PrP and these lipids as well as the effect of the presence of these lipids on structural transitions and fibril formation: A common, V3-like sphingolipid-binding domain could be detected that allows interaction of PrP with galactosyl cerebroside and sphingolipids (Mahfoud *et al*., 2002). This and other works suggest that the interaction of PrP with sphingolipid-rich membrane fractions, i.e. rafts, caveolae-like domains or artificial raft-like liposomes stabilizes PrP in its normal, cellular isoform (Naslavsky *et al*., 1999; Baron & Caughey, 2003; Sanghera & Pinheiro, 2002). To the contrary, depletion of cholesterol leads to a reduction of PrP^{Sc}-levels (Taraboulos *et al*., 1995). Taken together the mentioned data suggests that there are a number of factors involved in structural transition and fibril formation for PrP.

Earlier investigations in our group have demonstrated that it is possible to induce the reverse reaction, i.e. a structural transition from a PrP^{Sc}-like to a PrP^{C}-like form *in vitro*: The PrP^{Sc}-like PrP 27-30 from prion rods purified from brains of scrapie-infected hamsters can be solubilized by treatment with 0.2 % SDS followed by sonication (Riesner *et al*., 1996). The resulting preparations of solubilized PrP 27-30 designated sol PrP 27-30 showed ~10 % of the infectivity of the starting material, i.e. PrP 27-30. Reconstitution experiments aiming at creation of *de novo* infectivity with preparations of sol PrP 27-30 were carried out *in vitro* by diluting the SDS in the samples from 0.2 % to 0.01 %. This treatment resulted in gain of partial PK-resistance, induction of a β-structure and formation of amorphous aggregates as revealed by electron microscopy (Post *et al*., 1998). However, bioassays revealed that the newly formed aggregates from sol PrP 27-30 did not show a significantly increased infectivity in comparison to untreated, tetra- to hexameric sol PrP 27-30: The infectivity levels increased by no more than 1 log ID_{50}/ml which lies within the inaccuracy of a bioassay. To verify

whether this increase in infectivity-levels was generated *de novo*, the background infectivity as measured for sol PrP 27-30 needed to be abolished. Only when infectivity can be measured following reconstitution experiments that start from non-infectious material one can be sure that this infectivity was generated *de novo*. To abolish the background infectivity of sol PrP 27-30, the solubilization procedure for PrP 27-30 was extended by elution of sol PrP 27-30 from SDS polyacrylamide gelelectrophoresis (SDS-PAGE). This extra step yielded the PrP^{C}-like, solubilized, gel-eluted PrP 27-30 designated elu PrP 27-30: Elu PrP 27-30 is monomeric, has a mainly α-helical secondary structure, is sensitive to PK-digestion and is not infectious (cf. Figure 1.7) (Leffers 1999). Elu PrP 27-30 is suitable for reconstitution experiments: Measuring low levels of infectivity following reconstitution of the PrP^{C}-like elu PrP 27-30 to a PrP^{Sc}-like form would be a clear, self-evident sign of *de novo* infectivity generated *in vitro*. This would immediately proof the "*protein-only*"-hypothesis and is therefore one of the major aims of this study.

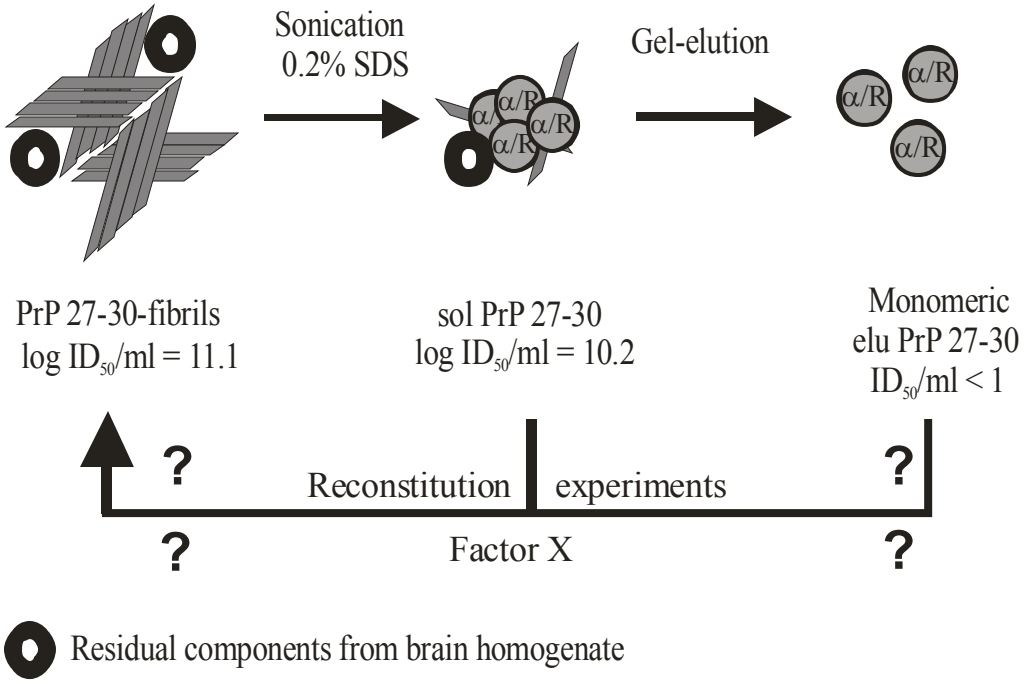

Figure 1.7: *in vitro* conversion of PrP 27-30. The PrP^{Sc}-like PrP 27-30 from prion rods of scrapie-infected hamsters can be solubilized by treatment with 0.2 % SDS and following sonication. The resulting sol PrP 27-30 reveals background infectivity which can be abolished by elution of the protein from SDS polyacrylamide gelelectrophoresis. This procedure yields the PrP^{C}-like elu PrP 27-30.

1.8 Aims of this thesis

Generation of *de novo*-infectivity *in vitro* would be the final proof of the "*protein-only*"-hypothesis. Preparations of PrP from brains of animals infected with a prion disease that contain amyloid fibrils reveal high levels of infectivity. This observation resulted in the design of countless *in vitro*-experiments that aimed at *de novo* generation of amyloid fibrils and infectivity starting from PrP^{C}-like isoforms of the prion protein. Also the basic understanding of the conversion process from PrP^{C} to PrP^{Sc} and identification of all factors involved is of major interest. Assuming that the "*protein-only*"-hypothesis is correct, it should be possible to generate *de novo*-infectivity *in vitro* by induction of a structural transition from PrP^{C} to PrP^{Sc}.

In the studies preceding this study an SDS-dependent *in vitro* conversion system was established that allowed induction of amorphous aggregates from low-infectious, solubilized PrP 27-30 by dilution of the SDS present in the samples (cf. above). Furthermore a procedure was established that allowed elimination of the background-infectivity of sol PrP 27-30 by elution from SDS-PAGE resulting in elu PrP 27-30. The main objective of this study was to induce transitions starting from this non-infectious, PrP^{C}-like conformation to a PrP^{Sc}-like conformation including formation of amyloid fibrils. These newly formed amyloid fibrils could then be tested for generation of *de novo* infectivity *in vitro*.
The desired transitions were studied for various forms of PrP including
a.) recombinant (rec) PrP (90-231),
b.) solubilized, gel-eluted PrP 27-30 designated elu PrP 27-30 from brains of hamsters infected with 263K hamster-adapted scrapie and
c.) natural, full length PrP^{C} from brains of uninfected Syrian Golden Hamsters.

All these forms of PrP have in common that they are free of infectivity. Thus, if bioassays of these forms would reveal measurable infectivity, it would be self-evident that this infectivity would have been generated *in vitro* and *de novo* (cf. above).
Apart from this property, the named forms of PrP differ in various ways:
Since rec PrP (90-231) lacks posttranslational modifications, i.e. it carries neither a GPI-anchor nor the two N-glycosylations mentioned above it could be studied whether these modifications are necessary for fibril formation of PrP. Also rec PrP (90-231) and elu PrP 27-30 only consist of amino acids 90-231 of the prion protein which resembles the PK-resistant

core of infectious PrP. Hence, in comparison to natural, full length PrP^C the role of the first 89 amino acids in fibril formation could be studied.

To keep PrP solubilized, SDS was used also revealing some membrane-like characteristics. SDS does not chemically modify PrP; hence the "correct" structure for PrP^C or PrP^{Sc} should always be in the range of inducible structures. Since other studies have shown that SDS can not only be used to solubilize PrP, but also allows induction of various intermediate structures depending on the concentration of SDS added to a sample (Jansen *et al*., 2001), this interaction was further investigated.

Moreover, the role of sodium chloride in transition and aggregation processes of PrP was investigated since it has been shown before and during this study that when sodium chloride is added to PrP in concentrations that are close to the physiological, extracellular concentration of 150 mM, slow aggregation including fibril formation is induced (Jackson *et al*., 1999; Swietnicki *et al*., 2000; Baskakov *et al*., 2001; Xiong *et al*., 2001).

One of the consequences of working with conditions close to the *in vivo* situation meant working at neutral pH, since PrP^C is enriched at the cell surface in raft- or caveolae-like domains (cf. above). These domains are enriched with lipids like sphingomyelin, galactosyl cerebroside and cholesterol which are also found in prion rods (Klein *et al*., 1998); therefore the role of these lipids in fibril formation was investigated.

In summary this work focused on two major subjects:

1.) The influence of a number of factors on the structural transition from a PrP^C-like to a PrP^{Sc}-like state and on fibril formation was investigated. These factors include protein modifications and secondary components like SDS, sodium chloride and lipids. The effect of these factors was investigated over various incubation times with the aim to derive a general model for a mechanism for fibril formation of the prion protein *in vitro*.

2.) If aim number 1.) can be achieved the newly, *in vitro* generated fibrils should be analyzed in regard to the other typical markers associated with the transition of the prion protein from PrP^C to PrP^{Sc}, i.e. PK-resistance and infectivity. The latter was determined in bioassays to evaluate whether factors affecting fibril formation can also lead to generation of *de novo* infectivity in this *in vitro* conversion system.

2. Materials & Methods

2.1 Chemicals

If not stated otherwise, chemicals were of the highest purity grade available and obtained from regular commercial suppliers.

2.2 Lipids

The composition of the residual lipids in prion rods has been previously analyzed (Klein *et al*., 1998). For the current experiments, the sphingomyelin found was purchased from Sigma (St. Louis, Missouri) and the cerebrosides were purchased from Avanti Polar Lipids (Alabaster, Alabama). Cholesterol was purchased from Sigma. Lipids extracted from prion rods were not used in the experiments.

2.3 Samples of sol PrP 27-30, rec PrP (90-231) and native, full length PrP^C

PrP 27-30 from brains of scrapie-infected Syrian Gold Hamsters was prepared as described elsewhere (Prusiner *et al*., 1983). In the last step of this protocol the protein was purified through a discontinuous sucrose gradient ultracentrifugation ranging from 25 % to 56 % sucrose. The infectious material was regularly found in fractions of 40 % to 52 % sucrose. The samples were stored at -70 °C. Solubilized PrP 27-30 was obtained by sonication of 1mg/ml PrP 27-30 in 10 mM HEPES pH 7.2 / 0.2 % SDS (Riesner *et al*., 1996). Sonication was carried out with a Bandelin HD 2070 sonicator (Bandelin Electronic, Berlin). The probe was immersed in the sample and the power setting was fixed to 65%. The samples were kept on ice and sonicated for 15 seconds at 65 % power followed by a one minute pause to cool down the sample. These cycles were repeated 11 times. Subsequent centrifugation in a TL-100 ultracentrifuge (Beckman Instruments, USA) using the swinging bucket rotor TLS-55 for 2 h at 210,000 x *g* at 4 °C served to separate the soluble PrP 27-30 from the insoluble pellet

fraction. The concentration of PrP in the supernatant denoted ‘sol PrP 27-30’ was determined by amino acid analysis (Jones *et al*., 1986) to be about 125 µg/ml.

Recombinant Syrian Golden Hamster Prion Protein denoted SHa rec PrP (90-231) was expressed and purified as described (Jansen *et al*., 2001; Mehlhorn *et al*., 1996). The lyophilised protein was adjusted to a concentration of 5 mg/ml in distilled water and then unfolded by incubation in 6 M guanidinium hydrochloride (GdnHCl) for 30 minutes. Refolding of the protein was carried out by fast dilution of the GdnHCl with 25 mM Tris/acetate pH 8.0 / 5 mM EDTA down to 0.6 M and a protein concentration of 0.5 mg/ml. Afterwards the buffer was exchanged to the buffer needed in the respective experiment by centrifugation in Amicon tubes (Amicon Inc., Beverly, MA, USA).

PrP^C from brains of uninfected hamsters was provided by Dr. Keh-Ming Pan, UCSF; it was prepared as described (Pan *et al*., 1993).

2.4 Commonly used solutions and buffers

NaP_i (Sodium Phosphate buffer)

100 mM Disodiumhydrogenphosphate (Na_2HPO_4) and

100 mM Sodiumdihydrogenphosphate (NaH_2PO_4)

were mixed to achieve the desired pH-value. If not stated otherwise the buffer was used at a final concentration of 10 mM at pH 7.2.

HEPES (N-[2-Hydroxyethyl]piperazine-N’-[2-ethansulfonic acid])

100 mM HEPES was adjusted to pH 7.2 using NaOH and unless stated otherwise used at a final concentration of 10 mM.

TBS-T (Tris Buffered Saline, Tween)

10 mM Tris/HCl pH 8.0

150 mM NaCl

0.01 % Tween 20

PBS (Phosphate Buffered Saline)

10 mM	Potassium phosphate pH 7.0
150 mM	NaCl

Acrylamide stock solution

30 %	Acrylamide (600 g)
0.8 %	N, N'-bisacrylamide
ad 2 l	distilled water

The solution was stirred for at least 30 minutes after addition of amberlite MB3 (ionic exchanger), filtered and stored at 4°C.

2.5 Protein gel electrophoresis (SDS-PAGE)

Protein gel electrophoresis was carried out in a Hoefer SE 600 chamber by Amersham Pharmacia Biotech (San Francisco, USA) according to the protocol of Laemmli (Laemmli *et al*., 1970). Gel electrophoresis was carried out in 1x Laemmli buffer in the presence of 0.1 % SDS for 30 minutes at 180 V followed by approximately 90 minutes at 220 V or until the bands had reached the desired position in the gel. As marker the "Benchmark Prestained Protein Ladder" (Gibco BRL, USA) was used.

10 x gel electrophoresis buffer (10 x Laemmli buffer)

1.9 M	Glycine (288 g)
0.25 M	Tris (60 g)
ad 2 l	distilled water

pH will adjust to 8.3

Running gel (12 %)

380 mM	Tris/HCl pH 8.8
12 %	Acrylamide/Bisacrylamide (30:0.8)
0.1 %	SDS
0.1 %	TEMED
0.1 %	APS

Stacking gel

124 mM	Tris/HCl pH 6.8
3 %	Acrylamide/Bisacrylamide (30:0.8)
0.1 %	SDS
0.1 %	TEMED
0.1 %	APS

Sample buffer (2x)

62.5 mM	Tris/HCl pH 6.8
5 %	SDS
10 %	Glycerol
0.016 %	Bromphenolblue

2.6 Dot-blot

When carrying out a dot-blot procedure the protein is directly applied to a polyvinylfluoride-(PVDF-) membrane (Millipore GmbH, Neu Isenburg, Germany) using a weak vacuum. The device allows processing of 96 samples at the same time (S & S Minifold I, Schleicher & Schuell, Dassel, Germany). After moistening the PVDF-membrane with ethanol it was shortly equilibrated in TBS-T pH 8.0 along with a sheet of Whatman paper (Whatman 3 MM Chr). The device was then assembled by putting the Whatman paper on top of the lower chamber, then the PVDF-membrane and then the 96-well cover on top. Samples of 100 µl volume were applied to the slots under a weak vacuum. Then the slots were washed twice using distilled water and a slightly increased vacuum. Detection of the protein was carried out using the monoclonal antibody 3F4 (UCSF, San Francisco, USA). Since 3F4 only recognizes denatured protein, the membrane was incubated for five minutes in 1 % KOH and then briefly washed in TBS-T prior to the immunologic reaction (cf. 2.8).

2.7 Semi-dry-blot

This technique allows transfer of proteins from SDS-PAGE to a PVDF-membrane. After gel electrophoresis the polyacrylamide gel is briefly incubated in 1x gel electrophoresis buffer (cf. 2.5) without SDS along with 6 sheets of Whatman paper and the PVDF-membrane that was moistened with ethanol prior to equilibration in 1x gel electrophoresis buffer. Then the "Semi-Dry Electrophoretic Transfer Cell" (Biorad, Hercules, USA) was assembled as follows (from + to -): Three sheets of Whatman paper, PVDF-membrane, polyacrylamide gel and again three sheets of Whatman paper. Transfer was carried out for 45 - 60 minutes at 1.5 mA/cm² and a maximum of 25 V. Then the protein was detected using an immunologic reaction (cf. 2.8).

2.8 Immunologic protein detection

The immunologic detection of PrP was carried out using the PrP-specific primary antibody 3F4 (Kascsak *et al*., 1987). PVDF-membranes with bound proteins after dot-blot or semi-dry-blot treatment were incubated in TBS-T pH 8.0 containing 5 % milk powder (Frema-Reform, DE-VAU-GE, Lüneburg, Germany) for 1 - 2 h at room temperature (optional: overnight at 4°C) to block unspecific protein binding sites on the PVDF-membrane. After washing the membrane briefly in TBS-T pH 8.0 it was incubated with the primary antibody 3F4 (1:10,000 in TBS-T pH 8.0) for 1 - 2 h at room temperature or overnight at 4 °C. Then the membrane was washed twice in TBS-T pH 8.0 for 10 minutes each step and afterwards incubated in the secondary antibody SaM-PO (sheep-anti-mouse-Ig G-antibody labeled with horseradish-peroxidase; Amersham Pharmacia Biotech Europe GmbH, Freiburg, Germany) at a dilution of 1:5,000 in TBS-T pH 8.0 for 1 - 2 h at room temperature. Antibody that did not bind to 3F4 was washed out in three steps using TBS-T pH 8.0 for 10 minutes each. Detection was carried out using a chemoluminescence reaction: The detection reagent contains luminol, which is oxidized by the peroxidase that is coupled to the secondary antibody. This reaction releases energy in the form of light. The membrane was incubated with the detection reagent kit ECL (Amersham, Freiburg, Germany) for one minute. The emission of light lasts for approximately one hour. To make the protein visible, the membrane was exposed to x-ray film (Hyperfilm, Amersham, Freiburg, Germany) for approximately 15 - 30 seconds.

2.9 Differential ultracentrifugation

The solubility of the prion protein under a given condition was determined according to the standards of Hjelmeland and Chrambach (Hjelmeland & Chrambach, 1984), defining that particles that remain in the supernatant after a 100,000 x *g* spin for 1 h are regarded as soluble. When a sample was prepared that contained SDS it was important to adjust the SDS-concentration to the final value before adding the protein. Samples were incubated with SDS and analyzed by centrifugation. Pellets were resuspended in sample buffer (cf. 2.5) and the relative amounts of protein in supernatant and pellet were determined by dot-blot or semi-dry-blot.

2.10 Gel-elution of prion proteins and dialysis

Proteins can be recovered from SDS-PAGE in high yields (Jacobs & Clad, 1986) using the S&S Elutrap Electro-Separation System (Schleicher & Schuell, Keene, USA): Following SDS/PAGE using 10 µg PrP per slot the area ranging from 14 - 35 kDa was cut from the gel and cut into small pieces for optimal elution results. Each elution chamber was filled with gel-pieces resulting from two slots corresponding to 20 µg PrP. The tank-buffer used for elution was 1x Laemmli Tris-Glycine containing 0.025 % SDS. The gel pieces were eluted at 200 V for 7 h. Since the PrP-molecules are saturated with SDS they have a negative total charge and could be collected from a trap which is bordered by two membranes (cf. Figure 2.1): The membrane designated BT 2 allows entry of protein molecules into the trap whereas the membrane designated BT 1 keeps the proteins from leaving the trap with an exclusion size of 5 kDa. The BT 2-membrane keeps gel particles from entering the trap. At the end of each elution the polarity of the chamber was inversed for 30 seconds to release protein molecules that stuck to the BT 1-membrane. Volumes of eluates ranged from 500-800 µl. Afterwards the buffer of the eluate was changed to the buffer needed in each respective experiment by carrying out a dialysis for 48 h using 3 ml Slide-A-Lyzer cassettes with an exclusion size of 10 kDa (Pierce, Rockford, USA) against 1 liter of the desired buffer which was frequently exchanged.

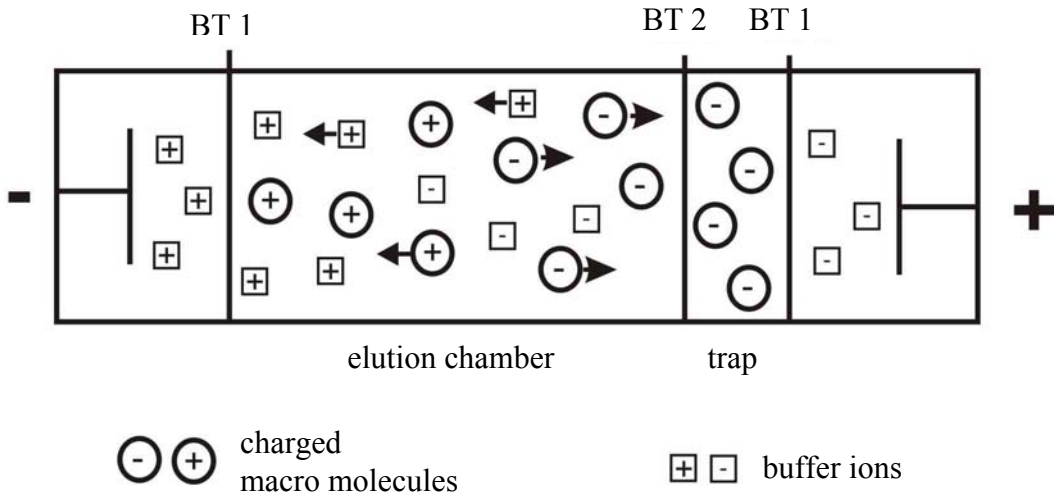

Figure 2.1: Schematic picture of an elution chamber.

2.11 Circular dichroism

Chiral substances like most asymmetric carbon atoms are optically active. This activity results in interactions with linear polarized light: The circular polarized components that add up to a linear polarized wave are not equally absorbed by optical active substances indicating that the absorption coefficients for the two circular polarized components differ from each others. When analyzing the secondary structure of a protein by CD-spectroscopy, the difference between these two coefficients in the region of far UV (170 nm – 260 nm) is measured. This analysis allows differentiation of typical secondary structure elements for proteins, i.e. α-helices, β-sheets or β-turns (cf. Figure 2.2). When a protein contains more than one of these elements, a mixed spectrum results that allows conclusions with regard to the structural elements that are present. For CD-spectroscopy the Spectropolarimeter J715 (Jasco, Labor- und Datentechnik GmbH, Groß-Umstadt, Germany) was used. The cuvettes (Helma, Muehlheim, Germany) had a 1 cm pathlength. The minimum concentration for a protein sample was 10 ng/µl with a total volume of 80 µl. During measurements the sample-chamber was flooded with 8 l gaseous nitrogen per minute. Spectra were measured at room temperature from 195 - 260 nm at a resolution of 1 nm and a response time of 4 seconds. Per sample five to ten spectra were measured, averaged and corrected using the respective buffer spectrum.

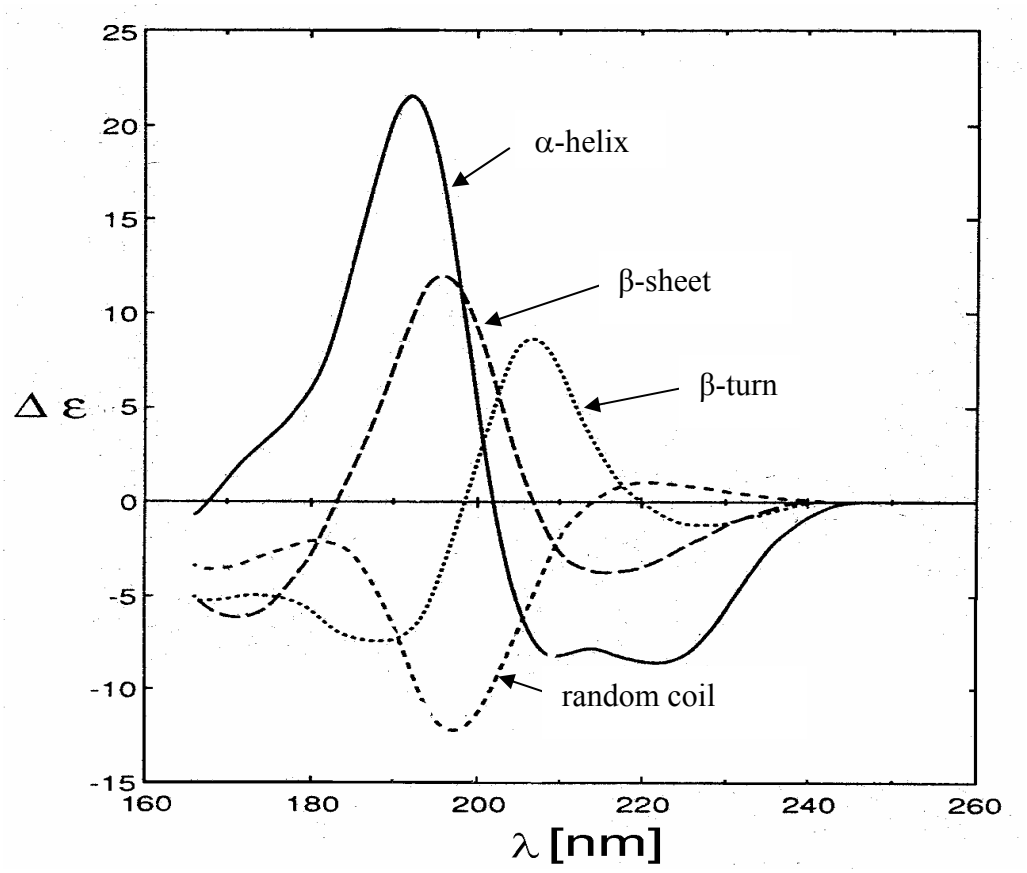

Figure 2.2: CD-spectra of typical elements of secondary structure of proteins. Modified after Brahms & Brahms, 1980.

2.12 Measuring the binding of SDS to PrP with the Methylen Blue binding assay

The assay was modified from a protocol to determine the amount of molecules of SDS bound to proteins (Reynolds & Tanford, 1970) and applied to determine the number of molecules of SDS bound to PrP at low concentrations of SDS (≤ 0.01 %). An excess of Methylen Blue was added to a protein-free, aqueous solution of SDS. The resulting SDS/Methylen Blue-complex was extracted into an organic chloroform-phase. The optical density of the chloroform-phase at 655 nm in comparison to a blank sample that did not contain SDS allowed generating a calibration curve. To determine the amount of protein-bound SDS in a sample this procedure

was modified as follows: rec PrP (90-231) (100 ng/µl) in 10 mM NaP_i pH 7.2 at SDS-concentrations between 0 – 0.01 % SDS was incubated at 25°C overnight. Under these conditions the protein binds a certain amount of SDS and most if not all of the protein aggregates. To remove the aggregated protein-SDS complex from the sample, a 100,000 x *g* spin was carried out. Then 1 ml Methylen Blue and 4 ml chloroform were added to 10 µl of the supernatant. After vortexing the sample for 15 seconds all of the SDS in the supernatant formed SDS/Methylen Blue complexes and was extracted to the chloroform-phase. The absorption of the chloroform-phase was recorded at 400 - 700 nm exactly 1 minute after filling the cuvette. The concentration of SDS in the supernatant of the original sample was then calculated by comparison of the A_{655}-value with the calibration curve, and the amount of SDS that pelleted with the aggregated protein could be determined.

2.13 Modified Hill plot

In order to evaluate the amount of cooperative SDS binding to PrP within the transition from a PrP dimer to a PrP oligomer, the Hill equation had to be modified. A similar modification was derived earlier by Jansen et al. (Jansen *et al*., 2001) for a dimer-tetramer transition. Since the oligomeric state was determined as a 12 - 16mer (Jansen 2002), the corresponding equation had to be derived. It should be noted, that unfortunately several misprints were present in the earlier derivation but the final equation used for the fit to the experimental data was correct. The reaction mechanism is assumed as: A transition from dimers (PrP_2) with n molecules of SDS bound ($PrP_2 \cdot SDS_n$) to a dodecamer PrP_{12} results in the cooperative release of 6 n SDS in the reaction:

$$6\,(PrP_2 \cdot SDS_n) \overset{K}{\leftrightarrow} PrP_{12} + 6\,n\,SDS$$

The degree of transition as calculated from the transition curve in Fig. 3.2 is:

$$\theta = \frac{12\,[PrP_{12}]}{12\,[PrP_{12}] + 2\,[PrP_2 \cdot SDS_n]} = \frac{12\,[PrP_{12}]}{PrP_o}$$

with $\theta = 1$ for the β-structure PrP at 0.03% SDS, and $\theta = 0$ for the α-helical PrP at 0.06% SDS, total PrP = $PrP_0 = 2\,[PrP_2 \cdot SDS_n] + 12\,[PrP_{12}]$, and total SDS = $SDS_0 = n\,[PrP_2 \cdot SDS_n] + [SDS_f]$ where SDS_f = free SDS.

The resulting equilibrium constant K for cooperative binding or release, respectively, of 6 n SDS together with the dimer dodecamer transition of PrP, is:

$$K = \frac{[PrP_2 \cdot SDS_n]^6}{[PrP_{12}] \cdot [SDS]^{6n}}$$

Inserting the expression for θ, PrP_0 and SDS_f yields the modified Hill plot:

$$6 \log (1-\theta) - \log (\theta = 6n \log [SDS_f] + \log \frac{K}{PrP_0^5} + \log \frac{16}{3}$$

2.14 Proteinase K assays

Two different protocols were used for proteinase K assays: For limited proteolysis PrP was incubated with proteinase K at a ratio of 3:1 (m/m) for 5 minutes at 25 °C. The reaction was then stopped by adjusting the sample to 7.5 mM PMSF. The degree of digestion was then determined by comparing the sample to an undigested control-sample on a western blot using antibody 3F4.

For standard proteinase K digestion PrP was incubated with proteinase K at a ratio of 1:25 (m/m) for 1 h at 37 °C. The reaction was then stopped by adjusting the sample to 1.5 mM PMSF. Again the degree of digestion was determined by comparing the sample to an undigested control-sample on a western blot using antibody 3F4.

2.15 Electron microscopy

To analyze the structure of protein aggregates transmission electron microscopy (TEM) was carried out using a Philips / FEI Tecnai F20 electron microscope. This microscope uses a field emission gun as electron source (cathode). When the cathode is heated up, electrons can be extracted and accelerated by an anode using a voltage of routinely 80 - 100 kV. The anode has a central hole that allows an electron beam to pass through. Then the electrons pass two condenser lenses to focus the beam on the level of the specimen. Lenses are generally composed of spools that generate electromagnetic fields when electric currents are applied. After passing these condenser lenses the electrons pass through the specimen in three different ways: Unaffected, scattered without loss of energy (elastic deflection) or scattered with loss of energy (inelastic deflection). The different scattering angles produce a contrasting image because all angles scattered more than 0.5 degrees are stopped by an objective aperture (cf. Figure 2.3) situated below the specimen. The following intermediate lens and projective lens increase the resulting magnification of the picture that can be observed on a fluorescence screen or documented using x-ray films or a digital camera. The brightness of the image of each region will be proportional to the number of unscattered electrons which pass through the aperture. Therefore, light atoms, such as carbon, will appear light while heavier atoms like iron will appear darker. This phenomenon is the basis of the negative staining techniques as used here (cf. 2.15). Generally phases, fractures and other properties that are 2 to 3 angstroms across can be seen. Biological samples normally don't allow higher resolutions than 1 nm. Electron microscopes require a high vacuum to exclude interactions of the electron beam with anything else but the specimen itself like gas molecules, etc.

Usually 200 mesh formvar/carbon-coated nickel grids (Ted Pella, Inc., USA) were used as specimen holder. These were glow discharged prior to use to make the surface hydrophilic and to allow adsorption of macromolecules from the sample solution.

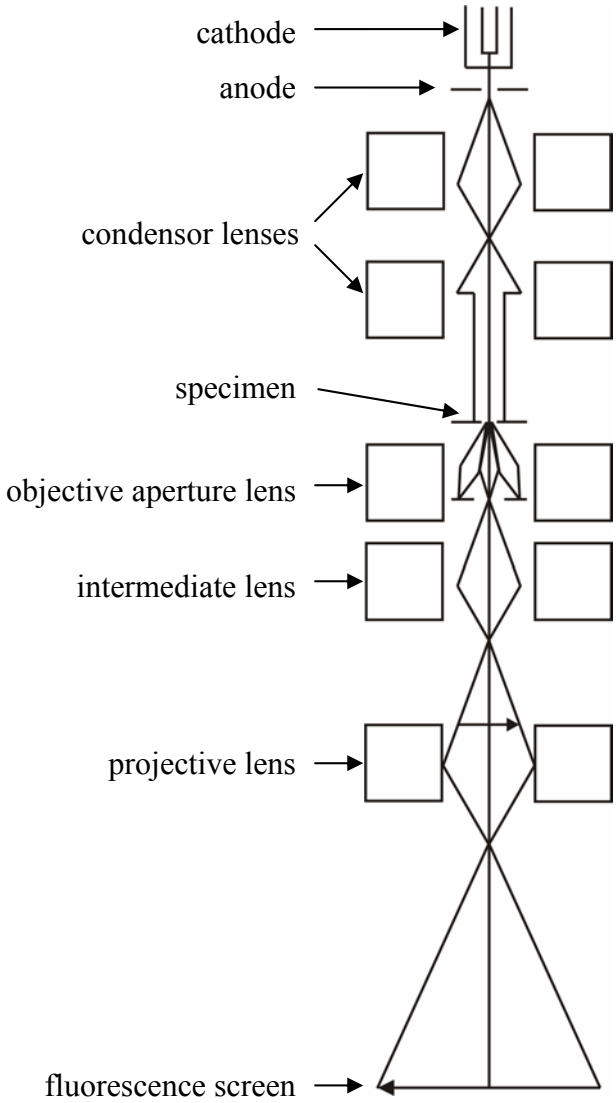

Figure 2.3: Schematic picture of an electron microscope.

2.16 Negative stain and immunolabeling

To visualize protein molecules and aggregates, the negative staining procedure was applied using ammonium molybdate. This heavy metal salt is especially well suited for staining of membranes and fibrillar proteins. Additionally PrP was immunolabeled using the antibody huFab D18 (Williamson *et al*., 1996; Williamson *et al*., 1998; Peretz *et al*., 1997) to prove the PrP-content of the observed structures. For this purpose the following protocol was applied: 200 mesh formvar/carbon-coated nickel grids (Ted Pella, Inc., USA) were glow discharged prior to immunolabeling. Samples of 5 µl were adsorbed for 1 - 2 minutes and then briefly

washed with 0.1 M and 0.01 M ammonium acetate (pH 7.4). The washing solution is partially removed from the grids and afterwards the grids were blocked by placing them on a droplet of 1 % BSA in HEPES buffered saline (HBS: 10 mM NaHEPES pH 7.2, 150 mM NaCl, 0.1 M NaN_3) for 90 minutes. The grids were then briefly washed in HBS and incubated on a droplet containing the primary antibody huFab D18 in 0.1 % BSA in HBS for 2 h at room temperature or overnight at 4 °C. Then the grids were again briefly washed in HBS and incubated on a droplet containing the secondary antibody α-hu Ig G (mouse, whole antibody, Jackson Laboratory, Maine, USA) in 0.1 % BSA in HBS for 2 h at room temperature. Then the grids were briefly washed in HBS and incubated on a droplet containing 10 nm gold particles coupled to protein A molecules in a 1:1 anticipated ratio in 0.1 % BSA in HBS for 1 h. Protein A gold was obtained from J. Griffiths (Utrecht University Medical School Department of Cell Biology). After another brief washing step in HBS the material was fixed by incubation with 2.5 % glutaraldehyde for five minutes. Finally the grids were briefly washed in H_2O and negatively stained for a few seconds with freshly filtered 2 % (w/v) ammonium molybdate. The staining solution is removed from the grid with filter paper and the dried samples were then viewed in a Philips / FEI Tecnai F20 electron microscope at 80 kV and standard magnifications of 25,000 and 40,000, respectively.

2.17 Bioassays

Bioassays were performed by inoculating 30 µl samples intracerebrally into transgenic mice overexpressing PrP^C of Syrian Golden Hamsters (SHa PrP^C) approximately 8-fold compared to Syrian Hamsters (Scott *et al*., 1997b). The Tg ($SHaPrP^{+/+}$) 7 *PrnP* $^{0/0}$ mice are homozygous for the SHa PrP transgene array and were crossed onto a mouse-PrP deficient background (Bueler *et al*., 1992). Samples were diluted 10-fold into phosphate-buffered saline with 5 mg/ml bovine serum albumin as a carrier. Prion titers were calculated by measuring the incubation time intervals from inoculation to onset of neurological illness. The equation used was derived from 12 independent end-point-titration experiments with Tg ($SHaPrP^{+/+}$) 7 *PrnP* $^{0/0}$ mice overexpressing $SHaPrP^C$ (Prusiner *et al*., 1999):

$\log ID_{50}/ml = 3680 * x^{-1.622}$ with x = incubation time in days and

$1\ ID_{50}$ = **i**nfectious **d**ose that is sufficient to infect 50 % of inoculated mice

Plotting the end-point titer against the incubation time allows to calculate a calibration curve (cf. Figure 2.4):

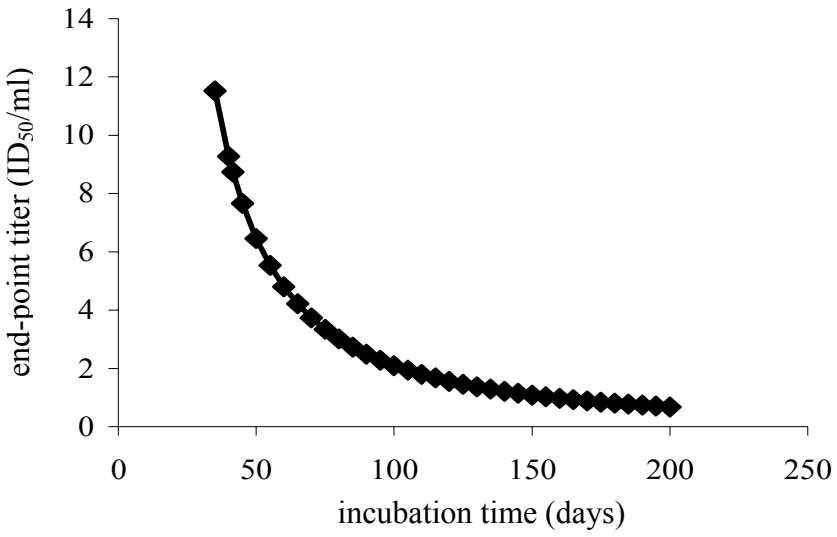

Figure 2.4: Calibration curve for the Sc 237 isolate of hamster scrapie prions in Tg (SHaPrP$^{+/+}$) 7 *PrnP* $^{0/0}$ mice. The mice exhibit an minimum incubation time of 45 days when infected with scrapie. The experiments were terminated 200 days after inoculation and the endpoint titer was calculated by the method of Spearman and Karber (Dougherty *et al*., 1964). Bioassays were carried out by Edna Kiyono and coworkers at the Hunters Point animal facility, UCSF.

3. Results

The prion hypothesis stipulates that PrP^{Sc} induces a structural transition in host-PrP^{C} to form new PrP^{Sc}. This transition process is followed by aggregation of PrP^{Sc}. Quantitative biophysical studies on the transition process, such as structural studies by CD-spectroscopy, require the protein in a soluble form. It was shown previously that solubilization of PrP 27-30 requires a treatment with e.g. the partially denaturing detergent SDS followed by sonication (Riesner *et al*., 1996). But SDS not only solubilizes PrP 27-30 to sol PrP 27-30, it also has the ability to induce structural transitions in the prion protein (Post *et al*., 1998; Jansen *et al*., 2001). Since the main aim of this study was to create an *in vitro* conversion system that mimics the *in vivo* conformational transition and subsequent aggregation, the ability of SDS to induce such structural transitions was investigated further: In detail, it was the aim to find conditions can that induce reversible structural transitions in the prion protein that lead to β-structured intermediates which are prone to slow, highly ordered aggregation.

3.1 SDS Induced, Structural Transitions of PrP

The first series of studies was carried out with rec PrP (90-231). This recombinant form of the prion protein has the same amino acid sequence as PrP 27-30, but lacks the GPI-anchor and the N-linked carbohydrates. Since it is available in bigger amounts than e.g. PrP 27-30, studies are often carried out with rec PrP (90-231) to investigate the basic principles of the structural transitions of PrP. Earlier studies on intermediates of prion refolding using an SDS-dependent *in vitro* conversion system with rec PrP (90-231) revealed a three step transition process: At 0.2 % SDS, rec PrP (90-231) is in a monomeric, soluble and mainly α-helical state. When SDS is diluted to 0.01 % SDS, several consecutive transitions occur. These transitions include as intermediates a soluble, α-helical dimer at ~0.06 % SDS, a soluble, β-structured oligomer composed of 12-16 PrP-molecules at ~0.04 % SDS and finally insoluble, β-structured multimers are reached at 0.01 % SDS (Jansen, 2002). These transitions are reproducible and reversible; only the SDS-concentration at which the transitions occur may vary by ~0.01 % when a new batch of protein is used. Most probably this variability is due to residual detergent in the protein preparations, which then influences the free SDS-

concentration, particularly in the low range. To compensate for this variability it was necessary to reproduce the transition curve and to determine the exact SDS-range at which the respective intermediates occur for each protein preparation.

The first aim of this study was to investigate the reversibility of the transition process described above from a PrP^{C}-like to a PrP^{Sc}-like form of rec PrP (90-231) as induced by SDS. In particular, the effect of diluting the SDS-concentration, as described before (Jansen, 2002), was compared with the effect of increasing the SDS-concentrations starting from pure aqueous buffer.

3.1.1 Structural transition of rec PrP (90-231) from a predominantly α-helical to a β-structured state induced by dilution of SDS

When rec PrP (90-231) is solubilized in 10 mM NaP_i pH 7.2 / 0.2 % SDS and analyzed by CD-spectroscopy, it reveals a mixture of α-helical and random coil structure (cf. Figure 3.1).

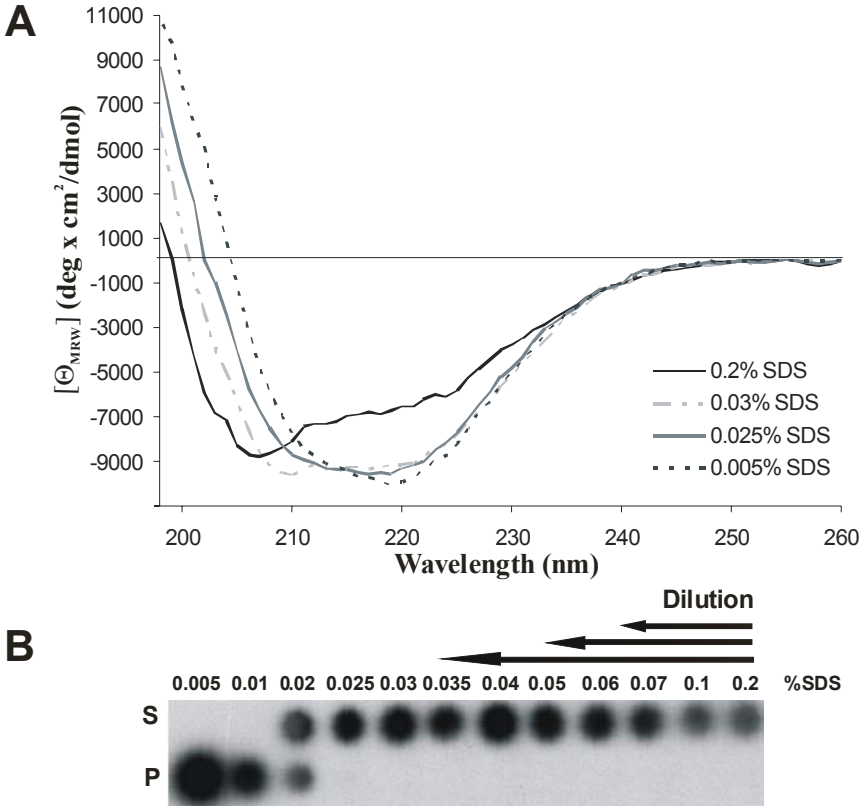

Figure 3.1: Structural transition and solubility of rec PrP (90-231) as induced by dilution of SDS. Rec PrP (90-231) at 1 mg/ml was solubilized in 10 mM NaP_i pH 7.2/0.2 % SDS. The SDS was then diluted to the concentrations shown at a final protein concentration of 20 ng/µl. **(A)** The secondary structure was analyzed by CD-spectroscopy directly after diluting the SDS, **(B)** solubility after an additional 1 h 100,000 x *g* ultracentrifugation and separation of supernatant (S) and pellet (P).

The SDS concentration was then diluted from 0.2 % down to the concentrations shown in Fig. 3.1 A and Fig. 3.1 B. Afterwards, a structural analysis was carried out as fast as possible given the respective experimental procedures, i.e. CD measurements within about 20 minutes and a solubility analysis using differential ultracentrifugation within one hour. It is evident from the CD-spectra that down to 0.03 % SDS the extent of α-helices increases and that the amount of random coil decreases. Below 0.03 % SDS the spectrum shifts to one characteristic of a β-structured conformation. From the dot blot analysis in Fig. 3.1 B it is seen that the β-structured conformation down to 0.02 % SDS is soluble and that below 0.02 % SDS it is in an aggregated state. Hence, the transition includes a soluble, β-structured intermediate at 0.025 % SDS (cf. Figure 3.1).

Collecting CD-spectra of rec PrP (90-231) over a range of SDS-concentrations allows to calculate a transition curve: When the ratio of the CD-signals at 218 nm (characteristic for β-structures) and 207 nm (characteristic for mainly α-helical structures) is plotted against the SDS-concentration, the structural transition of the protein can be followed (cf. Figure 3.2). Transition curves of otherwise identical samples but with e.g. different incubation times can easily be compared: A prolonged incubation of 24 h for the same samples as used above at 25°C results in a shift of the transition curve to higher SDS-concentrations (cf. Fig. 3.2):

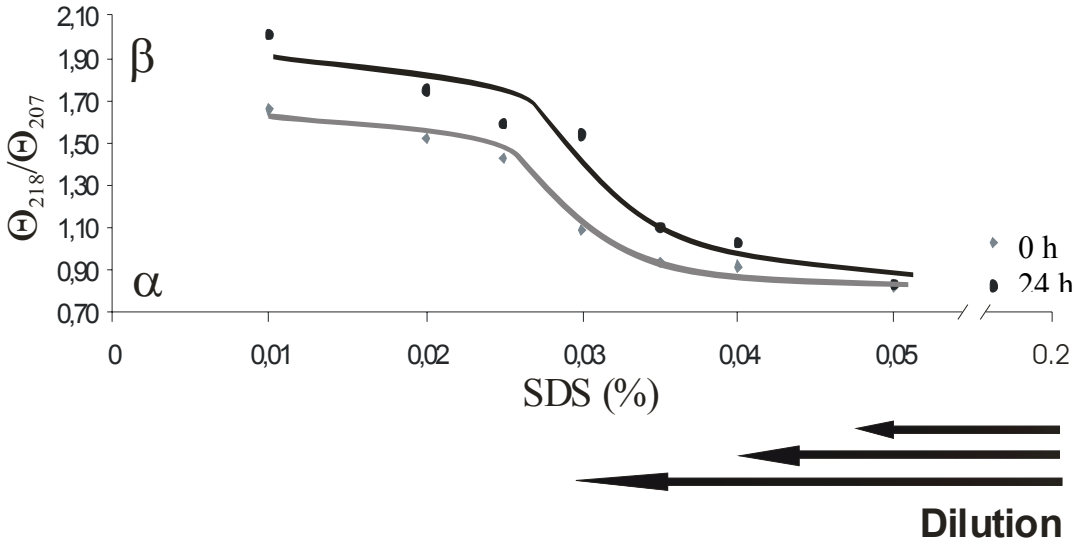

Figure 3.2: Slow formation of β-structure at intermediate SDS-concentrations. Rec PrP (90-231) at 1mg/ml was solubilized in 10 mM NaP_i pH 7.2 / 0.2 % SDS. The SDS was then diluted to the concentrations shown at a final protein concentration of 20 ng/µl. CD-spectroscopy was carried out either directly after dilution of the SDS or after 24 h at 25°C. High values of $\Theta_{218}/\Theta_{207}$ indicate a β-structured conformation whereas low values indicate a mainly α-helical structure.

The increase of the $\Theta_{218}/\Theta_{207}$-value over 24 h at intermediate SDS-concentrations (0.02 % - 0.05 %) indicates that formation of the β-structure is slow at these conditions, i.e. takes more than 30 minutes. In earlier studies the approach to the equilibrium between the α-helical and the β-structured state was observed at 0.0275 % SDS. This was achieved by frequently measuring the ratio of $\Theta_{218}/\Theta_{207}$ over 8 hours. The resulting exponential curve revealed a characteristic time of 2.5 h for the structural transition (Jansen, 2002). In conclusion it can be said that formation of the α-helical structure as well as of the soluble β-structure, starting from the partially denatured structure at 0.2 % SDS, is fast, whereas establishing the equilibrium between both structures at intermediate SDS-concentrations is very slow.

3.1.2 Structural transitions from native, α-helical PrP in aqueous solution induced by addition of SDS

After confirming the results of structural transition induced by dilution of SDS the reversibility of the transitions was tested by addition of SDS to samples completely free of SDS or other detergents. Rec PrP (90-231) is soluble in the absence of detergents when dissolved in 20mM NaAc pH 5.5. When the protein was adjusted to the conditions used otherwise in this study, i.e. 10 mM NaP_i pH 7.2, the protein does not remain stably soluble. The portion that can be pelleted after 1 h, 100,000 x *g* (cf. Fig. 3.3 B, t = 0 h) was discarded, and to the soluble portion SDS was added in concentrations as indicated in Fig. 3.3. At very low concentrations of SDS (≤0.005 % SDS) the structure of rec PrP (90-231) changes from the initial α-helical structure to a β-structure-rich state within the experimental time frame for CD-spectroscopy (20 minutes). This can be seen in the respective transition curve (Fig. 3.3 A). In addition the protein becomes completely insoluble at 0.005 % SDS as seen from the dot blot (Fig. 3.3 B). With a further increase of SDS-concentrations to ~0.04 % the secondary structure cannot be assessed reliably by CD-spectroscopy because of the insolubility of PrP. Above 0.05 % SDS PrP changes to a soluble, β-structured state which is known from previous experiments (see above, cf. 3.1.1). By increasing the SDS-concentration further, the transition from the soluble, β-structured to the α-helical state is induced; a transition that was also observed in the SDS-dilution experiments (cf. Fig. 3.2). The transition range, however, is shifted from ~0.03 % SDS (dilution of SDS) to ~0.06 % SDS (addition of SDS). This is most probably a kinetic effect: Adjustment of the equilibrium between α-helical and β-structured rec PrP (90-231) takes at least 7 days at intermediate SDS-concentrations (0.04 % - 0.07 %) (cf. Figure 3.3 A).

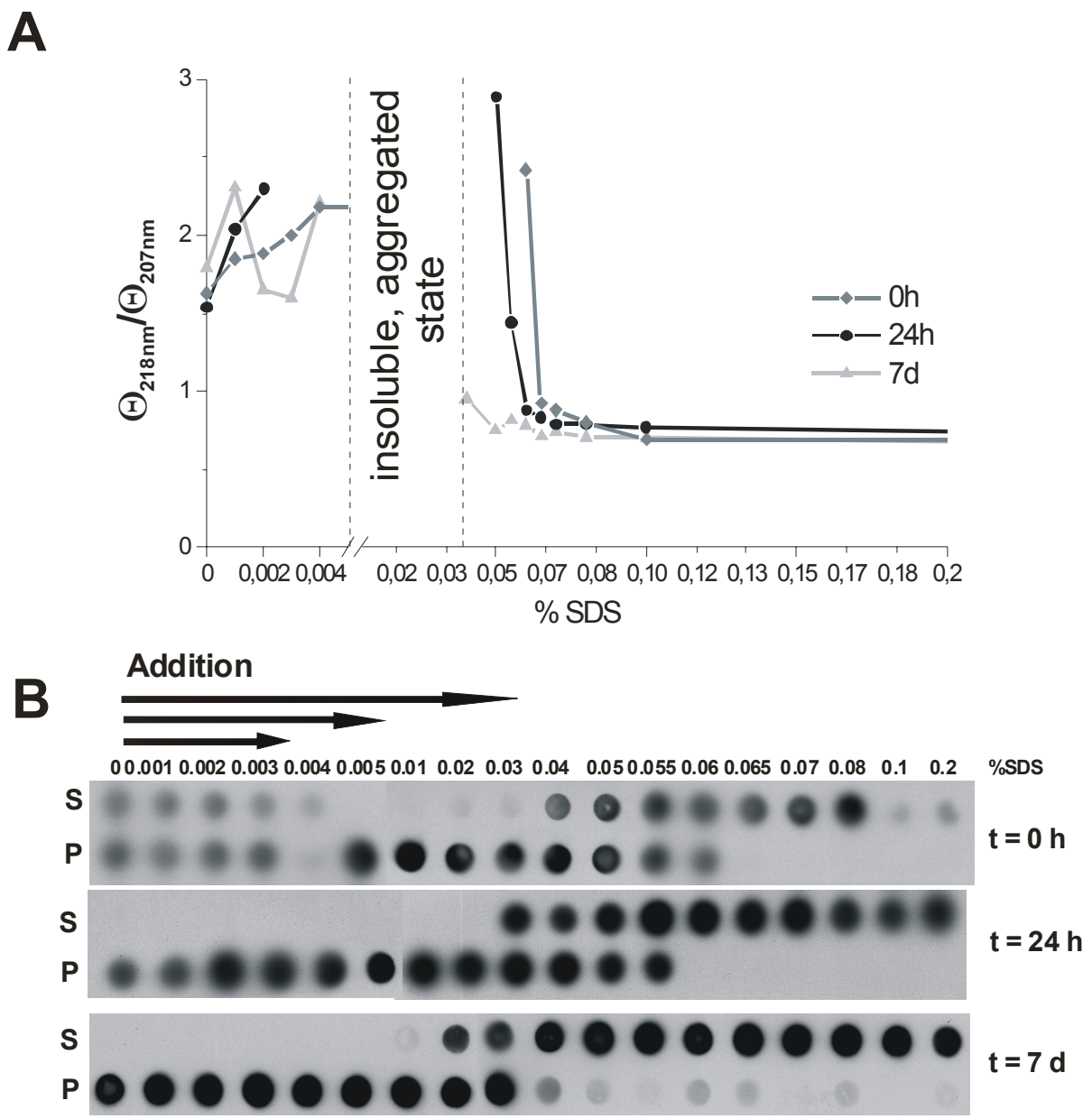

Figure 3.3: Structural transition and solubility of rec PrP (90-231) as induced by addition of SDS. Increasing amounts of SDS were added to 1 mg / ml rec PrP (90-231) at 20 mM NaAc pH 5.5. The samples were adjusted to a final concentration of 20 ng/µl rec PrP (90-231) in 10 mM NaPi pH 7.2 and the SDS-concentrations shown. **(A)** CD-spectroscopy was carried out either directly, after 24 h or after 7 days at 25 °C and a transition curve was calculated; high values of $\Theta_{218}/\Theta_{207}$ indicate high β-structure content. **(B)** Solubility was analyzed after the depicted incubation times by an additional 1 h 100,000 x *g* ultracentrifuge spin and separation of supernatant (S) and pellet (P).

These kinetic effects became more evident when the results from measurements after different incubation times were compared in greater detail: The transition curves in Fig. 3.3 A are incomplete because of the insolubility of one conformation involved. Nevertheless it is seen that at the same SDS-concentration, e.g. 0.04 %, without incubation and even after one day a

β-structure-rich conformation is established, but after 7 days the CD-spectrum of an α-helical conformation was obtained (cf. Fig. 3.4). At this SDS-concentration, without prolonged incubation, the PrP was partially insoluble (Fig. 3.3 B) but after 7 days at 0.04 % SDS PrP was predominantly soluble.

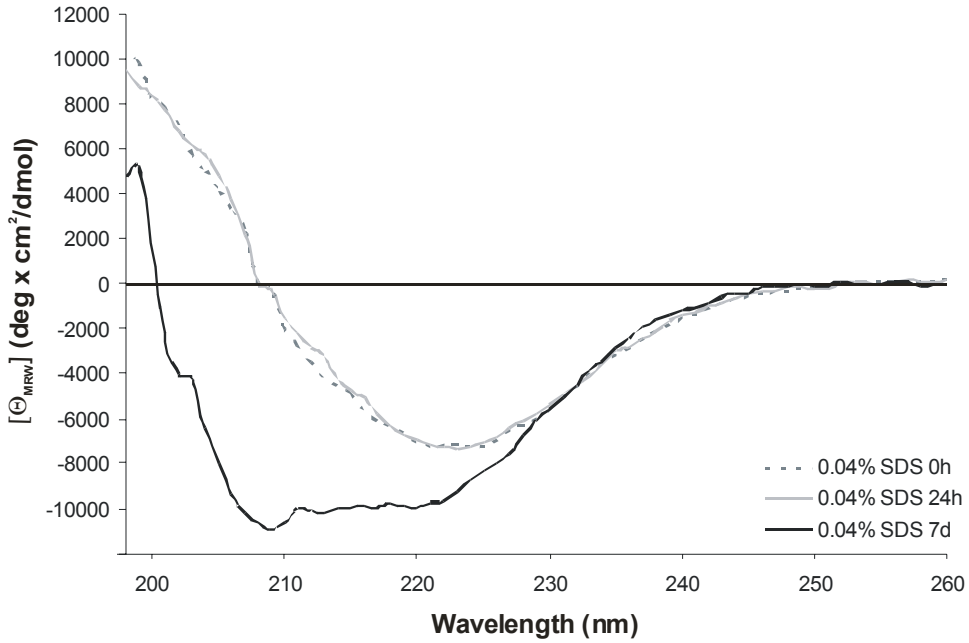

Figure 3.4: Slow equilibrium between β-structured and α-helical states. When 0.04 % SDS is added to rec PrP (90-231) in 10 mM NaP_i pH 7.2 the protein turns to a β-structured state. This state remains stable for 24 h, but within 7 days of incubation at 25°C the structure changes slowly to one that is predominantly α-helical as revealed by CD-spectroscopy.

The results confirm the finding from the SDS-dilution experiments that the equilibrium between the α-helical and β-structured conformations is very slow at intermediate SDS-concentrations. An even more drastic kinetic influence is revealed when the transition is induced starting from the aggregated, β-structured state (cf. above) compared to starting from soluble, α-helical states (cf. 3.1.1).

In earlier discussions the PrP conformation after dilution of SDS from 0.2 % to 0.01 % was described as the SDS-free conformation (Post *et al*., 1998). This interpretation was supported by the finding that the conformation as measurable in the aggregated state remains unchanged if the final SDS (0.01 %) was washed in SDS-free buffer several times. The present studies, however, demonstrate that addition of SDS lower than 0.005 % to a detergent-free protein solution leaves the conformation partially soluble and not in β-structured aggregates.

Consequently, the conformational state of rec PrP (90-231) in the concentration range between 0 % and 0.005 % depends upon the direction of establishing the SDS-concentration.

3.1.3 SDS binding to rec PrP (90-231) at very low concentrations of SDS

As described in the paragraph above low concentrations of SDS induce a shift to predominantly β-structured conformations followed by aggregation. Therefore, the binding of SDS to rec PrP (90-231) at low concentrations of SDS was studied quantitatively.

A modified version of the Methylen Blue assay (Reynolds & Tanford, 1970) was carried out (cf. 2.12). The concentration of free SDS in a rec PrP (90-231) containing sample was compared to a protein-free control with the same amount of total SDS. From this comparison the amount of SDS that was bound to the protein was determined. This method is applicable even easier when the protein is fully aggregated, i.e. at low SDS-concentrations, because the protein-SDS complex can easily be separated from the solution by ultracentrifugation. The amount of SDS remaining in the supernatant was determined with an absorption test (cf. 2.12). The graph in Fig. 3.5 shows that the amount of SDS that actually binds to the protein at SDS-concentrations of up to 0.01 % does not exceed 5 molecules of SDS per PrP molecule.

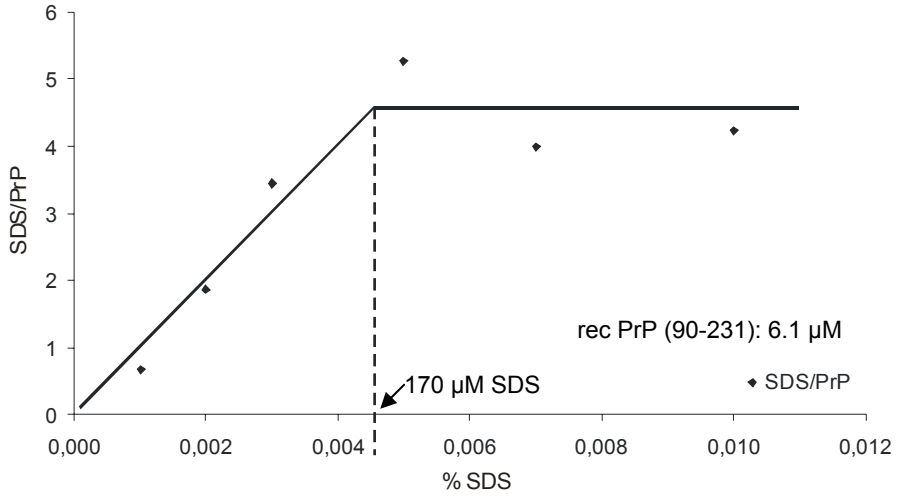

Figure 3.5: SDS binding to rec PrP (90-231) at low SDS-concentrations using the Methylen Blue binding assay: As little as 4-5 molecules of SDS bind per molecule of rec PrP (90-231) at 0.005 % SDS. At this SDS-concentration the PrP is in a β-structured state and fully aggregated (cf. Figure 3.3).

Thus, as little as 5 molecules induce the shift of from the SDS-free, α-helical rec PrP (90-231) to β-structured aggregates. As described above (cf. 3.1.2) this transition is not completely reversible. Since one of the working hypotheses of this study was that formation of amyloid

fibrils requires reversible transition processes this range of low SDS-concentrations (0 % - 0.005 %) was not used for experiments aiming at fibril formation (cf. below).

Instead a closer look was taken at the SDS/PrP stoichiometry for the reversible transition process of PrP at intermediate SDS-concentrations (>0.01 % SDS). At these SDS-concentrations it doesn't matter if the SDS-concentration is established starting from 0 % SDS or from 0.2 % SDS as the experiments described above have shown (cf. 3.1.1 & 3.1.2).

Earlier findings have revealed binding of 30-32 molecules of SDS bind per rec PrP (90-231) at 0.2 % SDS (Jansen, 2002). 21 molecules of SDS bind per rec PrP (90-231) at 0.06 % SDS, where rec PrP (90-231) is in a dimeric state (Jansen, 2002). Furthermore re-evaluation of earlier results (Jansen 2002) led to calculations of SDS-release during the transition from α-helical dimers to β-structured oligomers. These oligomers consist of 12-16 molecules of PrP per oligomer. From the transition curve (cf. Figure 3.2) it can be calculated, using a modified Hill plot, that at least 2-3 SDS per rec PrP (90-231) are released from the dimers described by Jansen (Jansen 2002) (cf. Figure 3.6). Hence, 18-19 molecules of SDS bind per molecule of rec PrP (90-231) in the β-structured, oligomeric state.

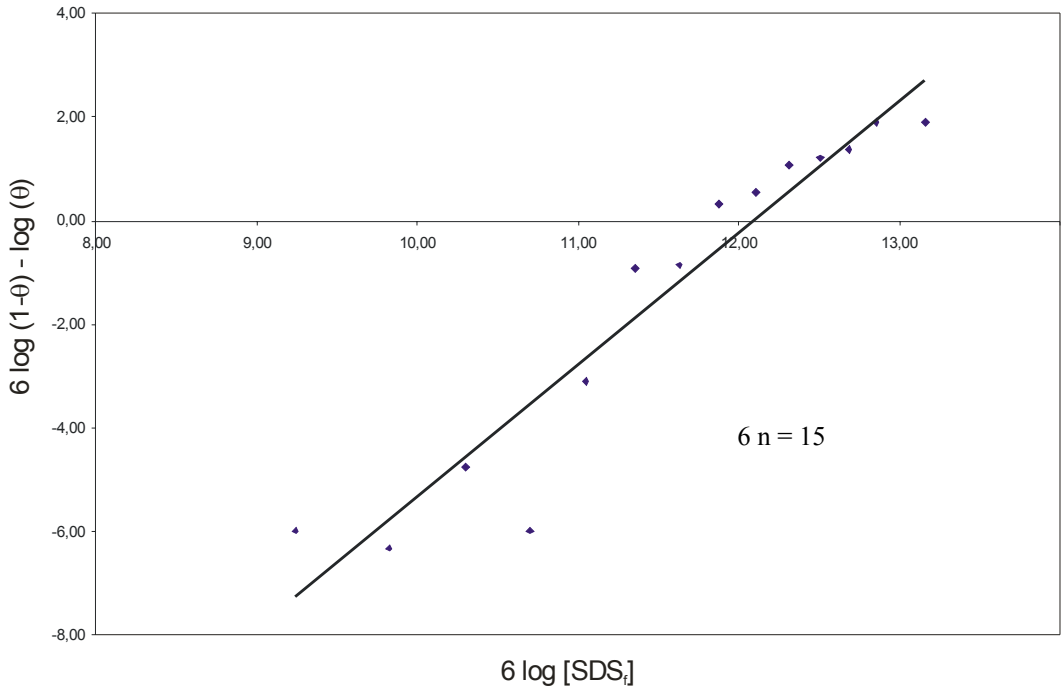

Figure 3.6: Modified Hill plot. To estimate the number of molecules of SDS that are released during the transition from the rec PrP (90-231)-dimer to the rec PrP (90-231)-dodecamer, the Hill plot was modified by inserting the expression for the degree of transition θ. Plotting of 6 log (1-θ) – log (θ) against 6 log [SDS_f] yields a slope of 6 n = 15, therefore n = 2.5, i.e. 2-3 molecules of SDS are released per molecule of PrP during the transition.

Since a β-structure like this one is required for the desired fibril formation, conditions inducing soluble β-structures that may allow slow, well ordered aggregation will be the focus of the following parts of this study.

3.2 Formation of fibrils of PrP and its dependence on solution conditions

In an earlier study a structural transition of PrP 27-30 from prion rods to the PrP^C-like, soluble PrP 27-30 was established by sonication in the presence of SDS and consecutive elution from denaturing gel electrophoresis (Leffers, 1999) (cf. 1.7). The gel electrophoresis and elution yielded a PrP sample free of any infectivity, but definitely with the complete chemical properties of infectious PrP. This feature was particularly important when it was tried to reverse the process and to design conditions *in vitro* that allow a transition back to a PrP^{Sc}-like form, i.e. reconstitution of a β-structured state followed by well ordered aggregation. These reconstitution experiments were carried out with two forms of solubilized PrP 27-30, namely sol PrP 27-30 and sol PrP 27-30 after gel electrophoresis designated elu PrP 27-30. In comparison, similar experiments with native, full length PrP^C from hamster brain were carried out. The whole procedure of solubilization and reconstitution is depicted in Fig. 3.7.

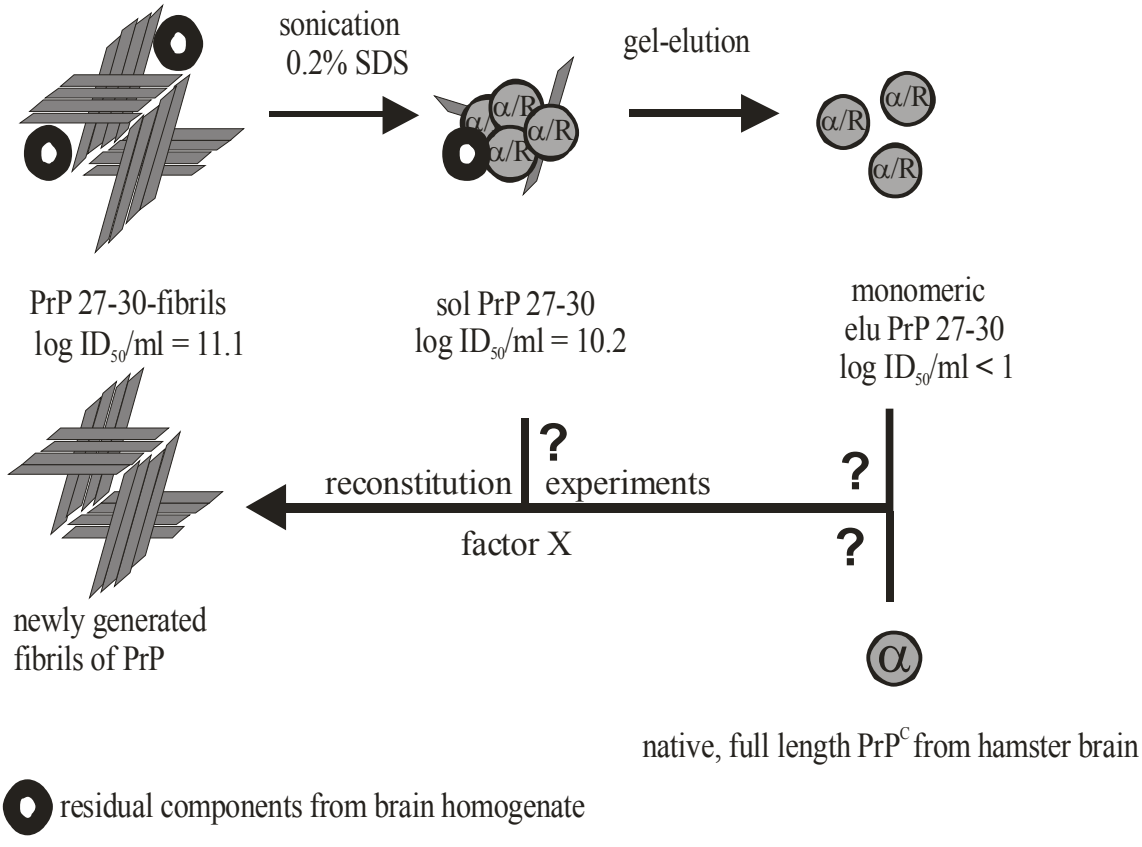

Figure 3.7: Fibril formation experiments for various forms of PrP *in vitro*. PrP 27-30 from prion rods can be solubilized by treatment with 0.2 % SDS and subsequent sonication. The resulting sol PrP 27-30 is tetra- to hexameric, PK-sensitive and retains a background infectivity which can be abolished by eluting the protein from SDS-PAGE gels. This procedure yields the PrP^C-like elu PrP 27-30. Reconstitution experiments with the aim to form amyloid fibrils from PrP were carried out with sol PrP 27-30, elu PrP 27-30 and native, full length PrP^C from brains of uninfected hamsters.

In Table 3.1 an overview for the forms of PrP used for the following reconstitution experiments with respect to their source is given.

Table 3.1: Forms of prion proteins used for reconstitution experiments.

Prion Protein	Source	Properties
PrP^C	PrP^C purified from brains of uninfected Syrian Gold Hamsters.	soluble monomeric α-helical not infectious
sol PrP 27-30	Solubilized PrP 27-30 purified by treatment of infectious prion rods containing insoluble PrP 27-30 with 0.2 % SDS and subsequent sonication.	soluble tetra- to hexameric mainly α-helical background infectivity
elu PrP 27-30	sol PrP 27-30 eluted from denaturing gel-electrophoresis (SDS-PAGE)	soluble monomeric mainly α-helical not infectious

To observe the aggregation state of PrP, electron microscopy was used (cf. 2.15). For this reason the buffer used in the previous experiments, i.e. 10 mM NaP_i pH 7.2 needed to be exchanged to one that is suitable for electron microscopy. The replacement buffer consisted of 10 mM Na-HEPES pH 7.2 since other experiments with rec PrP (90-231) had shown that the solubility and PK-resistance of PrP is identical in both buffers over a range of SDS-concentrations (Stoehr, 2003). Potential differences in secondary structure could not be assessed due to the fact that Na-HEPES interferes with CD-spectroscopy. However, since it is known that sol PrP 27-30 and elu PrP 27-30 are mainly in a soluble, β-structured state at 0.01 % SDS in 10 mM NaP_i pH 7.2 (Leffers, 1999) which also applies for PrP^C (Elfrink, personal communication), this SDS-concentration was used for 10 mM Na-HEPES pH 7.2

assuming that not only the solubility and PK-resistance, but also the secondary structure are identical in both buffers. Therefore the samples of sol PrP 27-30, elu PrP 27-30 and PrP^C that were used in the following experiments were adjusted to 10 mM Na-HEPES pH 7.2 and varying SDS-concentrations using Pierce Slide-A-Lyzer dialysis cassettes. Additional factors like sodium chloride or lipids as found in prion rods were added afterwards depending on the experimental setup (cf. below).

First the samples were analyzed for solubility in dependence on incubation time. When aggregation had occurred the samples were further analyzed by electron microscopy to determine the nature of the newly formed aggregates.

3.2.1 Solubility analysis of sol PrP 27-30 (before gel-elution)

Since other groups have shown that the presence of sodium chloride seems to be essential for highly ordered aggregation of PrP (cf. Introduction), the aggregation of sol PrP 27-30 was studied by adding varying concentrations of 0-500 mM NaCl to sol PrP 27-30 at 10 mM HEPES pH 7.2/0.01 % SDS (cf. Figure 3.7). These samples were incubated for 1, 21 or 42 days at 37 °C. For analysis they were subjected to a 1 h 100,000 x *g* ultracentrifugation to determine the solubility of the protein. The supernatant was separated from the pellet and analyzed by Western blot (cf. Figure 3.8).

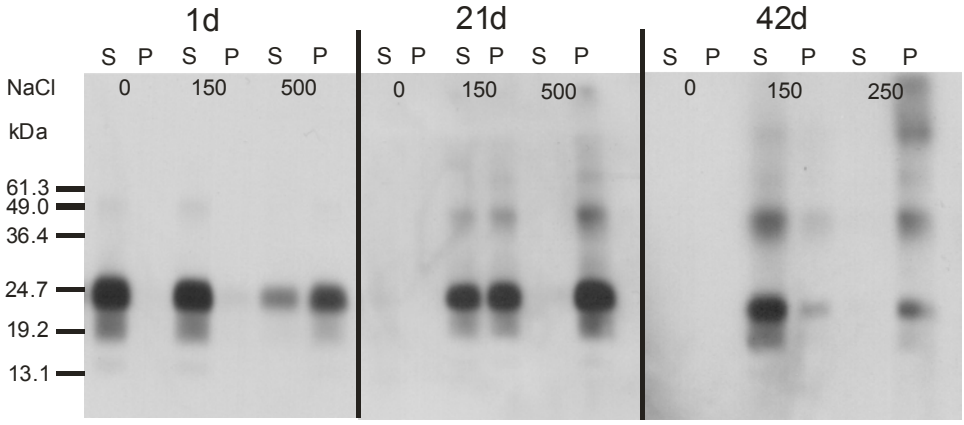

Figure 3.8: Determination of aggregation conditions for sol PrP 27-30 (before gel-elution):
Aggregation of sol PrP 27-30 was induced by adjusting the samples to 10 mM HEPES pH 7.2/0.01 % SDS, addition of different concentrations of NaCl (0, 150, 250 or 500 mM) and incubation at 37 °C for 1, 21 or 42 days. After the incubation period the solubility of the samples was determined by a 1 h 100,000 x *g* ultracentrifugation, separation of supernatant (S) and pellet (P) and subsequent Western blot analysis. Since 500 mM NaCl led to a complete aggregation of sol PrP 27-30 after 21 days, only 250 mM NaCl were used for the 42 d incubation. For absence of signals in samples without NaCl added after 21 and 42 d incubation see text.

It should be noted first that the minimal protein-concentration in the aggregation experiments was 10 ng/µl in order to obtain reproducible effects. The fact that no protein signal could be seen in the absence of sodium chloride after 21 and 42 days might be due to the fact that the protein sticks to the walls of the tubes after long incubation times.

Sol PrP 27-30 at 10 mM HEPES pH 7.2/0.01 % SDS fully aggregated upon addition of 500 mM NaCl and incubation for 21 days at 37 °C. When the samples were incubated for 42 days, addition of 250 mM NaCl was sufficient for complete aggregation of the protein. Under physiological conditions, i.e. addition of 150 mM NaCl, PrP showed variable aggregation properties; in this example about half of the material was aggregated after 21 days, but in a different sample that was incubated for 42 days, only small amounts were aggregated.

The variability of the distribution of sol PrP 27-30 between supernatant and pellet at 150 mM NaCl indicates that a certain threshold of oligomer-concentration or –size for the protein may have to be reached before aggregation occurs. In general threshold effects are difficult to control exactly. The probability of developing those oligomers may be low at 150 mM NaCl, whereas it is higher at 250 mM NaCl, where sol PrP 27-30 reproducibly fully aggregates after 42 days.

3.2.2 Solubility analysis of elu PrP 27-30 (after gel-elution)

The effect of sodium chloride on aggregation of elu PrP 27-30 was studied using the same concentration range as above: In contrast to sol PrP 27-30, long incubation of elu PrP 27-30 at 10 mM HEPES pH 7.2/0.01 % SDS with 0-250 mM NaCl does not lead to effective aggregation of the protein (cf. Figure 3.9 A). One of the differences between sol PrP 27-30 and elu PrP 27-30 is the presence of lipids in sol PrP 27-30: The mass ratio of lipids to PrP in prion rods equals about 1:50 in accordance to earlier studies (Klein *et al*., 1998). During an average solubilization process for PrP 27-30, about 10 - 20 % of the total protein is solubilized into sol PrP 27-30 (Riesner *et al*., 1996). Since it cannot be followed how much of the lipids are solubilized during the treatment with SDS and sonication, one can assume that at maximum the lipids are completely solubilized. The fact that lipids are solubilized from prion rods under these conditions is evident, since lipid vesicles can be seen in electron micrographs of sol PrP 27-30 (data not shown). Taking this information into account, the mass ratio of lipids to PrP might be at maximum 1:5 for samples containing sol PrP 27-30. When this amount of lipids, i.e. a mixture of sphingomyelin, galactosyl cerebroside and cholesterol in a ratio of 1:1:1 by mass as found in earlier studies for prion rods (Klein *et al.*, 1998), is added to

a sample of elu PrP 27-30 at 10 mM HEPES pH 7.2/0.01 % SDS/250 mM NaCl and incubated for 35 days at 37 °C, PrP fully aggregates (cf. Figure 3.9 B).

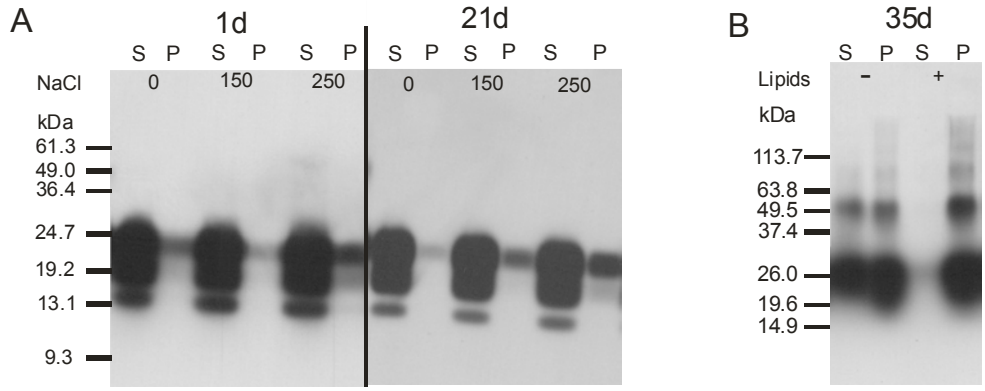

Figure 3.9: Determination of aggregation conditions for elu PrP 27-30 (after gel-elution): Aggregation of elu PrP 27-30 was induced by adjusting the samples to 10 mM HEPES pH 7.2/0.01 % SDS, addition of different concentrations of NaCl (0, 150 or 250 mM NaCl) and lipids as found in prion rods over a range of incubation times at 37 °C. After the incubation period the solubility of the samples was determined by a 1 h 100,000 x *g* ultracentrifugation, separation of supernatant (S) and pellet (P) and subsequent Western blot analysis **(A)** 0, 150 or 250 mM NaCl were added to elu PrP 27-30 and incubated for 1 or 21 days. **(B)** 250 mM NaCl were added to elu PrP 27-30 and incubated for 35 days at 37 °C in the absence (-) or presence (+) of lipids.

3.2.3 Fibril formation of PrP 27-30 before and after gel-elution

Following the solubility analysis, the structure of the aggregation products was analyzed by electron microscopy. Aliquots of the same samples as used for the solubility tests were analyzed. The starting material, i.e. PrP 27-30 from brains of scrapie infected Syrian Golden Hamsters, reveals a rod-like structure in electron micrographs (cf. Fig. 3.10 A). When PrP was solubilized and subjected to centrifugation, the supernatant contained sol PrP 27-30 at 10 mM HEPES pH 7.2/0.2 % SDS. This sol PrP 27-30 appeared in the shape of little, tetra- to hexameric particles confirming earlier studies (Riesner *et al*., 1996). In addition, bigger, amorphous fragments in complex with lipid-vesicles were also observed (cf. Fig. 3.10 C). When the SDS-concentration was lowered to 0.01 %, 250 mM NaCl was added, and the samples were incubated at 37 °C for 42 days. The samples contained approximately 5 - 10 % amyloid fibrils and 90 - 95 % amorphous aggregates (cf. Fig. 3.10 E; only fibril shown).

When sol PrP 27-30 is eluted from SDS-PAGE, monomeric, non-infectious elu PrP 27-30 results. Since these protein monomers cannot be seen under conventional staining-conditions (negative stain with 2 % ammonium molybdate, cf. Materials & Methods), the grid appears to be empty when viewed in an electron microscope (cf. Fig. 3.10 D).

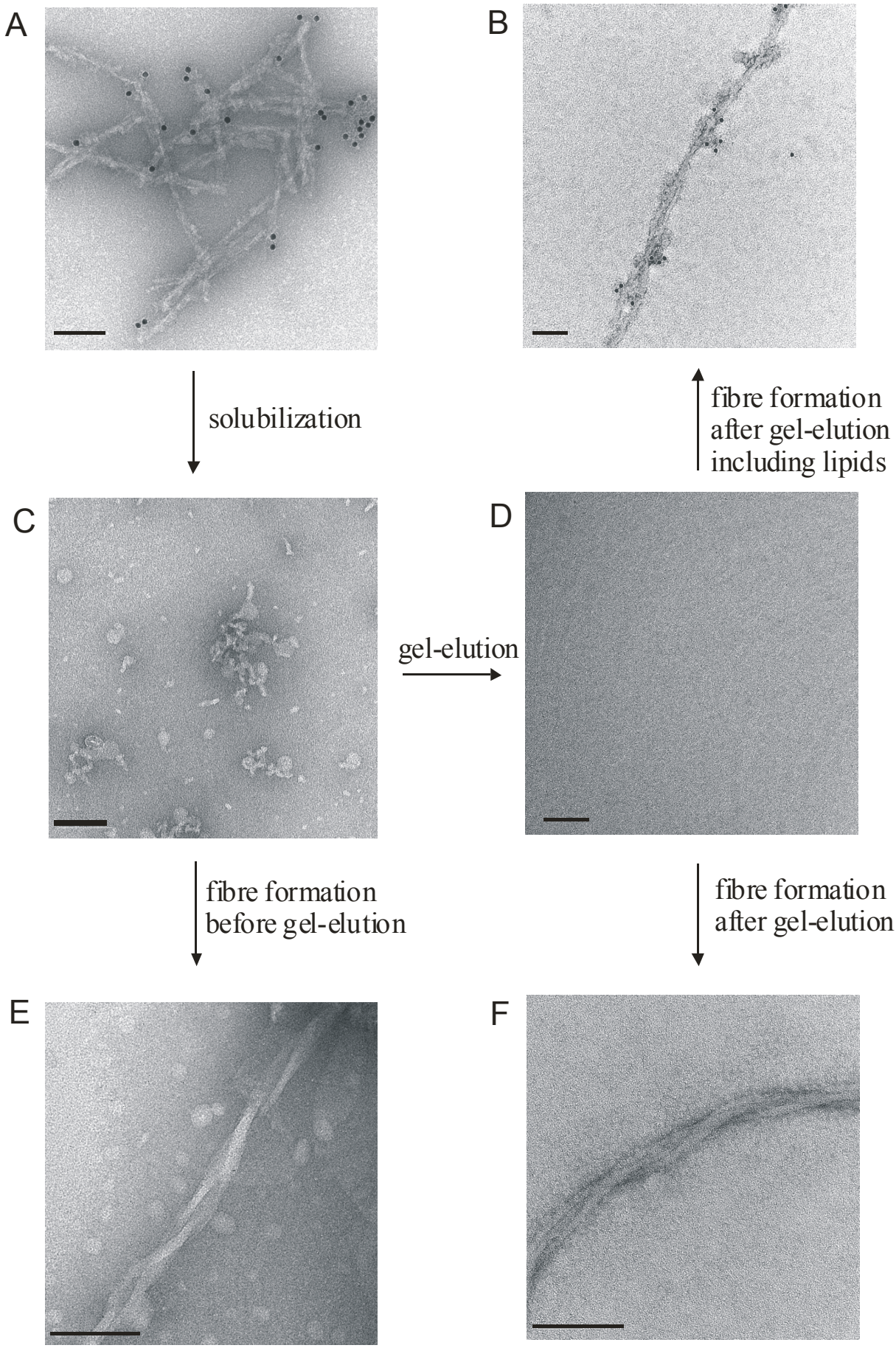
A
B
solubilization
fibre formation
after gel-elution
including lipids
C
D
gel-elution
fibre formation
before gel-elution
fibre formation
after gel-elution
E
F

Figure 3.10: Fibril formation of sol PrP 27-30 and elu PrP 27-30 as seen by electron microscopy
(A) PrP 27-30 from brains of scrapie-infected Syrian Golden Hamsters reveals a rod-like structure in electron micrographs (protein immunogold-labeled using huFab D18). **(B)** Fibres of elu PrP 27-30 formed in the presence of lipids. **(C)** sol PrP 27-30 at 10 mM HEPES/0.2 % SDS shows little, tetrameric to hexameric spherical particles as well as bigger fragments in complex with lipid-vesicles. **(D)** Monomeric elu PrP 27-30. The protein cannot be visualized in electron micrographs under the used conditions (cf. text). **(E)** Fibres of sol PrP 27-30. **(F)** Fibres of elu PrP 27-30 formed in the absence of lipids (protein immunogold-labeled using huFab D18). All samples negatively stained using 2 % ammonium molybdate; bars correspond to 100 nm.

Adjusting elu PrP 27-30 to 0.01 % SDS, 250 mM NaCl and incubation for 35 days at 37 °C in the absence (cf. Fig. 3.10 F) or presence of lipids (cf. Fig. 3.10 B) again led to formation of amorphous aggregates and amyloid fibrils. Analysis of multiple electron micrographs from grids containing reaggregated elu PrP 27-30 revealed that in the absence of lipids roughly 5 - 10 % of the protein forms fibrils while in the presence of lipids approximately 15 - 20 % of the protein formed fibrils. Moreover, the fibrils were substantially longer, i.e. about 5 µm in length without lipids and up to 20 µm in the presence of lipids. The diameter of the fibrils varied in both cases between 10 - 20 nm.

These results show that the established *in vitro* conversion system allows induction of formation of amyloid fibrils from the PrP^C-like isoform elu PrP 27-30. This fibril formation is not dependent on the presence of lipids, but lipids make the formation of fibrils more efficient. Like observed in other studies, aggregation including fibril formation is induced in or maybe even by the presence of sodium chloride.

3.2.4 Solubility analysis and fibril formation of native, full length PrP^C

Since the samples of PrP studied so far for fibril formation had undergone a partial denaturation in 0.2 % SDS or higher (elu PrP 27-30 has been incubated shortly in sample buffer; cf. 2.5), fibril formation was adapted to samples containing native, full length PrP^C. PrP^C was purified from brains of uninfected Syrian Golden Hamsters as described elsewhere (Pan *et al*., 1993). This purification process yields native, full length PrP^C in 10 mM NaP_i pH 7.5/150 mM NaCl and the non-denaturing detergent Zwittergent 3-12 at 0.12 %. In order to change the buffer to the one used in the *in vitro* conversion system described earlier, the material was dialyzed for 48 h against a 1000-fold volume of 10 mM HEPES pH 7.2/0.01 % SDS using Pierce Slide-A-Lyzer dialysis cassettes. After adjusting the samples to 250 mM NaCl and incubation at 37 °C for 35 days, a major proportion of the protein aggregated in the absence of lipids and the protein fully aggregated in the presence of lipids (sphingomyelin, galactosyl cerebroside and cholesterol, cf. above) (cf. Figure 3.11 A). An electron microscopic analysis of these samples revealed a mixture of amyloid fibrils and amorphous aggregates similar to the ones seen before for elu PrP 27-30 (cf. Figure 3.11 B, 3.11 C). The maximum length of the fibrils assembled in the presence of lipids was 20 µm, whereas in the absence of lipids the fibril length did not exceed 4 µm. The diameter of the fibrils again varied between 10-20 nm. Also, similar to the experiments with PrP 27-30, fibril formation was more efficient in the presence of lipids, but at least ~85 % of the protein appeared to be in the shape of amorphous aggregates. Immunogold-labeling of the samples using huFab D18 proved that the fibrils contained PrP (cf. Figure 3.11 B, 3.11 C). These experiments show that the transition from a PrP^C-like to a PrP^{Sc}-like form, as described above for PrP 27-30, is not affected - from a structural point of view - by the presence of SDS in a concentration of 0.2 %. Also, this is the first time that formation of amyloid fibrils from native, full length PrP^C could be demonstrated.

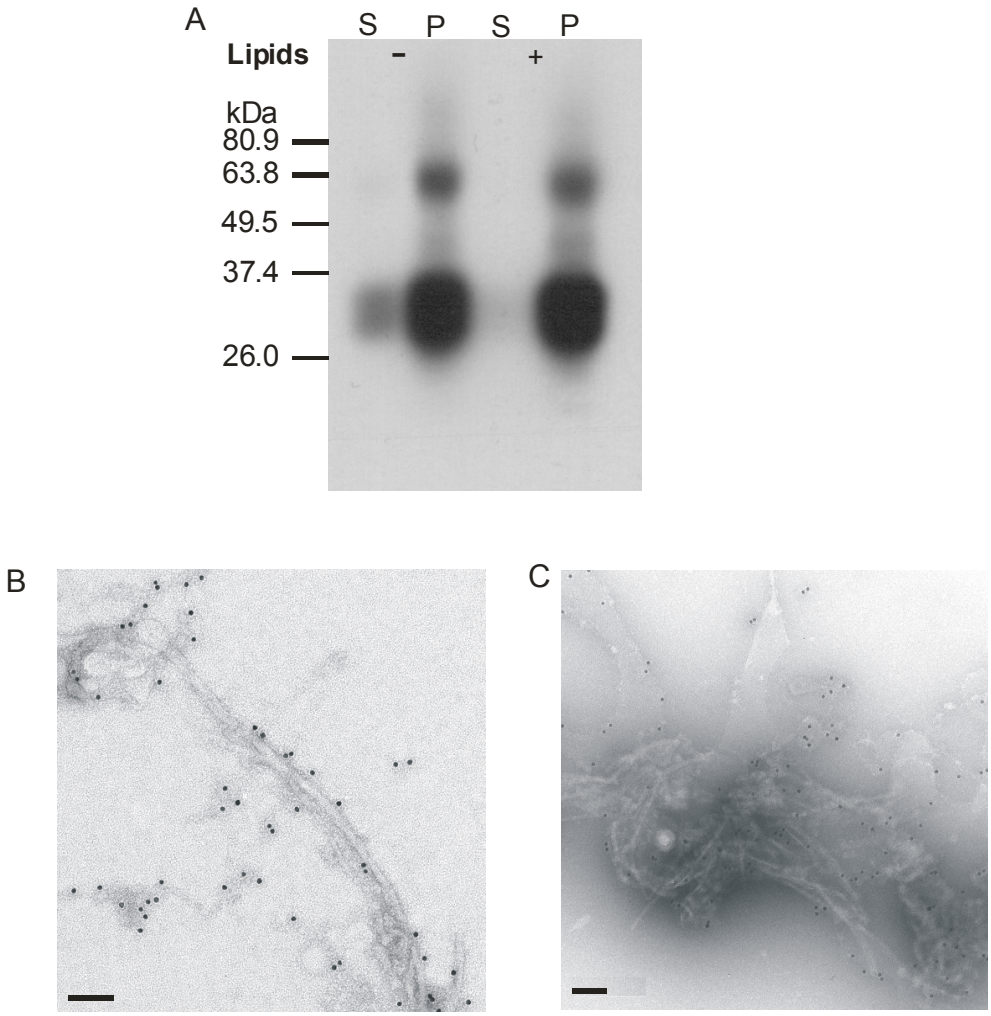

Figure 3.11: Solubility analysis and fibril formation of native, full length SHa PrP^C.
PrP^C was purified from brains of Syrian Golden Hamsters. The buffer was adjusted to 10 mM HEPES pH 7.2/0.01 % SDS by dialysis. **(A)** 250 mM NaCl were added and the sample was incubated for 35 days at 37 °C in the absence (-) or presence (+) of lipids. Then solubility was determined with a 1 h 100,000 x *g* ultracentrifugation, separation of supernatant (S) and pellet (P) and subsequent Western blot analysis. Electron microscopy of the pellets of the same samples in the absence **(B)** or presence **(C)** of lipids reveals formation of fibrils and amorphous aggregates. The samples were immunogold-labeled using huFab D18. All samples were negatively stained using 2 % ammonium molybdate; bars correspond to 100 nm.

3.3 Proteinase K resistance of *in vitro* generated amyloid fibrils of elu PrP 27-30 and PrP^C

After achieving the initial goal of this study, i.e. to establish an *in vitro* conversion system that allows formation of a PrP^{Sc}-like isoform from PrP^C, other markers were tested to verify the

PrP^{Sc}-like character of the products of the conversion. One marker often used for differentiation between PrP^{C} and PrP^{Sc} is digestion with proteinase K (PK): In general, PrP^{C} is sensitive to digestion with PK whereas digestion of PrP^{Sc} with PK results in a stable, still infectious fragment of PrP denoted PrP 27-30. It should be noted though, that in the past various studies have shown that development of PK-resistance does not necessarily correlate with development of infectivity. Furthermore it could be shown that PrP does not always lose infectivity when PK-resistance diminishes (*for review*: Wille *et al*., 2000). To evaluate whether the newly, *in vitro* generated fibrils from PrP^{C}, or elu PrP 27-30 show resistance to PK-digestion and to evaluate if the PK-resistance of these fibrils is higher than the resistance of the also present amorphous aggregates in the samples, the samples were subjected to a limited digestion with PK. Proteinase K was added to a sample containing PrP in the mass ratio of 1:3 (molar ratio of ≈ 1:5). The reaction was stopped after 5 minutes by adjusting the sample to 7.5 mM PMSF and the samples were analyzed by Western blot and electron microscopy. Most of the protein was degraded after 5 minutes of treatment with PK as revealed by Western blot analysis (cf. Figure 3.12).

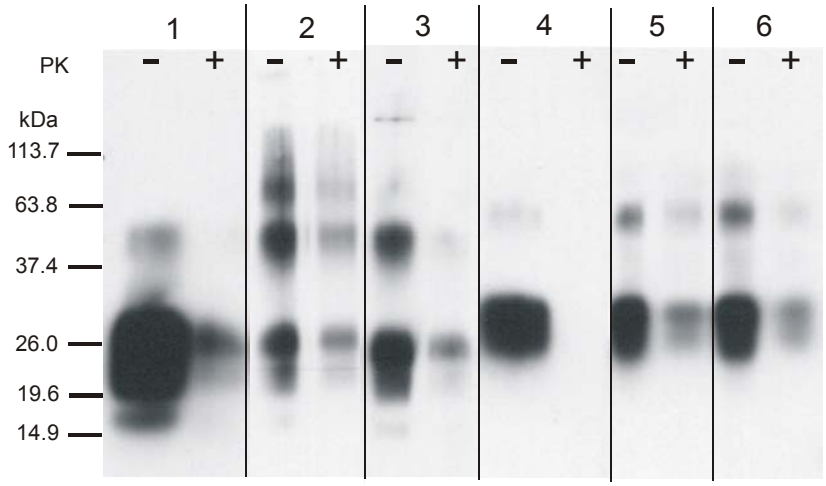

Figure 3.12: Limited PK-digestion of elu PrP 27-30 and PrP^{C}.

Aggregated elu PrP 27-30 and PrP^{C} was subjected to limited digestion with proteinase K: Samples containing 150 ng of PrP were treated with 50 ng of proteinase K for 5 minutes at room temperature. The reaction was stopped by adjusting the sample to 7.5 mM PMSF followed by Western blot analysis using the 3F4 antibody. Samples: (1) elu PrP 27-30 stock (10 mM HEPES pH 7.2/ 0.01 % SDS; control = no aggregation was induced), (2) reaggregated elu PrP 27-30, (3) reaggregated elu PrP 27-30 with lipids, (4) PrP^{C} stock (10 mM HEPES pH 7.2/0.01 % SDS; control = no aggregation was induced), (5) aggregated PrP^{C}, (6) aggregated PrP^{C} with lipids.

After the limited proteolysis, the ratio of amyloid fibrils and amorphous aggregates – in context with lipid vesicles - was unchanged, but the total amount was reduced by ~90 % (cf. Figure 3.13).

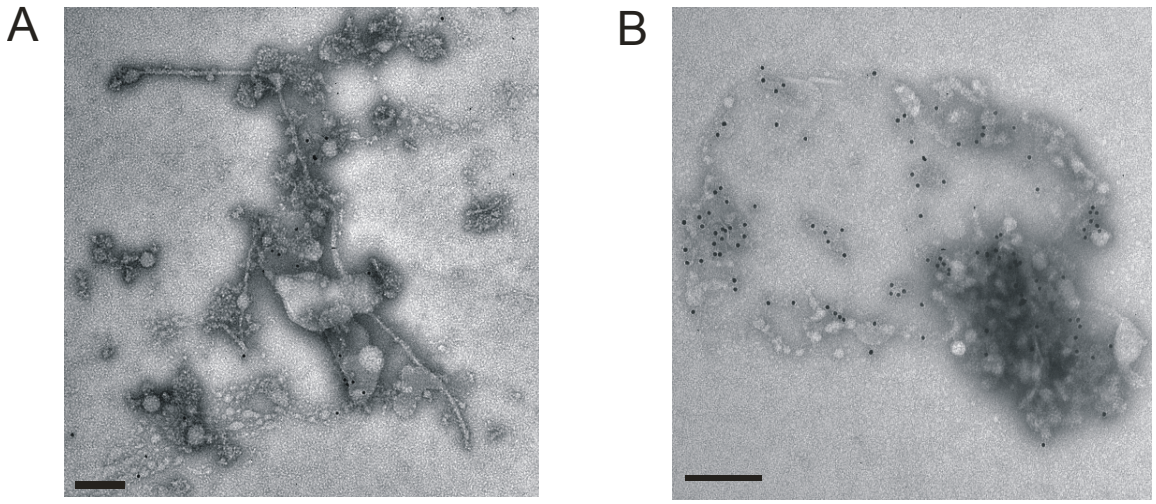

Figure 3.13: Limited PK-digestion of elu PrP 27-30 and PrP^C.
Aggregated elu PrP 27-30 and PrP^C was subjected to limited proteolysis with proteinase K: Samples containing 150 ng of PrP were treated with 50 ng of proteinase K for 5 minutes at room temperature. The reaction was stopped by adjusting the sample to 7.5 mM PMSF. A subsequent analysis by electron microscopy revealed the same ratio of fibrils, amorphous aggregates and lipid vesicles as before PK-digestion for elu PrP 27-30 **(A)** as well as for PrP^C **(B)**. Only the total amount of fibrils and aggregates was reduced by ~90 %. Samples negatively stained with 2 % ammonium molybdate and immunogold-labeled using huFab D18; bars correspond to 200 nm.

When the samples were subjected to standard PK-digestion, i.e. PK was added to PrP in a mass ratio of 1:25 (molar ratio of ≈ 1:39) and digested for 1 h at 37 °C, all forms of PrP were completely degraded by the protease (data not shown). These results indicate that formation of amyloid fibrils does not necessarily lead to PK-resistance and that the newly generated fibrils are no more resistant to digestion with PK than e.g. amorphous aggregates of PrP.

3.4 Bioassays of *in vitro* generated amyloid fibrils from elu PrP 27-30 and PrP^C

In the last step of this series of experiments the infectivity of the amyloid fibrils and amorphous aggregates was tested in bioassays: Each sample containing aggregated PrP was diluted 10-fold in 5 mg/ml BSA in PBS resulting in an end-concentration of 1 ng/µl protein

for the bioassay-sample. 30 µl of each sample was inoculated intracerebrally into transgenic mice overexpressing PrP^C of Syrian Golden Hamsters (SHa PrP^C) approximately 8-fold compared to Syrian Golden Hamsters. These Tg ($SHaPrP^{+/+}$) 7*PrnP* $^{0/0}$ mice are homozygous for the SHa PrP transgene array and were crossed onto a mouse-PrP deficient background. Five mice per sample were inoculated (cf. Table 3.2). As positive controls the starting material for experiments with PrP 27-30 was used, i.e. PrP 27-30 from prion rods of scrapie infected hamsters. This sample of PrP 27-30 revealed very high titers of scrapie infectivity with 11.1 log ID_{50}/ml. Infectivity levels were still very high after solubilizing the protein resulting in sol PrP 27-30 with 10.2 log ID_{50}/ml. This reduction in infectivity by 90 % through solubilization is in good accordance to earlier results (Riesner *et al*., 1996). PrP^C, elu PrP 27-30 and the lipids used in the aggregation experiments served as negative controls. However, Table 3.2 shows that none of the samples containing newly, *in vitro* aggregated PrP in the form of amyloid fibrils and amorphous aggregates induced significant rates of infectivity.

Table 3.2: Bioassay of *in vitro* generated fibrils of PrP

Samples from all stages of the *in vitro*-conversion system were inoculated intracerebrally into Tg ($SHaPrP^{+/+}$)7*PrnP* $^{0/0}$-mice overexpressing SHa PrP^C approximately 8-fold on an ablated background. Prion titers were calculated by measuring the incubation time intervals from inoculation to onset of neurological illness.

Sample	Time of death (d)	Average (d)	log ID_{50}/ml
PrP 27-30	41, 42, 42, 42, DAT	41.75 ± 1	11.1
sol PrP 27-30	43, 43, 47, 47, DAT	45 ± 1.7	10.2
elu PrP 27-30	0/5@ 422 d		
Lipids	0/5@ 422 d		
Reformed fibrils of elu PrP 27-30	0/5@ 457 d		
Reformed fibrils of elu PrP 27-30 with lipids	0/5@ 457 d		
PrP^C	0/5@ 408 d		
Reformed fibrils of PrP^C	0/5@ 422 d		
Reformed fibrils of PrP^C with lipids	1/5@ 422 d		

(DAT = death atypical; non-scrapie). Positive control: PrP 27-30. Negative controls: elu PrP 27-30, lipids alone and PrP^C.

It should be recalled though that only a small portion of the inoculated samples containing reformed PrP-fibrils are actually amyloid fibrils (cf. 3.2.3 & 3.2.4): When fibril formation was induced under the described conditions, at least 80 % of the PrP aggregated into amorphous plaques. Thus, if amyloid fibrils should be necessary for infectivity the samples containing reformed fibrils contained a much smaller portion of potentially infectious protein: While the positive controls contained 30 ng of protein assembled in amyloid fibrils, the samples with reformed fibrils had only ~6 ng of protein assembled into fibrils.

To evaluate whether any PK-resistant protein had accumulated in the brains of the inoculated mice, 2/5 mice of each sample were sacrificed after 250 days of incubation (cf. Figure 3.14).

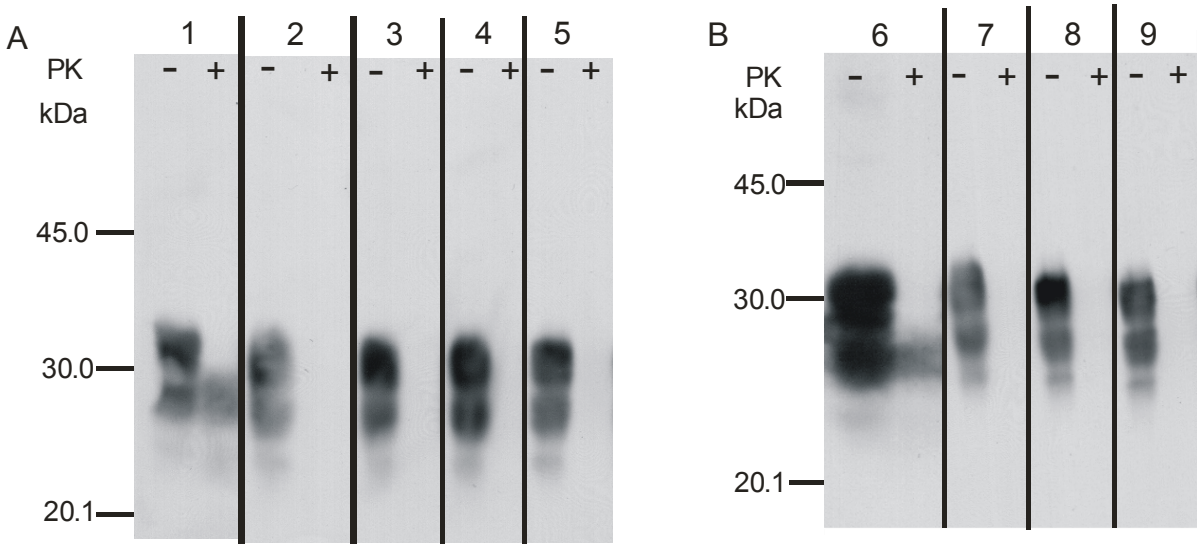

Figure 3.14: Search for PK-resistant PrP in brains of transgenic mice inoculated with *in vitro* generated amyloid fibrils. Samples from all stages of the described *in vitro*-conversion system were inoculated intracerebrally into Tg (SHaPrP$^{+/+}$)7*PrnP* $^{0/0}$-mice overexpressing SHa PrP^{C} approximately 8-fold on an ablated background. 2/5 mice were sacrificed after 250 days. 200 µl of a 10 % brain homogenate were adjusted to 50 ng/µl PK or left PK-free (controls) and incubated for 1 h at 37 °C. The PK-digestion was stopped by addition of 1 volume 2x sample buffer (cf. Materials & Methods). 50 µl of the resulting sample were run on SDS-PAGE and analyzed by Western blot using 3F4. Samples: (1) PrP 27-30 (starting material; positive control); (2) PrP^{C} (starting material; negative control); (3) aggregated PrP^{C}; (4) aggregated PrP^{C} with lipids; (5) lipids alone (negative control); (6) sol PrP 27-30 (positive control); (7) elu PrP 27-30 (negative control); (8) reaggregated elu PrP 27-30; (9) reaggregated elu PrP 27-30 with lipids.

Western blot analysis revealed that no PK-resistant protein had accumulated in the brains of the mice except in the positive controls, i.e. mice inoculated with PrP 27-30 and sol PrP 27-30.

Summarizing the results of the described studies it can be concluded that the established SDS-dependent *in vitro* conversion system allows induction of reversible transitions of PrP that can lead to formation of amyloid fibrils. However, these fibrils lack resistance to digestion with proteinase K and significant infectivity. Thus, the correlation between factors affecting fibril formation and generation of *de novo* infectivity needs to be further discussed (cf. below).

4. Discussion

According to the "*protein-only*"-hypothesis the event that initiates a transmissible spongiform encephalopathy or prion disease is a structural transition from PrP^{C} to PrP^{Sc}. Without any experimental exception the transition is connected with an aggregation of the misfolded PrP^{Sc} resulting in deposits composed of amorphous aggregates or sometimes of highly ordered amyloid fibrils. Until today the exact mechanism of the *in vivo* structural transition process and the subsequent aggregation process are not understood. This lack in understanding may explain why it has not yet been possible to mimic the transition process from PrP^{C} to infectious PrP^{Sc} *in vitro.* Nevertheless working with the prion protein *in vitro* is indispensable since it allows working with highly purified protein. Moreover, it allows to dissect the transition of PrP^{C} into the infectious form into several steps and to clarify which step is actually missing to generate *de novo* infectivity.

The aim of this study was therefore to improve an earlier established *in vitro* conversion system for PrP to a better adaptation to the *in vivo* situation (cf. Introduction). The system should allow

a.) to differentiate between reversible and irreversible structural transitions on the pathway from PrP^{C}-like to PrP^{Sc}-like conformations,

b.) an induction of highly ordered aggregation following the structural transition process and

c.) to study the newly formed structures not only in regard to commonly accepted markers like PK-resistance but finally also to infectivity.

Such a conversion system would also allow studies on the influence of additional components that may play a role in the transition process or the following aggregation. Any factor or component could selectively be added to the system at any stage of the transition or aggregation process and be analyzed for their influence.

The SDS-dependent *in vitro* conversion system that was improved in this study is based on earlier investigations of this group (Riesner *et al*., 1996). It had been shown that SDS can be used not only to solubilize PrP 27-30, but also to induce structural transitions between various conformations of the prion protein on the pathway from PrP^{C}-like to PrP^{Sc}-like isoforms (Post

et al., 1998 ; Leffers, 1999; Jansen *et al*., 2001; Jansen, 2002). In the first part of this study the reversibility of the transition process from PrP^{C}-like to PrP^{Sc}-like isoforms was analyzed using the described SDS-dependent *in vitro* conversion system.

4.1 Reversibility, irreversibility and kinetics of structural transitions of the prion protein as induced by SDS

Earlier studies had shown that it is possible to induce a structural transition of the PrP^{C}-like, SDS-solubilized rec PrP (90-231) to a PrP^{Sc}-like isoform, i.e. β-structured multimers (Post *et al*., 1998). This was achieved by diluting the SDS in the samples down to concentrations ≤ 0.01 % SDS. This finding could be reproduced in this study (cf. 3.1.1). The transition process included intermediates like an α-helical dimer at ~0.06 % SDS and soluble, β-structured oligomers at ~0.04 % SDS. Analyzing the kinetics of the processes (cf. Figure 3.2) confirmed earlier findings: Formation of the α-helical as well as of the soluble β-structure starting from a partially denatured structure at 0.2 % SDS was fast. In contrast, shifting the equilibrium between both structures was very slow (Jansen, 2002).

In the present study also the reverse direction of the transitions was examined: Various concentrations of SDS were added to the detergent-free, soluble and α-helical rec PrP (90-231) (cf. 3.1.2). Low amounts of SDS (0.005 - 0.01 %) led to an instant transition to β-structured, aggregated rec PrP (90-231). This process was so fast that up to SDS-concentrations of 0.03 % SDS it was not possible to follow the transition within the experimental time for conventional CD-spectroscopy, i.e. 20 minutes (cf. Figure 3.3). Further addition of SDS led to soluble, β-structured rec PrP (90-231) at 0.04 - 0.06 % SDS which was in a slow equilibrium with the mainly α-helical rec PrP (90-231) (cf. Figure 3.4). When more SDS was present, rec PrP (90-231) was transformed into a soluble, mainly α-helical seconddary structure (cf. Figure 3.3).

By comparing these two sets of experimental data a number of effects were observed:

At intermediate SDS-concentrations, i.e. 0.02 % - 0.06 %, a slow equilibrium between mainly α-helical and β-structured forms of PrP can be observed. The β-structured forms can assemble into oligomers, the structural transition is reversible. Moreover it does not matter whether the SDS-concentration is adjusted starting from 0 % or 0.2 % SDS, since both treatments result in establishment of the described slow equilibrium (cf. 3.1.1 & 3.1.2).

In contrast, at low SDS-concentrations (0 % - 0.01 %) it is important from which direction the SDS-concentration is adjusted: When SDS is diluted from 0.2 % e.g. to 0.01 % SDS, PrP changes its conformation to a β-structure in connection with fast aggregation (Post *et al.*, 1998). When the remaining SDS is now washed out, the secondary structure and the state of aggregation of the PrP does not change measurably any more. The present studies, however, have demonstrated that addition of SDS lower than 0.005 % to a detergent-free protein solution leaves the conformation partially soluble and not in β-structured aggregates. Consequently, the conformational state of rec PrP (90-231) in the concentration range between 0 % and 0.01 % depends upon the direction of establishing the SDS-concentration.

4.2 A Mechanistic model for the structural transitions of rec PrP (90-231) as induced by SDS *in vitro*

Both treatments, i.e. addition of low amounts of SDS to detergent-free rec PrP (90-231) and dilution of SDS from rec PrP (90-231) solubilized in 0.2 % SDS to ≤0.01 % SDS, allow induction of β-structured multimers. When the binding of SDS to PrP at these low SDS-concentrations was further investigated it could be shown that as little as 5 molecules of SDS bind per molecule of rec PrP (90-231) at 0.005 - 0.01 % SDS (cf. Figure 3.5). This result suggests that distinct binding sites for SDS must exist that lead to a transition of rec PrP (90-231) to a β-structured, aggregated state.

Together with other studies in our group we have now a fairly complete picture of the SDS-binding to the different conformations of rec PrP (90-231) (cf. Figure 4.1):

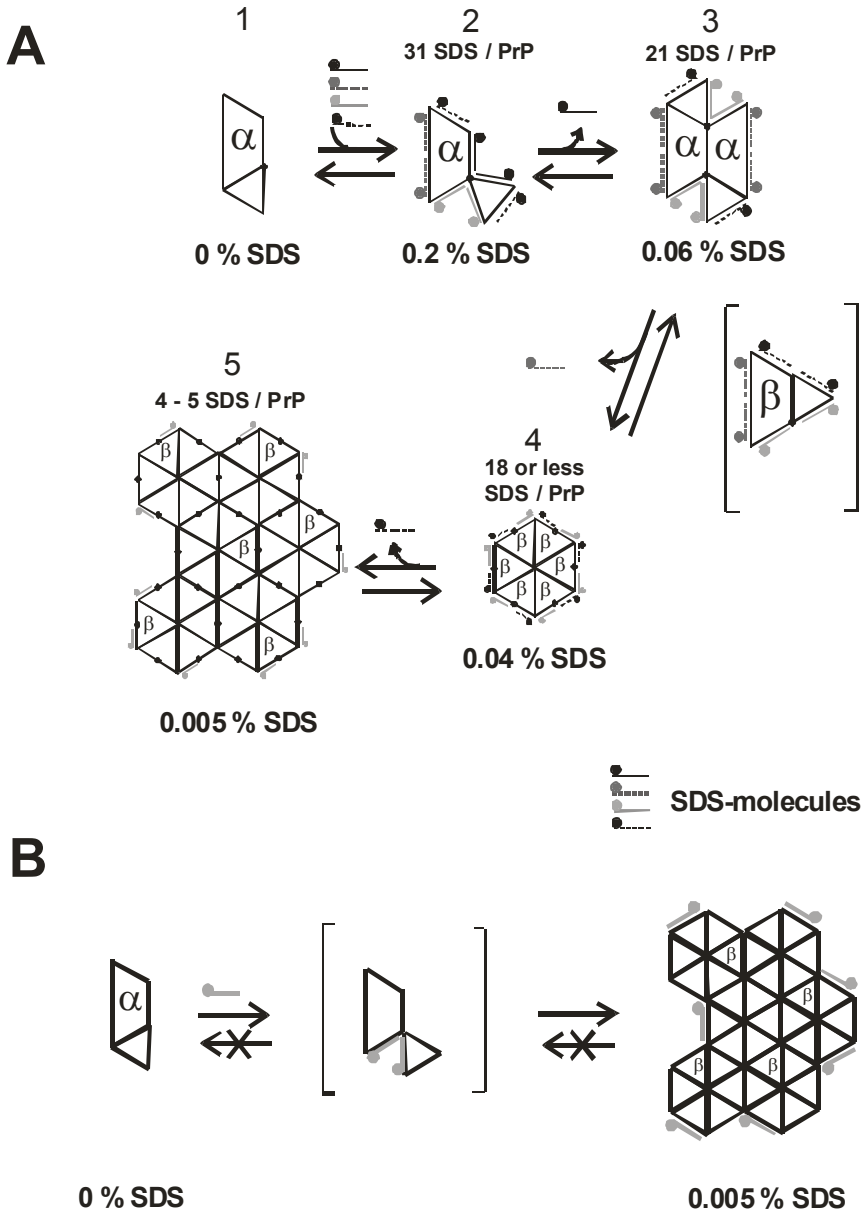

Figure 4.1: Model for the *in vitro*-conversion of rec PrP (90-231) induced by SDS.
(A) SDS-decrease: Model for the structural transitions that occur when rec PrP (90-231) is solubilized in 0.2 % SDS followed by subsequent, gradual removal of SDS. **(B)** SDS-increase: Model for the structural transition that occurs when small amounts of SDS are added to detergent-free, soluble rec PrP (90-231).

a.) Structural transitions and aggregation induced by SDS-decrease

Four conformational transitions and consequently at least five different conformational states were identified for rec PrP (90-231) in the presence of varying concentrations of SDS. Thus, it has to be concluded that at least four different types of binding sites for SDS are present on the surface of PrP: As determined by CD-spectroscopy and sedimentation equilibrium runs in an analytical ultracentrifuge ~31 SDS molecules bind to a slightly denatured but otherwise α-

helical monomeric PrP at 0.2 % SDS (Jansen, 2002). Given as a weight ratio it means that 0.5 g SDS binds to 1 g protein which corresponds roughly to normal binding of SDS to proteins at room temperature. One can assume, however, that in this state a portion of the SDS molecules are bound to interior sites of PrP and lead to a partial denaturation (cf. Fig. 4.1 A, state 2). Further analysis again using sedimentation equilibrium runs in an analytical ultracentrifuge revealed that about 10 SDS molecules are released from PrP after lowering SDS to ~0.06 %. Also renaturation to a higher α-helix content was achieved (cf. Fig. 4.1 A, state 3). This renaturation is concomitant with dimerization of PrP as shown before by Jansen et al. (Jansen *et al*., 2001). Therefore one can assume that the additional α-helical structure is stabilized by intermolecular hydrophobic interactions. These become accessible after the release of ~10 SDS molecules per molecule of PrP.

The transition from an α-helical dimer to a β-structured 12- to 16-mer (cf. Figure 4.1 A, state 4) is induced by the cooperative release of at least ~2-3 SDS molecules per PrP molecule. This can be concluded following calculations using a modified Hill plot (cf. 3.1.3, Figure 3.6). Additionally, it is obvious from the transition curve that the whole transition reaches its equilibrium only after 24 hours (cf. Fig. 3.2). Although the transition states can not be investigated experimentally, one can speculate that the α-helical dimers dissociate and that single molecules switch to a β-structured conformation. This form may then, however, be stabilized only by intermolecular interaction of at least 12 molecules of rec PrP (90-231). Consequently two factors may contribute to the slow reaction: (1) The high energy intermediate as suggested in Fig. 4.1 (in brackets) and (2) the oligomolecular reaction type, transferring six dimers into one dodecamer – or even larger. At least a significant contribution to the activation barrier must originate from the suggested high-energy intermediate: It was shown earlier by Post et al. (Post *et al*., 1998) that β-structured oligomers were formed much faster (in 10 to 20 minutes), when they were formed directly from the partially denatured, α-helical monomers without passing through the α-helical dimers.

Dilution of the SDS-concentration below 0.03 % leads to a continuous release of SDS molecules with concomitant aggregation and insolubility.

b.) Structural transitions and aggregation induced by SDS-increase

The question was raised how the transition of PrP can be induced without passing through the whole series of transition as depicted in Fig. 4.1 A, i.e. adding 0.2 % SDS and diluting it out stepwise. Indeed, when small amounts of SDS were added to an aqueous solution of rec PrP (90-231) (cf. Fig. 4.1 B), it directly switched over to a state similar to state 5 as seen in

Fig. 4.1 A. As little as 5 SDS molecules per PrP had to be bound to establish the β-structured aggregates (cf. 3.1.3, Fig. 3.5). Presumably, they occupy the strongest binding sites. It can be assumed that the binding of 5 SDS molecules partially denatures the α-helical structure (SDS molecules shown in light grey in Fig. 4.1 B) and thereby facilitates the switch to the β-structure.

Altogether re-evaluation of earlier data (Jansen 2002) and the new data presented here allows the following conclusions: Depending on the amount of SDS added to a protein sample or diluted from 0.2 % SDS the detergent induces a specific, structural transition that keeps the protein in a PrP^{C}-like or a PrP^{Sc}-like form. At intermediate SDS-concentrations not only reversibility between α-helical and β-structure-rich secondary structures in PrP can be observed but also reversibility between PrP-oligomers and -polymers. This situation is expected to be ideal for the formation of ordered structures like amyloid fibrils.
Therefore the next part of this study dealt with finding conditions for the SDS-dependent *in vitro* conversion system that resulted in formation of amyloid fibrils as sometimes found in association with prion diseases.

4.3 Fibril formation of the prion protein *in vitro* requires an initial soluble β-structure, the presence of sodium chloride and long incubation times

Very small amounts of SDS induce a fast aggregation into amorphous plaques as earlier studies have shown (Post *et al*., 1998). The working-hypothesis of this study was that conditions inducing soluble β-structures might allow a slow, well ordered aggregation and lead to formation of amyloid fibrils as observed in association with neurodegenerative diseases *in vivo* (cf. above).
Other groups have shown that the presence of sodium chloride is essential for highly ordered aggregation of PrP (Jackson *et al*., 1999; Swietnicki *et al*., 2000; Baskakov *et al*., 2001; Xiong *et al*., 2001). Hence, the systematic aggregation studies of this work included variation of sodium chloride (0 - 250 mM), which is close to the physiological concentration of 150 mM. Prior to this treatment the samples were forced into a soluble β-structure using SDS. The samples were then analyzed in respect to solubility and formation of highly structured aggregates over longer incubation times at 37 °C:

It was possible to induce *in vitro* aggregation - including fibril formation - for various forms of PrP (cf. 3.2, Figures 3.8 - 3.11). Earlier studies have shown that formation of amyloid fibrils can be induced with rec PrP (90-231) as minimal construct using the same SDS-dependent *in vitro* conversion system as described in this study (Stoehr 2003). Rec PrP (90-231) consists of amino acids 90-231 of the prion protein and does not carry any posttranslational modifications. Hence, the first 89 amino acids and the posttranslational modifications are not necessary for formation of amyloid fibrils. On the other side the presence of the complete amino acid chain and posttranslational modifications does not constrict formation of amyloid fibrils as the present study has shown. Both sol PrP 27-30 and elu PrP 27-30 carry all posttranslational modifications typical for PrP but lack the first 89 amino acids. Formation of amyloid fibrils could be induced by slight variation of the conditions found by Stoehr for rec PrP (90-231): Samples containing rec PrP (90-231) needed to be adjusted to 0.03 % SDS to force the protein into a soluble β-structure resulting in slow aggregation including amyloid fibrils (Stoehr 2003). In contrast, samples containing sol PrP 27-30 or elu PrP 27-30 needed to be adjusted to 0.01 % SDS to induce the same effect (cf. 3.2.1 & 3.2.2). Most important, it was possible to induce fibril formation *in vitro* even with native, full length PrP^{C} indicating that PrP^{C} is capable to form structures comparable to the ones of PrP^{Sc} as found in scrapie-affected animals (cf. 3.2.4, Figure 3.11).

Additionally, the effect of the presence of lipids as found in caveolae- or raft-like domains, i.e. sphingomyelin, galactosyl cerebroside and cholesterol, was studied: These lipids made fibril formation of posttranslationally modified PrP more efficient (cf. 3.2.3 & 3.2.4). Control experiments without these lipids revealed though that they were not strictly necessary for fibril formation (cf. Figure 3.10, 3.11 C). These results allow the formulation of a general model for the conversion from PrP^{C}-like to PrP^{Sc}-like states (cf. Figure 4.2):

PrP 27-30 can be solubilized and eluted from SDS-PAGE resulting in the PrP^{C}-like form elu PrP 27-30. This and other forms of PrP, i.e. rec PrP (90-231) (Stoehr, 2003) and native, full length PrP^{C} can be converted into a PrP^{Sc}-like structure: This is achieved by adjusting the samples to conditions that allow formation of higher aggregates including amyloid fibrils probably via an intermediate designated PrP*. According to the present study, PrP* might be a high-energy intermediate that contains an increased β-structure and is soluble (cf. 3.1.1). Since the conditions used in this SDS-dependent *in vitro* conversion system led to slow aggregation it can be suggested that PrP* is in an equilibrium with soluble, β-structured oligomers and to a low degree with soluble, α-helical dimers. From the β-structured oligomers

higher aggregation resulting mainly in amorphous aggregates or sometimes in amyloid fibrils may occur as shown in the model.

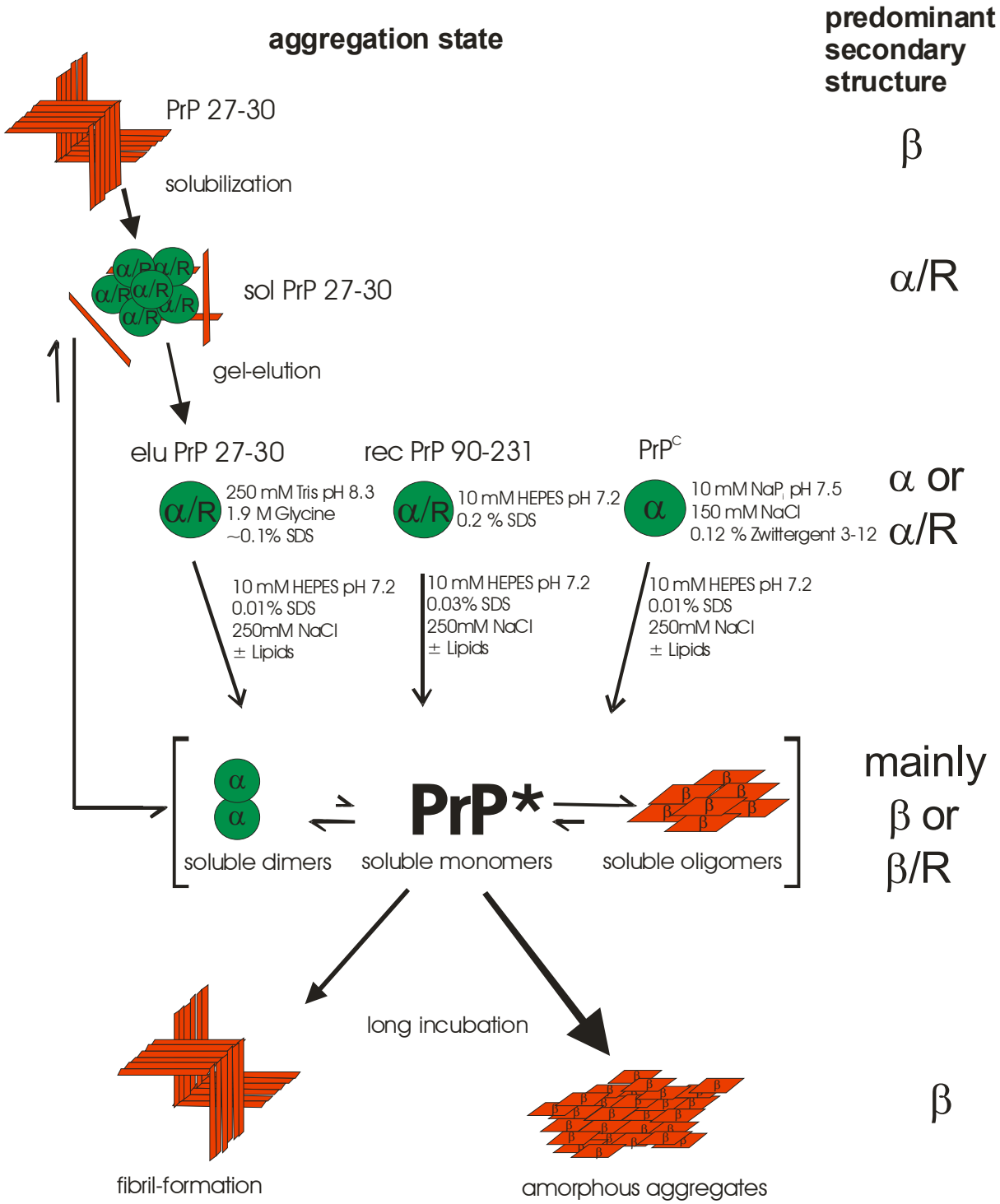

Figure 4.2: Model for *in vitro*-conversion including fibril formation of various forms of PrP.
PrP 27-30 can be solubilized into a monomeric, non-infectious form by treatment with 0.2 % SDS and sonication followed by elution from SDS-PAGE gels. This from of PrP designated elu PrP 27-30 has properties similar to rec PrP (90-231) and PrP^C. When these forms of PrP are adjusted to low concentrations of SDS and 250 mM NaCl, a soluble, β-structured state designated PrP* is favoured which is in an equilibrium with soluble, β-structured oligomers and with soluble, α-helical dimers. After prolonged incubation times of 5 – 6 weeks mainly amorphous aggregates form, but amyloid fibrils can also be observed. In the presence of sphingomyelin, galactosyl cerebroside and cholesterol fibril formation is enhanced.

4.4 Amyloid fibrils of PrP can be generated *in vitro* using various approaches

The present study has shown that the described SDS-dependent *in vitro* conversion system can be used to induce slow aggregation of the prion protein including formation of amyloid fibrils. It has been shown before and during this study that other approaches led to similar results:
A recombinant form of N-terminally truncated human PrP designated human rec PrP 91-231 could be forced into a β-structured conformation by reduction of the disulfide bond and lowering the pH to 4.0 (Jackson *et al.*, 1999). Like in our conversion system, the transition from α-helical to β-structured conformations was reversible, in this case induced by variation of the pH: At pH 8.0 the α-helical conformation dominates, whereas lowering the pH induced a reversible transition to a β-structured conformation. Moreover, e.g. the addition of salt, i.e. 150 mM NaCl or KCl, led to formation of amyloid fibrils starting from the soluble, β-structured conformation. However, since it could be shown that infectious PrP 27-30 has an intact disulfide bond (Turk *et al.*, 1988; Welker *et al.*, 2002), the relevance of these findings remained unclear. The conversion system described in the present study allows induction of amyloid fibrils from PrP leaving the disulfide bond intact thus being closer to the *in vivo* situation.
In another study that was carried out parallel to this work conditions could be found that force SHa rec PrP (90-231) and Mo rec PrP (89-231) into a slow equilibrium between monomeric, α-helical and oligomeric, β-structured isoforms similar to the one described in this study (Baskakov *et al.*, 2001; Baskakov *et al.*, 2002). In this case the protein was refolded after total

denaturation in 10 M urea. At intermediate urea concentrations (4 M) the equilibrium between α-helical and β-structured isoforms could be established. Fibril formation occurred – again in the presence of salt (200 mM NaCl) – within several hours to days depending on the pH of the solution. In contrast to the conversion system described in the present study, this system required an initial total denaturation of the protein followed by a refolding procedure that led to formation of amyloid fibrils under yet harsh conditions compared to *in vivo* conditions.

Finally studies have been carried out using other detergents to induce formation of amyloid fibrils (Xiong *et al.*, 2001): In the presence of 0.01 % sarkosyl SHa rec PrP (23-231) forms a small fraction of amyloid fibrils after 4 - 40 days of incubation when at the same time the pH is adjusted to pH 6.5 and 100 mM NaCl are added. However, in these studies no detailed information was collected about the transition process thus it remains unclear if addition of sarkosyl also leads to an equilibrium between α-helical and β-structured isoforms as described in the present study and the studies mentioned above.

Other studies in the same group have focused on the effect of the association of the prion protein to raft-like membranes rich in sphingomyelin and cholesterol in respect to conversion reactions (Baron *et al.*, 2002). These studies revealed that PrP^{C} resists conversion to a PrP^{Sc}-like form when attached to a membrane. Only when the PrP^{C} was removed from the membranes or when the incoming PrP^{Sc} was inserted into the raft-like membranes a conversion could be induced. However, in this case the conversion reaction was induced using a seed of PrP^{Sc} which makes it difficult to follow *de novo* generation of PrP^{Sc} from PrP^{C}. Formation of amyloid fibrils in the presence of lipids as shown in the present study could not be shown. Moreover, the marker used for detection of the conversion reaction was PK-resistance which has not proven to be a reliable marker for PrP^{Sc} (*for review*: Wille *et al.*, 2000).

4.5 Several models describe transition and aggregation processes of the prion protein

A number of approaches have been made to explain the replication process of PrP^{Sc}. The three most commonly accepted models dealing with this process are (1) the "*template assistance*"-model by Cohen & Prusiner (*for review*: Cohen & Prusiner, 1998), (2) the "*cooperative Prusiner*"-model derived by Eigen (Eigen 1996) and (3) the *"seeded nucleation"*-model by

Lansbury & colleagues (*for review*: Rochet & Lansbury, 2000) (cf. Introduction). All models involve a structural transition of PrP via an intermediate that is characterized by a partially denatured secondary structure with increased β-sheet content. Comparing these models with the model derived from experiments with the SDS-dependent *in vitro* conversion system described in the present study, several similarities can be found:

All models describe a structural transition from PrP^{C} or PrP^{C}-like conformations to PrP^{Sc} or PrP^{Sc}-like conformations. This transition might occur via a high energy barrier. According to the mentioned models this barrier might be due to the formation of an intermediate with increased β-structure. Moreover, the structural transition is in some way connected to aggregation processes that - in the case of the *"seeded nucleation"*-model and our model - might include formation of well ordered aggregates like amyloid fibrils. The other mentioned models do not exclude this possibility, but neither do they postulate a correlation between infectivity and formation of amyloid fibrils. In contrast e.g. the "*template assistance*"-model favours the hypothesis that the information for infectivity is at least to a high degree if not completely enciphered in the secondary structure of PrP^{Sc}. This hypothesis is difficult to prove e.g. with bioassays since degradation and "clearance effects" in the brains of humans and animals lead to fast washing out of intracerebrally inoculated samples. Single molecules, however, even if potentially infectious, might be degraded or washed out before they can induce an infection. It can be assumed that bigger aggregates composed of infectious PrP have a better chance to resist the described processes at least for the time needed to induce infection of the inoculated host. The following replication circle for PrP^{Sc} is thought to be faster than degradation and clearance-mechanisms once a certain threshold is crossed.

The major advantage of the model described in this study is that almost all of the intermediate stages depicted in Fig 4.2 except PrP* could be stabilized *in vitro* and characterized thoroughly in this or other studies in our group (Jansen 2002). The fact that PrP* could not be stabilized can simply be explained by the fact that PrP* might be a high-energy intermediate as suggested before (cf. 4.2 & 4.3). Moreover, the model described in the current study was verified by carrying out similar experiments with various forms of PrP. Taken together these experiments led to a comprehensive model of the structural transition and aggregation of the prion protein. However, bioassays needed to be carried out to verify how close the *in vitro* characterized protein structures and aggregates come to the *in vivo* occurring, infectious prion protein. This will be discussed in further detail below.

4.6 Amyloid fibrils generated using the SDS-dependent *in vitro* conversion system are PK-sensitive and do not reveal significant infectivity

In the last part of this study the relationship between formation of amyloid fibrils, proteinase K (PK)-resistance and infectivity of PrP was further investigated. The experiments revealed that no significant proteinase K resistance was generated by the formation of fibrils *in vitro* (cf. Figure 3.12). Furthermore, it could be shown that the generated fibrils are no more resistant to digestion than the amorphous aggregates (cf. 3.3, Figure 3.13). This similar behaviour in regard to PK-resistance in spite of the different ultrastructure might be a matter of spatial accessibility to PK: The amorphous aggregates were fairly large and therefore poorly accessible to PK. In contrast, the fibrils were narrower but of higher order and thus more tightly packed, which might have made it difficult for the proteinase to degrade the protein.

Even though the newly generated fibrils differ from PrP^{Sc} in respect to PK-resistance, the samples were tested for infectivity. This was done since this is the first time that infectivity tests for fibrils formed *in vitro* from native, full length PrP^{C} could be carried out. Additionally other studies have shown that infectivity does not always correlate with PK-resistance (*for review*: Wille *et al.*, 2000), which makes this marker questionable as basis for differentiation between PrP^{C} and PrP^{Sc}. However, as shown in table 3.1, no significant infectivity could be measured for the *de novo*, *in vitro* generated fibrils after 408-457 days of incubation.

The fact that the mice infected with *in vitro* generated fibrils did not develop clinical signs of scrapie after this long incubation time might have different reasons:

The simplest explanation for the lack of infectivity in the samples might be a so called “clearance effect”: It is known that protein inoculated intracerebrally is washed out to a high degree within a very short time after inoculation. Since the samples of newly generated fibrils only contained a small fraction of fibrils and their precursors, the concentration of the infectious agent might simply not have been high enough to lead to effective infection of the animals as infection of 1/5 mice inoculated with newly formed fibrils from PrP^{C} in the presence of lipids might indicate. To rule out this possibility the experiments would have to be repeated with higher amounts of amyloid fibrils. Moreover, the brain homogenate of the mice could be passaged to a second generation to evaluate whether subclinical amounts of the scrapie agent were present in the animals that might become clinical when inoculated to the second generation of mice. Similar observations have been reported before in context with other infectivity studies (Lasmezas *et al*., 1996).

A more complex explanation for the lack of infectivity might be found in connection with the problems associated with *in vitro* studies of the prion protein: Purifying PrP and inducing transitions *in vitro* leads to changes in the protein samples that cannot fully be detected by the methods used in this study. This indicates that it is unclear how close the newly, *in vitro* generated fibrils of PrP are to the infectious PrP^{Sc} or PrP 27-30 as found in prion rods even if they are structurally very similar to infectious PrP. Obviously factors affecting fibril formation lead to a PrP^{Sc}-like conformation, but this does not include infectivity. There may still be a factor or a combination of factors missing to induce a scrapie-infection. One possible factor might be the polyglucose scaffold found in association with prion rods. The role of this scaffold in regard to infectivity is currently analyzed in another study in our group (*see also*: Dumpitak 2003).

Taking current models into account to explain the lack of infectivity, fibrils may actually not lead to infection with prion diseases, but only play a role in the pathogenesis of the disease: Instead of being responsible for the infection, the fibril or other higher aggregates might instead be a neuroprotective end-product to inhibit neurotoxicity: This suggestion is based on the hypothesis that precursors of fibrils, i.e. oligomeric intermediates or protofibrils, might be responsible for neurotoxicity. This may occur through the formation of pores similar to the pore-forming fibrils of α-synuclein or Aβ, which can compromise the integrity of membranes (*for review*: Caughey & Lansbury, 2003). Also it has been observed that *in vitro* formed aggregates of PrP have often caused neurotoxicity but so far never infectivity (Post *et al*., 2000). It should be noted that it has been shown before that PrP^{Sc} can induce neurotoxicity, but this requires the expression of PrP^{C} (Brandner *et al*., 1996). Altogether it remains unclear how and if infectivity and neurotoxicity are related in respect to structural aspects in prion diseases.

4.7 Conclusions / Outlook

In regard to the aims set at the beginning of this study (cf. 1.8) it can be concluded that

1.) Further studies on the earlier established SDS-dependent *in vitro* conversion system have shown that induction of reversible structural transitions from PrP^{C}-like to PrP^{Sc}-like isoforms was possible at intermediate SDS-concentrations. Moreover, structural transitions at low SDS-concentrations proved to be irreversible.

2.) When the described SDS-dependent *in vitro* conversion system is tuned to conditions that induce formation of soluble β-structured PrP the protein slowly aggregated in the presence of sodium chloride. This aggregation included the formation of amyloid fibrils.

3.) Formation of amyloid fibrils was enhanced by the presence of sphingomyelin, galactosyl cerebroside and cholesterol, but the presence of these lipids was not necessary for fibril formation itself.

4.) Amyloid fibril formation could be induced with rec PrP (90-231 (Stoehr 2003), elu PrP 27-30 and with native, full length PrP^{C}; hence, the first 89 amino acids of the protein sequence and the posttranslational modifications were not necessary for fibril formation in this system.

5.) Amyloid fibrils generated using the SDS-dependent *in vitro* conversion system were PK-sensitive and did not reveal significant infectivity; therefore factors affecting fibril formation do not necessarily affect generation of infectivity as well.

Looking at future projects in this context it should be possible to stabilize several of the intermediate states in the aggregation process of PrP^{Sc}-like isoforms analyzed in this *in vitro* conversion system. Further studies can be carried out to evaluate the role of fibrils as well as their precursors in respect to infectivity and neurotoxicity: Since the transitions are very slow, it should be possible to prepare aggregates of different sizes and to test them for their function.
In regard to the electron microscopic analysis this study has shown that it was possible to specifically label the newly, *in vitro* generated amyloid fibrils using the antibody huFab D18

(cf. Figure 3.10). This antibody recognizes both PrP^{C} and PrP^{Sc} which made it impossible to verify whether the newly formed fibrils had a mainly PrP^{C}-like or PrP^{Sc}-like character. The design of an antibody specific for PrP^{Sc} would allow verification of the PrP^{Sc}-like character of the newly, *in vitro* generated amyloid fibrils starting from PrP^{C}-like isoforms. There are reports about such an antibody (Korth *et al*., 1997), but in this special case the reported antibody 15B3 is not specific for hamster-PrP as used in this study. Moreover it remains to be tested whether such an antibody would be suitable for the immunogold-labeling techniques used in this study.

In summary the described experiments resulted in the design of a convenient *in vitro* conversion system that allowed induction of structural transitions from PrP^{C}-like to PrP^{Sc}-like states including a range of intermediates for various forms of PrP. The transition is followed by a partially specific aggregation resulting in structures similar to the ones found in association with prion diseases *in vivo*. This allows comparative studies as well as collection of detailed information on amorphous and specific structures including their precursors that may help to find the missing link between structure formation and generation of infectivity in prion diseases.

5. Summary

Prions are the causative agent of neurodegenerative diseases affecting animals and humans. To date all attempts to prove the "*protein-only*" hypothesis by *de novo* generation of infectivity *in vitro* have failed. The main aim of these attempts was to mimic the structural transition from the normal, non-infectious PrP^{C} to the abnormal, infectious PrP^{Sc} *in vitro*. This study focused on designing an *in vitro* conversion system that would allow induction of the described transition process followed by specific aggregation resulting in amyloid fibrils as sometimes found in association with prion diseases. Furthermore, the resulting structures were analyzed for scrapie-related markers, i.e. resistance to digestion with proteinase K and infectivity as measured in bioassays.

In order to reach these aims, the transition process from PrP^{C}-like to PrP^{Sc}-like isoforms was further analyzed using an SDS-dependent *in vitro* conversion system. It could be confirmed that PrP can be converted to a soluble β-structure at intermediate SDS-concentrations. This aggregation prone intermediate was then incubated *in vitro* at conditions close to the *in vivo* situation using neutral pH, close to physiological concentrations of sodium chloride and a temperature of 37 °C for several weeks. Additionally, the effect of lipids - as found in prion rods - was analyzed.

The experiments revealed that starting from soluble, β-structured PrP a slow and to some degree specific aggregation, i.e. formation of amyloid fibrils, could be induced. The presence of sphingomyelin, galactosyl cerebroside and cholesterol enhanced fibril formation, but was not necessary to induce it. It could be shown for the first time that native, full length PrP^{C} from brains of uninfected hamsters can form amyloid fibrils similar to those found in association with prion diseases.

However, the *in vitro* generated fibrils showed neither the scrapie-related PK-resistance nor significant infectivity after incubation of ~420 days.

The SDS-dependent *in vitro* conversion system allowed the collection of detailed information on the structural transition and subsequent aggregation process of PrP: Various intermediate stages of these processes can be stabilized and analyzed in greater detail, moreover the effect of various other secondary components can be investigated which may help to finally find the missing link between structure formation and generation of infectivity in prion diseases.

6. Zusammenfassung

Prionen sind die Erreger einer neurodegenerativen Erkrankung, die Prionkrankheit genannt wird und sowohl Tiere als auch Menschen befällt. Bisher sind alle Versuche, die "*protein-only*"-Hypothese durch *de novo* Generierung von Infektiosität *in vitro* zu beweisen, fehlgeschlagen. Ziel dieser Versuche war, die strukturelle Umfaltung des normalen, nicht infektiösen PrP^{C} in das abnormale, infektiöse PrP^{Sc} *in vitro* zu induzieren. Im Rahmen dieser Arbeit sollte ein *in vitro*-Konversionssystem entwickelt werden, dass die Induktion der beschriebenen strukturellen Umfaltung erlaubt, gefolgt von einer spezifischen Aggregation. Dies sollte zur Bildung amyloider Fibrillen führen wie sie manchmal in Kontext mit Prionkrankheiten gefunden werden. Außerdem sollten die neu entstandenen Strukturen auf Scrapie-typische Marker wie z.B. PK-Resistenz und Infektiosität hin untersucht werden.

Um diese Ziele zu erreichen wurde zunächst der Umfaltungsprozess von PrP^{C}-ähnlichen zu PrP^{Sc}-ähnlichen Isoformen mit Hilfe eines SDS-abhängigen *in vitro*-Konversionssystems weitergehend analysiert. Es konnte bestätigt werden, dass PrP bei mittleren SDS-Konzentrationen in eine lösliche β-Struktur überführt werden kann. Dieses zu Aggregation neigende Intermediat wurde dann *in vitro* inkubiert unter Bedingungen, die der *in vivo*-Situation nahe kommen: Neutraler pH, 250 mM Natriumchlorid und eine längere Inkubation bei 37 °C. Des Weiteren wurde der Effekt von Lipiden, die in prion rods gefunden wurden, analysiert.

Die Experimente zeigten, dass unter den beschriebenen Bedingungen und ausgehend von löslichem, β-strukturiertem PrP eine langsame und zum Teil geordnete Aggregation induziert werden kann, d.h. es entstanden u.a. amyloide Fibrillen. Die Gegenwart von Sphingomyelin, Galaktosylcerebrosid und Cholesterol verstärkt die Bildung amyloider Fibrillen, ist aber nicht nötig, um die Bildung der Fibrillen zu induzieren. Es konnte zum ersten Mal gezeigt werden, dass natürliches Volllängen-PrP^{C} aus dem Hirn nicht infizierter Hamster amyloide Fibrillen bilden kann, wie man sie auch in Assoziation mit Prionkrankheiten finden kann. Dennoch zeigten diese *in vitro* generierten Fibrillen weder die Scrapie-typische PK-Resistenz noch signifikante Infektiosität nach einer Inkubationszeit von ~420 Tagen. Das etablierte SDS-abhängige *in vitro*-Konversionssystem erlaubt nun das Sammeln weiterer, detaillierter Informationen bezüglich des Umfaltungsprozesses von PrP samt folgender Aggregation: Einige Intermediate des Systems können stabilisiert und weitergehend analysiert werden. Des Weiteren kann der Effekt von anderen sekundären Komponenten analysiert werden. Dies könnte helfen die fehlende Verbindung zwischen Strukturbildung und Infektiosität bei Prionkrankheiten zu finden.

7. References

Alper, T., Cramp, W. A., Haig, D. A., & Clarke, M. C. (1967). Does the agent of scrapie replicate without nucleic acid? *Nature* **214**, 764-766.

Appel, T. R., Dumpitak, C., Matthiesen, U., & Riesner, D. (1999). Prion rods contain an inert polysaccharide scaffold. *Biol.Chem.* **380**, 1295-1306.

Baron, G. S., Wehrly, K., Dorward, D. W., Chesebro, B. & Caughey, B. (2002). Conversion of raft associated prion protein to the protease-resistant state requires insertion of PrP-res (PrP^{Sc}) into contiguous membranes. *EMBO* **21**, 1031-1040.

Baron, G. S. & Caughey, B. (2003). Effect of glycosylphosphatidylinositol anchor-dependent and -independent prion protein association with model raft membranes on conversion to the protease-resistant isoform. *J.Biol.Chem.* **278**, 14883-14892.

Baskakov, I. V., Legname, G., Prusiner, S. B., & Cohen, F. E. (2001). Folding of prion protein to its native {alpha}-helical conformation is under kinetic control. *J.Biol.Chem.* **276 (23)**, 19687-19690.

Baskakov, I. V., Legname, G., Baldwin, M. A., Prusiner, S. B. & Cohen, F. E. (2002). Pathway complexity of prion protein assembly into amyloid. *J.Biol.Chem.* **277 (24)**, 21140-21148.

Belay, E. D. (1999). Transmissible spongiform encephalopathies in humans. *Annu.Rev.Microbiol.* **53**, 283-314.

Bons, N., Mestre-Frances, N., Charnay, Y., Salmona, M., & Tagliavini, F. (1996). Spontaneous spongiform encephalopathy in a young adult rhesus monkey. *C.R.Acad.Sci.III* **319**, 733-736.

Brahms, S. & Brahms, J. (1980). Determination of protein secondary structure in solution by vacuum ultraviolet circular dichroism. *J.Mol.Biol.* **138**, 149-178.

Brandner, S., Raeber, A., Sailer, A., Blattler, T., Fischer, M., Weissmann, C., & Aguzzi, A. (1996). Normal host prion protein (PrPC) is required for scrapie spread within the central nervous system. *Proc.Natl.Acad.Sci.U.S.A* **93**, 13148-13151.

Brown, D. R., Qin, K., Herms, J. W., Madlung, A., Manson, J., Strome, R., Fraser, P. E., Kruck, T., von Bohlen, A., Schulz-Schaeffer, W., Giese, A., Westaway, D., & Kretzschmar, H. (1997). The cellular prion protein binds copper *in vivo*. *Nature* **390**, 684-687.

Brown, D. R., Wong, B. S., Hafiz, F., Clive, C., Haswell, S. J., & Jones, I. M. (1999). Normal prion protein has an activity like that of superoxide dismutase. *Biochem.J.* **344 Pt 1**, 1-5.

Bruce, M. E., Fraser, H., McBride, P. A., Scott, F. R., and Dickinson, A. G. (1992) Prion diseases of humans and animals. 497-508.

Bueler, H., Fischer, M., Lang, Y., Bluethmann, H., Lipp, H. P., DeArmond, S. J., Prusiner, S. B., Aguet, M., & Weissmann, C. (1992). Normal development and behaviour of mice lacking the neuronal cell- surface PrP protein. *Nature* **356**, 577-582.

Caughey, B., Kocisko, D. A., Raymond, G. J., & Lansbury, P. T., Jr. (1995). Aggregates of scrapie-associated prion protein induce the cell-free conversion of protease-sensitive prion protein to the protease-resistant state. *Chem.Biol.* **2**, 807-817.

Caughey, B. & Lansbury, P. T., Jr. (2003). Protofibrils, Pores, Fibrils, and Neurodegeneration: Separating the Responsible Protein Aggregates from the Innocent Bystanders. *Annu Rev Neurosci* **26**, 267-298.

Caughey, B., Raymond, G. J., Kocisko, D. A., & Lansbury, P. T., Jr. (1997). Scrapie infectivity correlates with converting activity, protease resistance, and aggregation of scrapie-associated prion protein in guanidine denaturation studies. *J.Virol.* **71**, 4107-4110.

Clarke, G., Collins, R. A., Leavitt, B. R., Andrews, D. F., Hayden, M. R., Lumsden, C. J., & McInnes, R. R. (2000). A one-hit model of cell death in inherited neuronal degradations. *Nature* **406**, 195-199.

Cohen, F. E., Pan, K. M., Huang, Z., Baldwin, M., Fletterick, R. J., & Prusiner, S. B. (1994). Structural clues to prion replication. *Science* **264**, 530-531.

Cohen, F. E. & Prusiner, S. B. (1998). Pathologic conformations of prion proteins. *Annu.Rev.Biochem.* **67**, 793-819.

Collinge, J. (1999). Variant Creutzfeldt-Jakob disease. *Lancet* **354**, 317-323.

Conway, K. A., Rochet, J. C., Bieganski, R. M., & Lansbury, P. T. (2001). Kinetic stabilization of the alpha-synuclein protofibril by a dopamine-alpha-synuclein adduct. *Science* **294**, 1346-1349.

Creutzfeldt, H. G. (1920). Über eine eigenartige herdfärmige Erkrankung des Zentralnervensystems. *Z.Gesamte Neurol Psychiatrie* **57**, 1-18.

Dobson, C. M. (1999). Protein misfolding, evolution and disease. *Trends Biochem.Sci.* **24**, 329-332.

Dougherty, R. (1964). Animal virus titration techniques in „Techniques in Experimental Virology“. Academic Press 169-224.

Dumpitak, C. (1998). Analyse von nicht-proteinartigen Komponenten in Prionen. *Master thesis*, Heinrich-Heine Universität Duesseldorf.

Dumpitak, C. (2003). Untersuchungen zu Struktur und Funktion von Polysacchariden und alterungsassoziierten Proteinmodifikationen bei Prionen. *Dissertation*, Heinrich-Heine Universitaet Duesseldorf.

Eigen, M. (1996). Prionics or the kinetic basis of prion diseases. *Biophys.Chem.* **63**, A1-18.

Fraser, H. (2000). Phillips report and the origin of BSE. *Vet.Rec.* **147**, 724-

Gajdusek, D. C. & Zigas, V. (1957). Degenerative disease of the central nervous system in New Guinea – The endemic occurrence of "kuru" in native population. *N.Engl.J.Med.* **257**, 974-978.

Gauczynski, S., Peyrin, J. M., Haik, S., Leucht, C., Hundt, C., Rieger, R., Krasemann, S., Deslys, J. P., Dormont, D., Lasmezas, C. I., & Weiss, S. (2001). The 37-kDa/67-kDa laminin receptor acts as the cell-surface receptor for the cellular prion protein. *EMBO J.* **20**, 5863-5875.

Gerstmann, J., Sträussler, E., & Scheinker, I. (1936). Über eine eigenartige hereditär-familiäre Erkrankung des Zentralnervensystems. Zugleich ein Beitrag zur Frage des vorzeitigen lokalen Alterns. *Z.Neurol.* **154**, 736-762.

Gibbons, R. A. & Hunter, G. D. (1967). Nature of the scrapie agent. *Nature* **215**, 1041-1043.

Griffith, J. S. (1967). Self-replication and scrapie. *Nature* **215**, 1043-1044.

Hill, A. F., Antoniou, M., & Collinge, J. (1999). Protease-resistant prion protein produced *in vitro* lacks detectable infectivity. *J.Gen.Virol.* **80 (Pt 1)**, 11-14.

Hjelmeland, L. M. & Chrambach, A. (1984). Solubilization of functional membrane proteins. *Methods Enzymol.* **104**, 305-318.

Hoernlimann, B., Riesner, D., and Kretzschmar, H. (2001). Prionen und Prionkrankheiten, Walter de Gruyter, Berlin New York.

Hutter, G., Heppner, F. L. & Aguzzi, A. (2003). No superoxide dismutase activity of cellular prion protein *in vivo*. *Biol. Chem.* **384**, 1279-1285.

Ironside, J. W. (1998). Neuropathological findings in new variant CJD and experimental transmission of BSE. *FEMS Immunol.Med.Microbiol.* **21**, 91-95.

Jackson, G. S., Hosszu, L. L., Power, A., Hill, A. F., Kenney, J., Saibil, H., Craven, C. J., Waltho, J. P., Clarke, A. R., & Collinge, J. (1999). Reversible conversion of monomeric human prion protein between native and fibrilogenic conformations. *Science* **283**, 1935-1937.

Jakob, A. (1921). Über eigenartige Erkrankungen des Zentralnervensystems mit bemerkenswerten anatomischen Befunden (spastische Pseudosklerose- Encephalomyelopathie mit disseminierten Degenerationsherden). *Z.Gesamte Neurol.Psychiatrie* **64**, 147-228.

Jacobs, E. & Clad, A. (1986). Electroelution of fixed and stained membrane proteins from preparative SDS-polyacrylamide gels into a membrane trap. *Anal.Biochem.* **154**, 583-589.

Jansen, K., Schafer, O., Birkmann, E., Post, K., Serban, H., Prusiner, S. B., & Riesner, D. (2001). Structural intermediates in the putative pathway from the cellular prion protein to the pathogenic form. *Biol.Chem.* **382**, 683-691.

Jansen, K. (2002). Dimere und Oligomere des Prion-Proteins als Modell fuer den Umwandlungsmechanismus von der zellulaeren Form des Prion Proteins in die pathogene Form. *Dissertation;* Heinrich-Heine Universitaet Duesseldorf.

Jeffrey, M., Goodsir, C. M., Bruce, M. E., McBride, P. A., Fowler, N., & Scott, J. R. (1994). Murine scrapie-infected neurons in vivo release excess prion protein into the extracellular space. *Neurosci.Lett.* **174**, 39-42.

Jeffrey, M., Goodsir, C. M., Bruce, M. E., McBride, P. A., Scott, J. R., & Halliday, W. G. (1992). Infection specific prion protein (PrP) accumulates on neuronal plasmalemma in scrapie infected mice. *Neurosci.Lett.* **147**, 106-109.

Jones, B. N. (1986). Amino acid analysis by o-Phthaldialdehyde precolumn derivatization and reverse phase HPLC. *Methods in Protein Microcharacterization*, 121-151.

Kaneko, K., Vey, M., Scott, M., Pilkuhn, S., Cohen, F. E., & Prusiner, S. B. (1997a). COOH-terminal sequence of the cellular prion protein directs subcellular trafficking and controls conversion into the scrapie isoform. *Proc.Natl.Acad.Sci.U.S.A* **94**, 2333-2338.

Kaneko, K., Zulianello, L., Scott, M., Cooper, C. M., Wallace, A. C., James, T. L., Cohen, F. E., & Prusiner, S. B. (1997b). Evidence for protein X binding to a discontinuous epitope on the cellular prion protein during scrapie prion propagation. *Proc.Natl.Acad.Sci.U.S.A* **94**, 10069-10074.

Kascsak, R. J., Rubenstein, R., Merz, P. A., Tonna-DeMasi, M., Fersko, R., Carp, R. I., Wisniewski, H. M., & Diringer, H. (1987). Mouse polyclonal and monoclonal antibody to scrapie-associated fibril proteins. *J.Virol.* **61**, 3688-3693.

Kellings, K., Meyer, N., Mirenda, C., Prusiner, S. B., & Riesner, D. (1992). Further analysis of nucleic acids in purified scrapie prion preparations by improved return refocusing gel electrophoresis. *J.Gen.Virol.* **73 (Pt 4)**, 1025-1029.

Klein, T. R., Kirsch, D., Kaufmann, R., & Riesner, D. (1998). Prion rods contain small amounts of two host sphingolipids as revealed by thin-layer chromatography and mass spectrometry. *Biol.Chem.* **379**, 655-666.

Korth, C., Stierli, B., Streit, P., Moser, M., Schaller, O., Fischer, R., Schulz-Schaeffer, W., Kretzschmar, H., Raeber, A., Braun, U., Ehrensperger, F., Hornemann, S., Glockshuber, R., Riek, R., Billeter, M., Wuthrich, K., & Oesch, B. (1997). Prion (PrP^{Sc})-specific epitope defined by a monoclonal antibody. *Nature* **390**, 74-77.

Kretzschmar, H. A., Prusiner, S. B., Stowring, L. E., & DeArmond, S. J. (1986a). Scrapie prion proteins are synthesized in neurons. *Am.J.Pathol.* **122**, 1-5.

Kretzschmar, H. A., Stowring, L. E., Westaway, D., Stubblebine, W. H., Prusiner, S. B & DeArmond, S. J. (1986b). Molecular cloning of a human prion protein cDNA. *DNA* **5**, 315-324.

Lansbury, P. T. (1999). Evolution of amyloid: what normal protein folding may tell us about fibrillogenesis and disease. *Proc.Natl.Acad.Sci.U.S.A* **96**, 3342-3344.

Lasmezas, C. I., Deslys, J. P., Demaimay, R., Adjou, K. T., Lamoury, F., Dormont, D., Robain, O., Ironside, J., & Hauw, J. J. (1996). BSE transmission to macaques. *Nature* **381**, 743-744.

Laemmli, U. K. (1970). Cleavage of structural proteins during the assembly of the head of bacteriophage T4. *Nature* **227**, 680-685.

Leffers, K.-W. (1999). Denaturierung, Renaturierung und Infektiosität von solubilisierten Prion-Proteinen. *Master Thesis;* Heinrich-Heine Universitaet Duesseldorf.

Liu, H., Farr-Jones, S., Ulyanov, N. B., Llinas, M., Marqusee, S., Groth, D., Cohen, F. E., Prusiner, S. B., & James, T. L. (1999). Solution structure of Syrian hamster prion protein rPrP(90-231). *Biochemistry* **38**, 5362-5377.

Lugaresi, E., Medori, R., Montagna, P., Baruzzi, A., Cortelli, P., Lugaresi, A., Tinuper, P., Zucconi, M., & Gambetti, P. (1986). Fatal familial insomnia and dysautonomia with selective degeneration of thalamic nuclei. *N.Engl.J.Med.* **315**, 997- 1003.

Mahfoud, R., Garmy, N., Maresca, M., Yahi, N., Puigserver, A., & Fantini, J. (2002). Identification of a Common Sphingolipid-binding Domain in Alzheimer, Prion, and HIV-1 Proteins. *J.Biol.Chem.* **277**, 11292-11296.

Manson, J. C., Clarke, A. R., Hooper, M. L., Aitchison, L., McConnell, I., & Hope, J. (1994). 129/Ola mice carrying a null mutation in PrP that abolishes mRNA production are developmentally normal. *Mol.Neurobiol.* **8**, 121-127.

Masters, C. L. & Richardson, E. P., Jr. (1978). Subacute spongiform encephalopathy (Creutzfeldt-Jakob disease). The nature and progression of spongiform change. *Brain* **101**, 333-344.

McGowan, J. P. (1922). Scrapie in sheep. *Scottish J.Agric.* **5**, 365-375.

McKinley, M. P., Bolton, D. C., & Prusiner, S. B. (1983). A protease-resistant protein is a structural component of the scrapie prion. *Cell* **35**, 57-62.

McKinley, M. P., Meyer, R. K., Kenaga, L., Rahbar, F., Cotter, R., Serban, A., & Prusiner, S. B. (1991). Scrapie prion rod formation in vitro requires both detergent extraction and limited proteolysis. *J.Virol.* **65**, 1340-1351.

Mehlhorn, I., Groth, D., Stockel, J., Moffat, B., Reilly, D., Yansura, D., Willett, W. S., Baldwin, M., Fletterick, R., Cohen, F. E., Vandlen, R., Henner, D., & Prusiner, S. B. (1996). High-level expression and characterization of a purified 142-residue polypeptide of the prion protein. *Biochemistry* **35**, 5528-5537.

Merz, P. A., Somerville, R. A., Wisniewski, H. M., & Iqbal, K. (1981). Abnormal fibrils from scrapie-infected brain. *Acta Neuropathol.(Berl)* **54**, 63-74.

Meyer, N., Rosenbaum, V., Schmidt, B., Gilles, K., Mirenda, C., Groth, D., Prusiner, S. B., & Riesner, D. (1991). Search for a putative scrapie genome in purified prion fractions reveals a paucity of nucleic acids. *J.Gen.Virol.* **72 (Pt 1)**, 37-49.

Mouillet-Richard, S., Ermonval, M., Chebassier, C., Laplanche, J. L., Lehmann, S., Launay, J. M. & Kellermann, O. (2000). Signal transduction through prion protein. *Science* **289**; 1925-1928.

Naslavsky, N., Shmeeda, H., Friedlander, G., Yanai, A., Futerman, A. H., Barenholz, Y., & Taraboulos, A. (1999). Sphingolipid depletion increases formation of the scrapie prion protein in neuroblastoma cells infected with prions. *J.Biol.Chem.* **274** , 20763-20771.

Pan, K. M., Baldwin, M., Nguyen, J., Gasset, M., Serban, A., Groth, D., Mehlhorn, I., Huang, Z., Fletterick, R. J., Cohen, F. E., & . (1993). Conversion of alpha-helices into beta-sheets features in the formation of the scrapie prion proteins. *Proc.Natl.Acad.Sci.U.S.A* **90**, 10962-10966.

Peretz, D., Williamson, R. A., Matsunaga, Y., Serban, H., Pinilla, C., Bastidas, R. B., Rozenshteyn, R., James, T. L., Houghten, R. A., Cohen, F. E., Prusiner, S. B., & Burton, D. R. (1997). A conformational transition at the N terminus of the prion protein features in formation of the scrapie isoform. *J.Mol.Biol.* **273**, 614-622.

Post, K., Pitschke, M., Schafer, O., Wille, H., Appel, T. R., Kirsch, D., Mehlhorn, I., Serban, H., Prusiner, S. B. , & Riesner, D. (1998). Rapid acquisition of beta-sheet structure in the prion protein prior to multimer formation. *Biol.Chem.* **379**, 1307-1317.

Post, K., Brown, D. R., Groschup, M., Kretzschmar, H. A., & Riesner, D. (2000). Neurotoxicity but not infectivity of prion proteins can be induced reversibly *in vitro*. *Arch.Virol.Suppl* , 265-273.

Prusiner, S. B. (1982). Novel proteinaceous infectious particles cause scrapie. *Science* **216**, 136-144.

Prusiner, S. B. (1991). Molecular biology of prion diseases. *Science* **252**, 1515-1522.

Prusiner, S. B. (1998). Prions. *Proc.Natl.Acad.Sci.U.S.A* **95**, 13363-13383.

Prusiner, S. B. (2001). Shattuck lecture – neurodegenerative diseases and prions. *N.Engl.J.Med.* **344**, 1516-1526.

Prusiner, S. B., Groth, D., Serban, A., Koehler, R., Foster, D., Torchia, M., Burton, D., Yang, S. L., & DeArmond, S. J. (1993). Ablation of the prion protein (PrP) gene in mice prevents scrapie and facilitates production of anti-PrP antibodies. *Proc.Natl.Acad.Sci.U.S.A* **90**, 10608-10612.

Prusiner, S. B., Groth, D. F., Cochran, S. P., Masiarz, F. R., McKinley, M. P., & Martinez, H. M. (1980). Molecular properties, partial purification, and assay by incubation period measurements of the hamster scrapie agent. *Biochemistry* **19**, 4883-4891.

Prusiner, S. B., Groth, D. F., McKinley, M. P., Cochran, S. P., Bowman, K. A., & Kasper, K. C. (1981). Thiocyanate and hydroxyl ions inactivate the scrapie agent. *Proc.Natl.Acad.Sci.U.S.A* **78**, 4606-4610.

Prusiner, S. B., McKinley, M. P., Bowman, K. A., Bolton, D. C., Bendheim, P. E., Groth, D. F., & Glenner, G. G. (1983). Scrapie prions aggregate to form amyloid-like birefringent rods. *Cell* **35**, 349-358.

Prusiner, S. B., Tremblay, P., Safar, J., Torchia, M., and De Armond, S. J. (1999). Bioassays of Prions in Prion Biology and Diseases, Cold Spring Harbor Laboratory Press 113-145.

Reynolds, J. A. & Tanford, C. (1970). Binding of dodecyl sulfate to proteins at high binding ratios. Possible implications for the state of proteins in biological membranes. *Proc.Natl.Acad.Sci.U.S.A* **66**, 1002-1007.

Riesner, D., Kellings, K., Post, K., Wille, H., Serban, H., Groth, D., Baldwin, M. A., & Prusiner, S. B. (1996). Disruption of prion rods generates 10-nm spherical particles having high alpha-helical content and lacking scrapie infectivity. *J.Virol.* **70**, 1714-1722.

Rochet, J. C. & Lansbury, P. T., Jr. (2000). Amyloid fibrillogenesis: themes and variations. *Curr.Opin.Struct.Biol.* **10**, 60-68.

Safar, J., Wang, W., Padgett, M. P., Ceroni, M., Piccardo, P., Zopf, D., Gajdusek, D. C., & Gibbs, C. J., Jr. (1990). Molecular mass, biochemical composition, and physicochemical behavior of the infectious form of the scrapie precursor protein monomer. *Proc.Natl.Acad.Sci.U.S.A* **87**, 6373-6377.

Safar, J., Wille, H., Itri, V., Groth, D., Serban, H., Torchia, M., Cohen, F. E., & Prusiner, S. B. (1998). Eight prion strains have PrP(^{Sc}) molecules with different conformations. *Nat.Med.* **4**, 1157-1165.

Sanghera, N. & Pinheiro, T. J. T. (2002). Binding of prion protein to lipid membranes and implications for prion conversion. *J.Mol.Biol.* **315**, 1241-1256.

Schmitt-Ulms, G., Legname, G., Baldwin, M. A., Ball, H. L., Bradon, N., Bosque, P. J., Crossin, K. L., Edelman, G. M., DeArmond, S. J., Cohen, F. E., & Prusiner, S. B. (2001). Binding of neural cell adhesion molecules (N-CAMs) to the cellular prion protein. *J.Mol.Biol.* **314**, 1209-1225.

Scott, M. R., Safar, J., Telling, G., Nguyen, O., Groth, D., Torchia, M., Koehler, R., Tremblay, P., Walther, D., Cohen, F. E., DeArmond, S. J., & Prusiner, S. B. (1997). Identification of a prion protein epitope modulating transmission of bovine spongiform encephalopathy prions to transgenic mice. *Proc.Natl.Acad.Sci.U.S.A* **94**, 14279-14284.

Scott, M. R., Groth, D., Tatzelt, J., Torchia, M., Tremblay, P., DeArmond, S. J., & Prusiner, S. B. (1997b). Propagation of prion strains through specific conformers of the prion protein. *J.Virol.* **71**, 9032-9044.

Scott, M. R., Will, R., Ironside, J., Nguyen, H. O., Tremblay, P., DeArmond, S. J., & Prusiner, S. B. (1999). Compelling transgenetic evidence for transmission of bovine spongiform encephalopathy prions to humans. *Proc.Natl.Acad.Sci.U.S.A* **96**, 15137-15142.

Sigurdsson, B. (1954). A Chronic Encephalitis of Sheep. *Brit.Vet.J.* **110**, 341-354.

Stahl, N., Baldwin, M. A., Burlingame, A. L. & Prusiner, S. B. (1990). Identification of glycoinositol phospholipid linked and truncated forms of the scrapie prion protein. *Biochemistry* **38**, 8879-8884.

Stahl, N., Baldwin, M. A., Teplow, D. B., Hood, L., Gibson, B. W., Burlingame, A. L., & Prusiner, S. B. (1993). Structural studies of the scrapie prion protein using mass spectrometry and amino acid sequencing. *Biochemistry* **32**, 1991-2002.

Stoehr, J. (2003). Moeglichkeiten der Fibrillenbildung bei rekombinanten Prion-Proteinen. *Master Thesis;* Heinrich-Heine Universitaet Duesseldorf.

Sunde, M. & Blake, C. C. (1997). The structure of amyloid fibrils by electron microscopy and X-ray diffraction. *Adv.Protein Chem.* **50**, 123-159.

Swietnicki, W., Morillas, M., Chen, S. G., Gambetti, P., & Surewicz, W. K. (2000). Aggregation and fibrillization of the recombinant human prion protein huPrP90-231. *Biochemistry* **39**, 424 -431.

Taraboulos, A., Scott, M., Semenov, A., Avrahami, D., Laszlo, L., Prusiner, S. B., & Avraham, D. (1995). Cholesterol depletion and modification of COOH-terminal targeting sequence of the prion protein inhibit formation of the scrapie isoform. *J.Cell Biol.* **129**, 121-132.

Taylor, J. P., Hardy, J., & Fischbeck, K. H. (2002). Toxic proteins in neurodegenerative disease. *Science* **296**, 1991-1995.

Telling, G. C., Scott, M., Hsiao, K. K., Foster, D., Yang, S. L., Torchia, M., Sidle, K. C., Collinge, J., DeArmond, S. J., & Prusiner, S. B. (1994). Transmission of Creutzfeldt-Jakob disease from humans to transgenic mice expressing chimeric human-mouse prion protein. *Proc.Natl.Acad.Sci.U.S.A* **91**, 9936-9940.

Telling, G. C., Scott, M., Mastrianni, J., Gabizon, R., Torchia, M., Cohen, F. E., DeArmond, S. J., & Prusiner, S. B. (1995). Prion propagation in mice expressing human and chimeric PrP transgenes implicates the interaction of cellular PrP with another protein. *Cell* **83**, 79-90.

Turk, E.; Teplow, D. B.; Hood, L. E. and Prusiner, S. B. (1988). Purification and properties of the cellular and scrapie hamster prion proteins. *Eur.J.Biochem.* **176**, 21-30.

Vey, M., Pilkuhn, S., Wille, H., Nixon, R., DeArmond, S. J., Smart, E. J., Anderson, R. G., Taraboulos, A., & Prusiner, S. B. (1996). Subcellular colocalization of the cellular and scrapie prion proteins in caveolae-like membranous domains. *Proc.Natl.Acad.Sci.U.S.A* **93**, 14945-14949.

Virchow, R. (1851). Struktur und Entwicklung der Staerkekoerner in Verhandlungen der physikalisch-medizinischen Gesellschaft zu Wuerzburg, F. Enke 49f.-

Walsh, D. M., Klyubin, I., Fadeeva, J. V., Cullen, W. K., Anwyl, R., Wolfe, M. S., Rowan, M. J., & Selkoe, D. J. (2002). Naturally secreted oligomers of amyloid beta protein potently inhibit hippocampal long-term potentiation *in vivo*. *Nature* **416**, 535-539.

Wang, J., Xu, G. L., Gonzales, V., Cornfield, M., Copeland, N. G., Jenkins, N. A., & Borchelt, D. A. (2002). Fibrillar inclusions and motor neuron degeneration in transgenic mice expressing superoxide dismutase 1 with a disrupted copper-binding site. *Neurobiol.Dis.* **10**, 128-138.

Weissmann, C., Bueler, H., Fischer, M., Bluethmann, H., & Aguet, M. (1993). Molecular biology of prion diseases. *Dev.Biol.Stand.* **80**, 53-54.

Welker, E.; Raymond, L. D.; Scheraga, H. A. and Caughey, B. (2002). Intramolecular versus intermolecular disulfide bonds in prion proteins. *J.Biol.Chem.* **277**, 33477-33481.

Wells, G. A. & McGill, I. S. (1992). Recently described scrapie-like encephalopathies of animals: case definitions. *Res.Vet.Sci.* **53**, 1-10.

Wells, G. A., Scott, A. C., Johnson, C. T., Gunning, R. F., Hancock, R. D., Jeffrey, M., Dawson, M., & Bradley, R. (1987). A novel progressive spongiform encephalopathy in cattle. *Vet.Rec.* **121**, 419 -420.

Wilesmith, J. W. & Wells, G. A. (1991). Bovine spongiform encephalopathy. *Curr.Top.Microbiol.Immunol.* **17221-38**38.

Will, R. G., Ironside, J. W., Zeidler, M., Cousens, S. N., Estibeiro, K., Alperovitch, A., Poser, S., Pocchiari, M., Hofman, A., & Smith, P. G. (1996). A new variant of Creutzfeldt-Jakob disease in the UK. *Lancet* **347**, 921-925.

Wille, H., Prusiner, S. B., & Cohen, F. E. (2000). Scrapie infectivity is independent of amyloid staining properties of the N-terminally truncated prion protein. *J.Struct.Biol.* **130**, 323-338.

Wille, H., Michelitsch, M. D., Guenebaut, V., Supattapone, S., Serban, A., Cohen, F. E., Agard, D. A., & Prusiner, S. B. (2002). Structural studies of the scrapie prion protein by electron crystallography. *Proc.Natl.Acad.Sci.U.S.A* **99**, 3563-3568.

Williams, E. S. (1980). Chronic wasting disease of mule deer: A spongiform encephalopathy. *J.Wildl.Dis.* **16**, 89-98.

Williamson, R. A., Peretz, D., Pinilla, C., Ball, H., Bastidas, R. B., Rozenshteyn, R., Houghten, R. A., Prusiner, S. B., & Burton, D. R. (1998). Mapping the prion protein using recombinant antibodies. *J.Virol.* **72**, 9413-9418.

Williamson, R. A., Peretz, D., Smorodinsky, N., Bastidas, R., Serban, H., Mehlhorn, I., DeArmond, S. J., Prusiner, S. B., & Burton, D. R. (1996). Circumventing tolerance to generate autologous monoclonal antibodies to the prion protein. *Proc.Natl.Acad.Sci.U.S.A* **93**, 7279-7282.

Xiong, L. W., Raymond, L. D., Hayes, S. F., Raymond, G. J., & Caughey, B. (2001). Conformational change, aggregation and fibril formation induced by detergent treatments of cellular prion protein. *J.Neurochem.* **79**, 669-678.

Zahn, R., Liu, A., Luhrs, T., Riek, R., von Schroetter, C., Lopez, G. F., Billeter, M., Calzolai, L., Wider, G., & Wuthrich, K. (2000). NMR solution structure of the human prion protein. *Proc.Natl.Acad.Sci.U.S.A* **97**, 145-150.

Eidesstattliche Erklärung

Hiermit erkläre ich an Eides statt, dass ich meine Dissertation selbständig verfasst und keine anderen als die angegebenen Quellen und Hilfsmittel benutzt sowie Zitate kenntlich gemacht habe.

Düsseldorf, im November 2003

(Karl-Werner Leffers)